Development of an online analyser for ore grade monitoring in gypsum mining

Doctoral Thesis

to be awarded the degree

Doctor of Engineering (Dr.-Ing.)

submitted by

M.Sc. Hessam Korei

from Tehran/Iran

approved by the Faculty of Energy and Economic Science,

Clausthal University of Technology,

Date of oral examination

12th January 2021

Dean:	Prof. Dr. rer. nat. habil. B. Lehmann
Chairperson of the Board of Examiners:	Prof. Dr. rer. pol. R. Menges
Chief Reviewers:	Prof. Dr.-Ing. habil. H. Tudeshki
	Prof. Dr. rer. nat. habil. B. Lehmann

Erklärung

Hiermit erkläre ich die vorliegende Dissertation eigenständig und ohne unerlaubte Hilfe verfasst habe. Es wurden ausschließlich die in der Arbeit angegebenen Quellen und Hilfsmittel benutzt.

Clausthal-Zellerfeld, 12.01.2021

Hessam Korei

Abstract

The efficient use of mineral deposits requires not only a detailed exploration but also permanent control of the ore grade during the exploitation. Manual sampling and analysis are time consuming and costly. For this reason, online analysers for ore grade control are used partly. The main disadvantages of these analysers are their sensitivity to dust, vibrations and atmospheric influences. The development of an online analyser without these disadvantages is the subject of the thesis. Based on the state of the art, a hypothesis for the development was established. The hypothesis assumes that in a mass flow of grains the ore content can be determined by passive acoustic measurement, assuming that the ore and the waste have different densities. The aim of the development was to implement such an analyser into the drilling rig to measure the ore content of cuttings from blast drillings.

The hypothesis was tested in several stages. Based on preliminary investigations, an online analyser was designed for laboratory use. For the evaluation two algorithms were developed. The laboratory tests were carried out for gypsum, anhydrite and their mixtures. In this context, the influence of the particle size and distribution, velocity and concentration of the mass flow as well as the moisture content were investigated. These test series confirm the hypothesis. In the second phase of the research, investigations were carried out to determine the ore grade. The investigations showed that the results of online analysis and chemical analysis of the samples vary from 0.07 % to 11.52 %. Based on laboratory results, an online analyser was designed for field tests and installed in the dust collector of a drilling rig. During the field test cuttings were continuously analysed online and subsamples were taken from the dust collector and analysed in the laboratory for validation. The comparison of the results shows that the online measurement deviates between 2.25 % to 8.99 % from the laboratory results.

Overall, the hypothesis has been confirmed. The analyser is currently used to detect the ore grade in a gypsum mine. Further potential to increase the accuracy of the online analyser was identified in the course of the field test.

Zusammenfassung

Die effiziente Nutzung von mineralischen Lagerstätten erfordert neben einer detaillierten Erkundung auch eine permanente Kontrolle des Rohstoffgehalts während des Abbaus. Manuelle Probenahme und Analyse sind zeitaufwendig und kostenintensiv. Aus diesem Grund werden teilweise im Bergbau Online-Analysatoren zur Qualitätskontrolle eingesetzt. Die Hauptnachteile dieser Analysatoren sind ihre Empfindlichkeit gegen Staub, Vibrationen und atmosphärische Einflüsse. Die Entwicklung eines Online-Analysators ohne diese Nachteile ist Gegenstand der vorliegenden Arbeit. Basierend auf dem Stand der Technik wurde eine Hypothese für die Entwicklung aufgestellt. Die Hypothese geht davon aus, dass in einem Massenstrom von Körnern der Rohstoffgehalt durch passive akustische Messung bestimmt werden kann. Das Ziel der Entwicklung war die Implementierung eines solchen Analysators in Sprengbohrgeräten zur Messung des Rohstoffgehalts des Bohrkleins.

Die Hypothese wurde in mehreren Stufen getestet. Basierend auf Voruntersuchungen wurde ein Online-Analysator für Laborversuche konzipiert. Für die Auswertung wurden zwei Algorithmen entwickelt. Die Laborversuche wurden für Gips, Anhydrit und deren Mischungen durchgeführt. Dabei wurde der Einfluss der Partikelgröße, Korngrößenverteilung der Stoffe sowie die Einflüsse der Geschwindigkeit und der Konzentration des Massenstroms und des Feuchtegehalts untersucht. Diese Versuchsreihen bestätigen die Forschungshypothese. In der zweiten Phase der Forschung wurden Untersuchungen zur Bestimmung des Gipsgehaltes durchgeführt. Die Untersuchungen zeigten, dass die Ergebnisse der Online-Analyse von den Ergebnissen der chemischen Analyse zwischen 0,07 % bis 11,52 % abweichen. Basierend auf Untersuchungen im Labor wurde ein Online-Analysator für den Test im Feld entwickelt und in einer Bohrmaschine eingebaut. Während des Feldtests wurde das Bohrklein kontinuierlich Online analysiert. Für die Validierung wurden Teilproben aus der Entstaubungsanlage der Bohrmaschine entnommen und im Labor analysiert. Der Vergleich der Ergebnisse zeigt, dass die Online-Messung zwischen 2,25 % und 8,99 % von den Ergebnissen der chemischen Analyse abweicht. Insgesamt hat sich die Forschungshypothese bestätigt. Der Analysator wird seit der Implementierung in einem Bergwerk genutzt. Die bisherigen Erfahrungen weisen Potenziale zur Erhöhung der Genauigkeit des Online Analysators auf.

Acknowledgement

I am honoured to have completed my PhD at the Clausthal University of Technology, a technical university with more than 246 years of tradition in education and research. After my two scientific stays at the Technical University of Clausthal within the framework of the IAESTE programme organised by the DAAD, I was given the opportunity to do my PhD at the Department of Surface Mining and International Mining.

With the research topic of developing an online analyser, I was able to combine my knowledge from my material science studies at the Iran University of Science and Technology with the tasks of analysis in the field of mineral resources. Working on this scientifically very challenging task in cooperation with industry gives me special experience. I would like to thank the Technical University and the Department of Surface Mining and International Mining for this opportunity.

I would like to thank the head of the department, Univ.- Prof. Dr.-Ing. habil. H. Tudeshki for defining the research task and his excellent scientific supervision and enormous support.

I would like to thank Prof. Dr. rer. nat. habil. B. Lehmann, head of the Department of Mineral Resources, for his scientific support and for taking over the co-lecture.

The thesis was carried out in technical cooperation and with the financial support of the company Knauf KG. I would like to thank them for the good cooperation and support.

I would like to thank my colleagues and the staff of the department for their collegial support.

I would like to thank my parents and my brother for their patience and encouragement during my studies and during the preparation of my doctoral thesis.

Clausthal, January 2021

Hessam Korei

Table of Content

Table of Figures

Table of Tables

Table of Graphs

1 Introduction

Annually about 35 bn. tons of mineral commodities are processed into products in various industries worldwide. In the mining industry raw materials are extracted, processed and enriched before being further processed. Mineral deposits are local accumulations of minerals to economic value because of geological and geochemical processes. The required enrichment factor for the classification of a deposit into reserve or resource depends on the mineral type. The ore grade of metal deposits varies from part per million to several tens of percent, while for industrial minerals such as salts or construction raw materials it is in the range of almost one hundred percent. The industrial use of raw materials usually requires very high material purity. The task of mining and ore processing is therefore to enrich ore grade from ppm or a few percent to almost 100 %. The task of mining and processing is also to reduce the impurities in some industrial minerals with a high ore grade. Therefore, ore grade control is one of the most important issues in mining and processing and this control takes place throughout the entire process. In the mine samples are taken from benches, from the cuttings of blast drillings and from the muck pile. After transport and crushing, the ore is stored for homogenization. Samples are then taken again from the stockpiles. In mineral processing several processes are carried out with the aim of enriching the ore. Separators, such as magnetic separators, electrostatic separators, cyclones, and flotation cells are some examples. During the entire processing, additional samples are taken and examined in the laboratory for ore grade determination. These repetitive sampling and analyses serve to control the processes and machines as well as to check the quality of the material. Lastly, the analytical results are used for the fleet and muck pile management. In mineral processing, the analyses are used for the optimal adjustment of the machines, for controlling them and the control of the entire process.

Sampling and sample analysis for the purpose of ore control is a central task in the mining and processing of mineral resources. The use of an online analyser to determine the ore grade would optimize the processes in many ways. Currently, samples are often taken manually from the run-of-the-mine (ROM) ore and sent to the laboratory where they are analysed, and results are reported to the mining and processing departments.

In a manual quality control process, intervention and changes in the process only can take place after the reporting of the laboratory results. Considering that in mining and processing, it is not uncommon to produce several thousand tons per hour, the results of the analysis are available very late. Almost too late for timely control. The development of an online analyser for use in mining and processing would fill a gap. There are some online analysers available on the market for this purpose, but they are sensitive devices. Dust, vibration, environmental temperature, or humidity of the analyte and much more are factors that do not allow the optimal use of these online analysers. Additionally, most of these analysers are often designed based on radiation which due to health and safety regulations have so far prevented a broad implementation of these technologies in mining and processing.

Since in all processes in mining and mineral processing in a very harsh environment the ore is present as grains and is always transported from one process step to the next as a mass flow, this industry needs an online analyser with special features. An online analyser that can be used in all settings, i.e. belt conveyor, hydraulic and pneumatic conveying and at the same time is not sensitive to dust, vibration and climatic factors would fulfil the requirements for the implementation very well.

The present work deals with the development of such an analyser. The research is based on the hypothesis that an online determination of ore grade is possible based on passive acoustic phenomena. Previous research has shown that this method allows an online particle size analysis of granules in a mass flow. This method makes use of the physical principle of impact based on the Hertz theory, which states that the force generated when a granule collides with an oscillator is proportional to the modulus of elasticity, Poisson's ratio and the particle size of the granules. The hypothesis of this work assumes that when grains with the same grain size, but different density collide with an oscillator, the momentum is proportional to the density of the granules. The deviation of the grain size of the grains, which can be tolerated for a successful online analysis, depends on the difference in density of the grains.

The verification of this hypothesis is done in a systematic investigation. The drill cuttings, which are produced during the production of blast drillings, are chosen as the object of investigation. The online analyser to be developed is to be implemented in drilling rigs. The cuttings produced during the drilling process will afterwards be analysed online. In this case the information from ore grade is available at the

beginning of the process and allows an immediate control of the following process steps. If this development is possible, online analysers for use in mineral processing can be built on the same technical concept. The investigations of this work are carried out with gypsum and anhydrite. Gypsum deposits contain anhydrite impurities due to gypsum's formation process. In some cases, there are enclosed anhydrite lenses or horizontal layers of anhydrite within the gypsum deposit. These impurities reduce the quality of the products. Ore control can therefore be an important tool for quality monitoring in gypsum mines.

The second chapter describes the state of the art for online ore grade determination. Due to the research hypothesis, this chapter also includes a description of the state of the art in acoustic material detection and acoustic online particle size analysis. In the third chapter the research hypothesis is described in more detail. An elementary component of the hypothesis is the acquisition and processing of acoustic signals. Therefore, in the fourth chapter of the thesis the basics of acoustic measurement are explained. In this context, the relevant parameters of a measurement system according to Hertz theory are discussed theoretically. These include the influence of particle size, particle size distribution, and the concentration and velocity of the mass flow. The basics of data acquisition and data as well as data reduction and data classification methods are described in this chapter as well. In chapter 5 the design of the online analyser for laboratory tests is presented. The individual components of the online analyser are selected according to the defined requirements and dimensioned by separate tests. The selection and dimensioning of the sensor, the Venturi nozzle, the shape and type of the oscillator as well as the supply of the analyser with compressed air are part of this section. In addition, the selection of the signal processing as well as the algorithms for the calibration of the online analyser are part of this section. The basic verification of the hypothesis with the online analyser is explained in chapter 6 of the thesis. The results for the determination of the influence of particle size, particle size distribution and moisture are described in chapter 7 to 9. Because gypsum deposits are partly associated with dolomite, the investigation is extended to test the possibility of online detection of dolomite. The results of these tests are presented in chapter 10. The online analyses will be more accurate the more similar the particle size distribution of the samples is. In this respect, the possibility of pre-classifying of the cutting will be investigated in chapter 11 and 12. After the basic proof of the measuring principle, the possibility of online ore grade analysis is further investigated. For this

purpose, a series of samples of different purity are tested online. The description of the samples as well as the tests and their results are presented in chapter 13. For the calibration two algorithms are selected and used. One algorithm is based on probability and statistical data analysis while the second algorithm is based on multivariate data analysis (PCR). The results of both calibration methods are compared to each other to assess the accuracy of the methods. Based on the results obtained, an online analyser will be designed for implementation in a drilling rig. The requirements for such a development and implementation will be explained in chapter 14. The field investigations will be carried out in two successive stages. In the first stage the basic function of data acquisition and data transfer to the electronic unit will be tested in an underground mine. The second stage will be based on the results of the first stage in an open-cast mine in combination with a modern drilling rig. The field tests are described in chapter 14 as well. After the description of the measuring concept, the online analyser implemented in the drilling instrument is presented. This chapter also contains the description of the field tests as well as data processing and calibration. Both algorithms are also used in this case. For the final verification of the hypothesis and proof of the repeatability a validation is performed after the calibration. For this purpose, an online ore grade determination is performed during a drilling process in an open pit. The results of the online analysis are compared with the results of the chemical analysis. At the same time the online results of the respective calibration methods are compared with each other. The results of the field tests are summarized. Finally, a summary of the thesis is given in chapter 15.

2 State of the art

The development of a new method for controlling ore grades in the mining industry requires the investigation of existing technologies according to the state of the art. The current technologies for determining the quality of raw materials can be divided into two major groups. The most commonly used measuring method is based on the physical principle of optics. The methods developed on the basis of optics are divided into two subgroups, visible and invisible, according to the wavelength of the light used. The methods with visible light use a wavelength of 400 nm to 700 nm. These methods are called VIS-Spectroscopy. The methods that use a wavelength of 0.1 nm to 100 nm belong to the invisible group. They are divided into gamma radiation and X-rays depending on the wavelength. These methods belong to the radiation spectroscopy. Some methods use the invisible spectrum between 700 nm and about 2,000 nm. This spectrum is called infrared. The typical method of this group is the Near Infrared, NIR-method. These methods use the spectrum between 100 nm and about 2,000 nm or from ultraviolet light to the infrared spectrum. These methods are called laser spectroscopy.

The second group, which is the subject of recent publications, is based on the physical measurement principle of acoustics. In this case the physical principle of friction is used for material detection. In the following, these methods are briefly described and the advantages and disadvantages of each method are explained. For the development of the hypothesis of this thesis the results are used.

2.1 Radiation based method

Near Infrared Spectroscopy (NIR)

The measuring principle of infrared spectroscopy is based on the harmonic vibrations of molecules. The intensity of the vibrations is proportional to the energy level. By absorbing infrared radiation, the molecules are set in motion. Through this motion, the vibrations of the intermolecular bonds can be measured, which is a characteristic of certain special materials. For the measurement of such vibrations, an infrared spectrum ranging from 700 nm to 2,400 nm is used. This spectrum is called near infrared (NIR). In the NIR spectroscopy a Fourier transform is used [1, 2, 3].

The use of NIR spectroscopy for minerals requires a complex and advanced calibration and the measurement results are highly dependent on the water content of the sample.

For this reason, this technology is often used in combination with an instrument to determine the water content of the minerals. Furthermore, the measurement system needs additional calibration for minerals with different water contents. The sensitivity of the system to water content is so high that it is partly used in industrial applications for the determination of water content. NIR spectroscopy is mainly used in medicine and the food industry. In the mining industry this technology is used for moisture measurement and material type determination. The online measurements of raw material mixtures in the cement industry can be named as such an example and is illustrated in Figure 2.1 [3].

Figure 2.1: An industrial example of Near Infrared Spectroscopy with the spectral flow analyser [3]

Laser-Induced Fluorescence Spectroscopy (LIF)

Laser-induced fluorescence spectroscopy (LIF) or Fluorescence spectroscopy makes use of the fact that atoms of all substances move to an excited state (higher energy level) when energy is supplied to them. When the atoms return to their original energy level, they release their excess energy by emit electromagnetic wave of certain wavelengths. With a constant energy source, the intensity of the emitted electromagnetic waves depends on the material. In case the energy source for atom excitation is a laser, the measuring principle is called Laser Induced Fluorescence Spectroscopy (LIF). The LIF method often used in the mining industry in combination with a belt conveyer and is referred to as a cross belt analyser which is used for determining the quality of raw materials. With such a method a chemical analysis or determination

of the individual minerals in the process is not possible. This technology is used both in mining and in the steel industry [4, 5, 3].

Laser Induced Breakdown Spectroscopy (LIBS)

The Laser Induced Breakdown Spectroscopy (LIBS) is based on the recording and analysis of the emitted electromagnetic waves by material entering the plasma state due to received energy from a high energy laser beam which is focused on it. Due to the high amount of energy the sample is evaporated and a plasma is generated. The emitted electromagnetic waves are picked up by optical detectors and are directed onto a spectrometer. The composition of the sample is then determined by the resulting spectral line where the position of the spectral lines is different for different elements. The intensity of the spectral lines corresponds to the mass ratio of an element present in the sample. This technology is used for elemental analysis of substances. An exception is the detection of sulfur and helium. For the analysis, databases for typical spectral lines of elements are created in advance. The problem is that several spectral lines exist for the same elements. The intensity is also very strongly dependent on the environmental conditions such as temperature and humidity. The change of the focus range has also an extraordinarily strong influence on the results of the analysis. Therefore, the LIBS analysers are mostly used in laboratory environments. There are efforts to use this technology in combination with conveyor systems, but the experience thus far has not been so positive [6, 7, 3, 8].

Fluorescence Spectroscopy (XRF)

This analytical method is based on irradiation of a sample with X-rays. Here an exceedingly high energy X-ray radiation hits the atoms of the elements. The supplied energy causes the electrons from the inner orbitals of the atoms to outer orbitals of the atoms. Due to the state instability of the atoms, the excess energy of the moved electrons is emitted in form of electromagnetic waves and the electrons return to their initial states. This radiation is picked up by detectors and is optically analysed. As the wavelength of the emitted electromagnetic wave is unique to a certain element, analysis of the radiation can be used to determine the element in the sample. The X-ray fluorescence spectrometer (XRF) is used both laboratory and in field applications in combination with conveyor belt systems for elemental analysis. In the latter case, the material is often separated and analysed by a bypass. For optimal analysis, samples should be smaller than 10 mm. A disadvantage of this measurement method

it the overly complex calibration process. For the results to be accurate, the calibration needs to be performed using the material which is going to be analysed later [9, 5, 3].

X-ray Diffraction (XRD)

In X-ray diffraction (XRD), an X-ray beam with a different defined angle of incidence is focused on the sample and the reflection of the beam is measured. The diffraction of this beam depends on the crystal structure of the samples and based on a calibration function it is possible to detect mineral phases. This technology is only used in the laboratory. A disadvantage of this method is that the samples need special preparation. Due to the necessary sample preparation, X-ray diffraction has not yet been used as an online measuring device in industry applications [10, 11].

Prompt Gamma Neutron Activation Analysis (PGNAA)

In this analysis technique, a sample is bombarded with neutrons where the atoms of the sample pick up these neutrons. Due to the new state the atomic nucleus becomes unstable. While the atomic nuclei tend to achieve a stable state again, they emit gamma radiation. The intensity of the gamma radiation is a fingerprint for a certain chemical element. This technology is used in combination with conveyor belt systems for online analysis of raw materials. For this purpose, a neutron source and a gamma radiation detector are installed closely together on the conveyor system. The accuracy of this measuring method depends on the water content of the sample. In addition, problems arise due to the matrix effect. Furthermore, calibration with reference samples is required for an accurate measurement. PGNAA is often used in the cement industry for online analysis of the raw material [12, 13, 3].

UV/VIS Spectroscopy

The measuring principle of UV/VIS spectroscopy is based on the excitation of valence electrons of atoms. By irradiating a sample with light in the visual (380 nm to 750 nm) or near ultraviolet (200 nm to 380 nm) spectrum, a light absorption occurs which is caused by electron transitions in the molecules. As mentioned above, the electron transitions are due to the excitation of valence electrons. By measuring the light transmission in transparent samples and the light reflection in opaque samples, a substance can be determined qualitatively. The measuring instruments consist of a light source and a photo-optical detector. With this measuring method it is only possible to determine the changes within a calibrated substance. Additionally, a premature

calibration of the system is required. Unknown substances cannot be detected with this method and the system is relatively sensitive to small changes and noise. Furthermore, changes in surface texture, moisture and particle size distribution influence the measurement results. UV/VIS spectroscopy is particularly used in the glass and plastics industries [14, 15, 5, 16, 3].

2.2 Acoustic based methods

Recently, several methods for material detection and particle size analysis based on acoustic emissions have been developed. These methods can be divided into two main groups. The first group of methods deals with the detection of soil types as well as the determination of soil mixtures. These methods are based on the principle of friction. Soils have different friction depending on their grain size. When a device is moved over Soil, the friction between Soil and the device generates an oscillation. The intensity of the vibration can be used as a fingerprint to determine the soil composition.

The second group of methods is used to determine the particle size distribution. In this case the physical principle of momentum is used. When granules, which are moved in a mass flow, collide with a device, impulses are generated. The characteristic of these oscillations depends on the particle size distribution of the mass flow. The particle size is determined by online measurement of the oscillations using a piezometer and further signal processing of the data. These methods are explained in more detail below.

Acoustic method using friction

In the patent application [17] a development is presented for the online determination of soil type. This method has been developed for civil engineering and mining applications for the online measurement of soil types, as well as the detection of interfaces (layer boundaries) during extraction and exploration. This invention is based on the measurement and evaluation of structure-borne noise. The structure-borne sound results from the friction which is produced by the relative movement of a device which is in contact with the soil. The acoustics or vibrations result from the friction between the device and the soil. The vibrations are measured with an accelerometer. A subsequent signal processing detects the material composition as well as the boundaries of the sediments [18]. The online analyser requires a calibration and the measurement results are influenced by the following parameters:

- Normal force

- Relative velocity between the sound body and the material
- Geometric properties and material characteristics of the oscillator
- Position of the acoustic sensor

This method has been successfully used in combination with Micro Tunneling, cone penetration test (CPT) and excavators in the mining industry [19].

Acoustic method using pulse energy or reflection

This method uses two system configurations. A distinction is made between passive acoustic methods and active acoustic methods.

With the active acoustic methods, an acoustic signal is sent from a transmitter. A receiver registers the incoming signal and the incoming signal is either reflected or attenuated. For these applications ultrasonic sensors are usually used as transmitters. In some configurations transmitter and receiver are combined in one device. In some other configurations, the transmitter and receiver are installed separately. Active methods are described for example in [20].

The active acoustic method is only used in connection with hydraulic mass flow. The accuracy of the measurement decreases with the increase of the solid's concentration.

The passive acoustic method is based on the physical principle of the impulse. Granules that are being transported in a mass flow generate impulses through collision with a device. As a result of the collision, the device starts to vibrate. The particle size of the granulate is determined by recording the vibrations using a piezoelectric vibration sensor and subsequent signal processing [21].

2.3 Summary of the state of the art

The evaluation of the state of the art for online determination of the ore grade shows that some measurement methods have become established in the industry. Most methods are based on the basic physical principle of optics. The measurement methods differ in the use of wavelengths or spectra. Color Line-Scanner (CCD), Near Infrared Spectrometer (NIR), Laser-Induced Breakdown Spectroscopy, Laser-Induced Florescence Spectroscopy (LIF), X-ray Diffraction (XRD), X-ray Transmission (XRT), X-ray Fluorescence (XRF), Prompt Gamma Neutron Activation Analysis (PGNAA) and Pulsed Fast Thermal Neutron Activation Analysis (PFTNAA) all belong to this group. Some of these methods can be used to determine the material composition while

others can only be used to determine the elemental composition. All these measurement methods are suitable for online measurement in combination with a bypass. From the above-mentioned methods all up to XRT and XRD are suitable for use on conveyor systems. The mentioned methods deliver the results in different time intervals. Laser based methods deliver up to 20 results per second. X-ray methods require up to 6 minutes. The accuracy of most methods depends on the water content of the material. Only the X-ray based methods are robust to fluctuations in material water content. Some methods such as NIR and XRF require powder for the measurement. The following disadvantages arise for industrial applications:

- Safety problems particularly for X-ray, laser and neutron sources
- vibration sensitivity
- dust sensitivity
- impact sensitivity
- Sensitivity to weathering

A comprehension of the presented state of the art is given in Table 2.1. In contrast to the optical methods, the acoustic methods have none of the disadvantages mentioned above. However, the acoustic methods do not allow quantitative analysis. The method allows only a relative qualitative determination of soil type. Considering the technical conditions in mining, the acoustic method offers some advantages, especially because of its robustness. Therefore, this thesis focuses on the development of an online analyser based on passive acoustics.

Table 2.1: Comparison table of different optical meaurement technologies [3]

	technology	physical	mineral composition	elementar composition	main conveyor belt	bypass belt	moisture influence	sureface measurement	measuring rate/ data output rate	environmental hazards	requirements
COLOR	CCD Color Line-Scanner	color, brightness	+	-	+	+	+	+	cont./ 1/min	UV	-
NIR	Near Infrared Spectrometer	absorption of light NIR	+	-	+	+	+	+	cont./ 1/min	-	Powder application
LIBS	Nd:YAG-Laser, Spectrometer	atoms emit spec. light	-	+	+	+	-	+	20/s	laser	-
LIF	laser, sensor	spec. fluorescence	+	-	+	+	-	+	20/s	laser	-
XRT	X-ray source, X-ray sensor	absorption of X-ray	-	+	-	+	+	-	cont./ 1/min	X-ray	-
XRF	X-ray source, X-ray sensor	element spec. fluorescence	-	+	+	+	+	-	cont./ max 6/min	X-ray	Restricted particle size
XRD	X-ray source, ring sensor	reflection X-ray diff. angles	+	-	-	+	-	+	cont./ 1/min	X-ray	Powder application
PGNAA PFTNAA	neutron source, Y-ray sensor	Y-ray emission	-	+	+	+	+	-	cont./ 1/min	Y-ray N-ray	-

3 Physical approach and research hypothesis

The physical approach of research is based on the passive acoustic principle. Previous research has shown that the application of this method allows the online particle size analysis of granules in a mass flow. The research results confirm that the particle size distribution of the granules in the mass flow can be derived from the waves that are generated when granules collide with an oscillator. A prerequisite for the implementation of this method is the development of a suitable signal processing and further algorithms to determine the particle size distribution. An overview of the principle of this system is shown in Figure 3.1 [21, 22, 23].

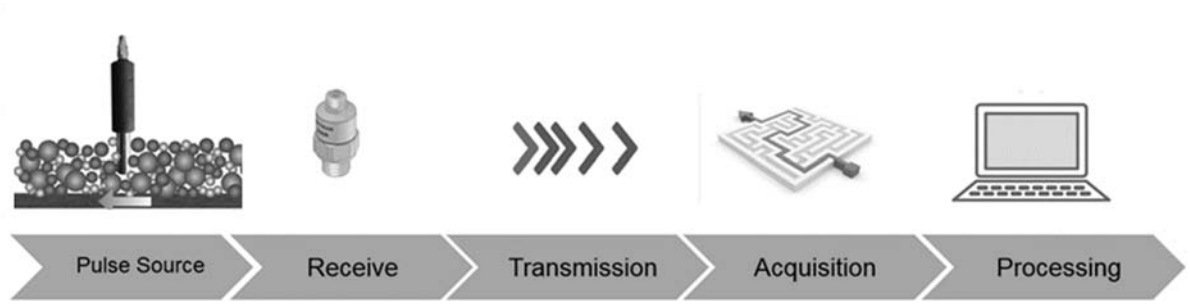

Figure 3.1: Principle of acoustic measurement

The research hypothesis assumes that this method can be further developed to calculate ore grade in a mass flow of granules. If granules of the same grain size and velocity collide with the oscillators, the pulse energy or signal intensity is a function of the density of the granules [24, 25, 26]. If the density of the grains in the mass flow changes, the pulse energy and the signal intensity also change. Therefore, based on the method, when grains with different densities are transported in a mass flow, an automatic detection of the materials can be carried out. The research hypothesis even goes further and assumes that it is even possible to determine the percentage of granules with different densities in a mass flow [27]. The verification of this hypothesis is the aim of this research. Graph 3.1 shows the change in pulse when density changes for different grain sizes. In this example grains of gypsum and anhydrite with a density of 2.32 t/m^3 and 2.97 t/m^3 were chosen.

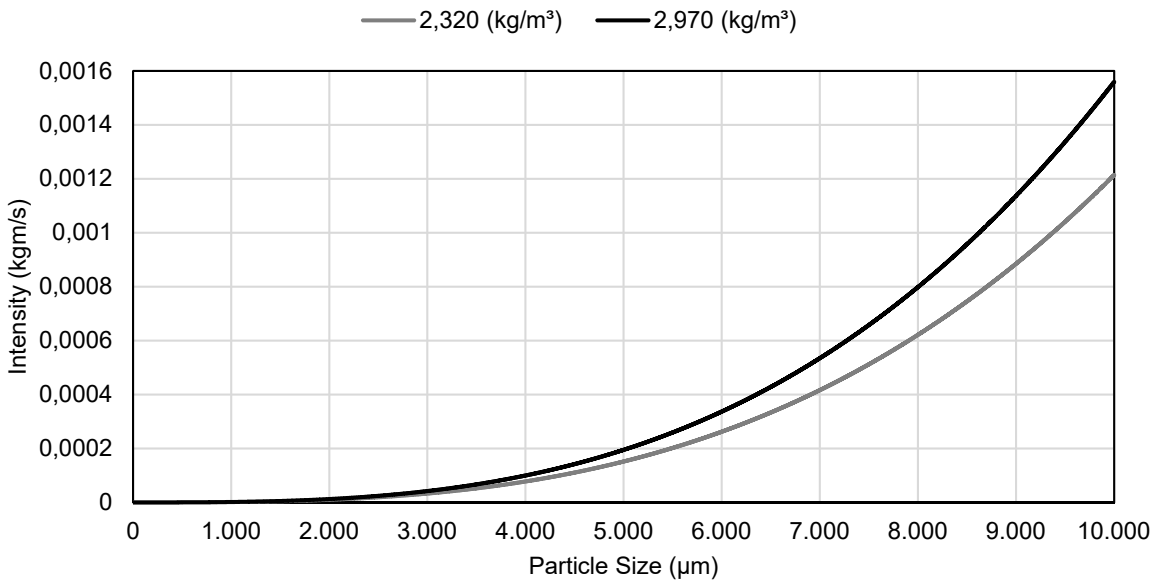

Graph 3.1: Relationship between pulse and density using the example of gypsum and anhydrite

Mineral deposits consist of ore and waste. The ore grade varies in a deposit depending on the mineral, the genesis of the deposit and the deposit type. The main purpose of deposit exploration is to identify the mineralized zones. The task of exploration is to determine the boundary between the ore body and the surrounding rocks and to determine the ore grade within the deposit itself. Based on this data, deposits are modelled, and the ore grade is determined, and the stripping ratio is calculated. The feasibility of a mining project depends on the results of the exploration. The ore processing also depends on the ore grade. Information on the ore grade is important for the entire processing chain. The ore is enriched in many machines such as sorters and classifiers. For the control of these machines the ore grade of the input and output materials is particularly important.

In all cases mentioned above, whether in exploration or processing, the materials are present as grains. The grains are transported in different ways as mass flows. In addition, ore and waste have different densities. The density difference depends on the type of deposit. For metallic ores, the difference is exceptionally large, whereas for non-metallic deposits the difference can be small.

The prerequisites for the development of an online analyser based on the research hypothesis are given in mining. The materials are present as grains, they have different densities and they are moved as a mass flow. Of importance is the actual need for such a development in mining. The use of such an analyser offers several technical, economic and even environmental advantages.

The verification of the research hypothesis is carried out in this thesis by means of investigations of drill cuttings. The investigations are carried out with the aim to develop an online analyser for the determination of ore grade in case of the verification of the hypothesis. The verification is focused on the investigation of cuttings that will be produced during the drilling of blast holes. Blast drillings are continuously produced in the mine. The cuttings from these drillings are available as grains and are usually transported with compressed air. A part of the quality management in the running mines is the sampling and analysis of the cuttings in the laboratory. Both the fleet management in the mine and the control of processing are based on this daily quality analysis. The hypothesis assumes that the cuttings produced during blast drilling are continuously analysed online at the drill site. The cuttings are to be continuously feed as a mass flow to a device where they collide with an oscillator. The oscillator contains a sensor. The waves resulting from the impact of the cuttings are detected by the sensor and processed in an electronic unit. From the data the ore grade is determined with a special software. Considering the time-dependent coordinates of the blast hole, signal processing can be used to create a quality dependent profile for the blast hole. As a result of the online analysis of the drill cuttings, a three-dimensional quality model of the deposit can be created, which can be updated and adjusted at any time by remote transmission of the analysis data. Figure 3.2 schematically illustrates the concept for this practical application.

For the verification of the hypothesis, the possibility of online analysis of the gypsum purity is investigated. Gypsum deposits often contain anhydrite and dolomite admixtures. These minerals have a higher density than gypsum.

For the systematic development of an online analyser the basics of acoustic measurement and data acquisition and data processing are considered and the requirements for such an analyser are derived. In successive steps an online analyser for laboratory purposes is developed and algorithms are set up. Based on the laboratory results an online analyser for drilling rig is developed and field tests are performed.

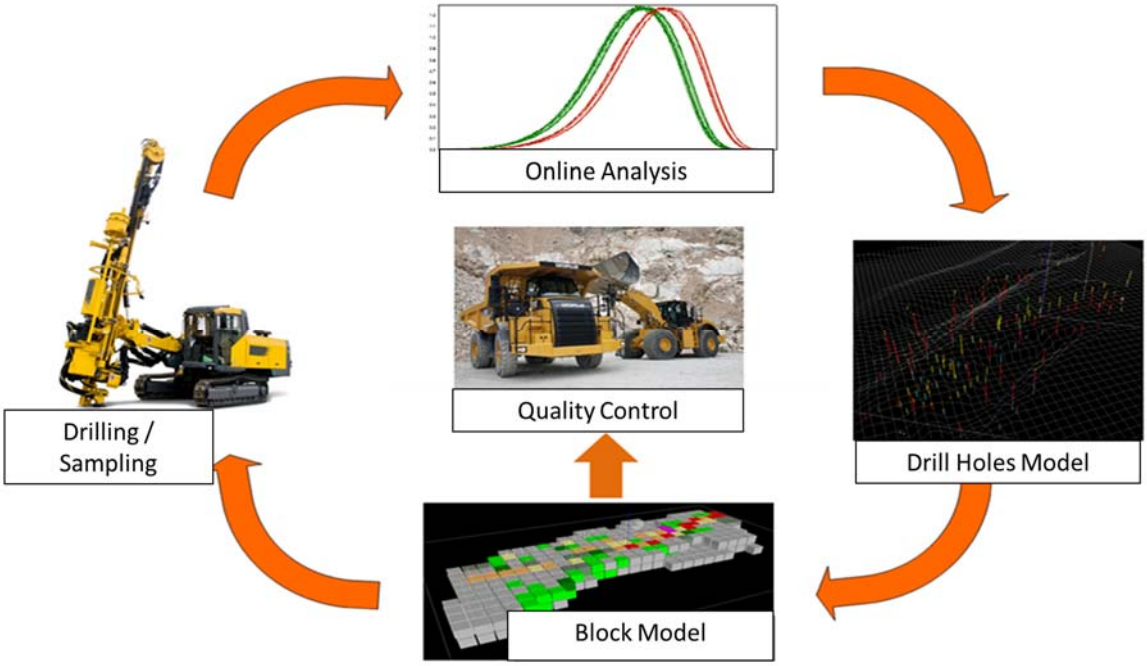

Figure 3.2: Conception for the practical application of sustainable quality control [25]

4 Basics of acoustic measurement

Acoustic measurement methods are based on the principle of acoustic emissions and make use of the produced oscillation from the collision of particles with a measurement element. The object which the particles collide with is usually metallic and is resistant to mechanical and chemical wear. When a particle collides with the surface of the rigid collision body, the impact energy creates a system of elastic waves within the body, which is formally equivalent to a source of acoustic emissions [28]. As an example, if a particle impacts upon a massive metallic collision plate, the measured acoustic signal A(t), which can be measured by the transducer, can be modelled as Equation (4-1):

$$A(t) = S(t) * G(t) * D(t) \tag{4-1}$$

where S(t), G(t) and D(t), respectively, denote the acoustic source, propagation and detector functions, as function of time t; the symbol * represents convolution [28]. In a more general sense, different research projects have shown that the generated acoustic signal can be written as in Equation (4-2) [29]:

$$U_{Acoustic} = f(\rho, v, d, T) \tag{4-2}$$

Here ρ is the density of particles colliding with the sensor, v is the particle transport velocity, d is the particle diameters, and T is the measurement environment temperature. In most applications the particle size d is to be found, therefore it is important to either keep the other factors constant, or somehow to measure and consider when analysing the output signal and calculating the particle size distribution. Another study which has determined the influential factors for the acoustic particle size measurement, has done this through the Hertz theory [30]. Here the duration of the impact t_{imp} and the amplitude of the force occurring during impact F_{Max} can be linked together. It has been shown that t_{imp} and F_{Max} are individually proportional to the density ρ, velocity v and the radius $\frac{d}{2}$ of the colliding particle with the sensor [31]. These relationships can be seen in Equation (4-3) and (4-4) below:

$$t_{imp} \approx (\alpha_1 + \alpha_2)^{0.4} \rho^{0.4} v^{-0.2} \frac{d}{2} \qquad (4\text{-}3)$$

with:

t_{imp}	duration of impact (s)
α_1	specific constant of material 1 (ms²/kg)
α_2	specific constant of material 2 (ms²/kg)
ρ	density (kg/m³)
v	velocity (m/s)
d	particle diameter (m)

$$F_{Max} \approx (\alpha_1 + \alpha_2)^{-0.4} \rho^{0.6} v^{1.2} \left(\frac{d}{2} \right)^2 \qquad (4\text{-}4)$$

with:

F_{Max}	maximum impact force (kgm/s²)
α_1	specific constant of material 1 (ms²/kg)
α_2	specific constant of material 2 (ms²/kg)
ρ	density (kg/m³)
v	velocity (m/s)
d	particle diameter (m)

Where α_n is determined by Equation (4-5):

$$\alpha_n = \frac{1 - \mu_n}{E_n} \tag{4-5}$$

with: α_n specific constant of material n (ms^2/kg)

μ_n Poisson's constant

E_n modulus of elasticity (kg/ms^2)

Here μ_1 is the Poisson's constant of particle material, μ_2 is the Poisson's constants of the measurement system impact material, E_1 is the modulus of elasticity of particle material, and E_2 is the modulus of elasticity of measurement system impact material.

The Hertz theory assumes that the energy generated by the collision of a particle with an oscillator is proportional to the density of the particle. The research hypothesis assumes that ore grade in a mass flow of granules can be determined online. In this case, these are grain collectives which simultaneously hit the oscillator. Therefore, the factors to be considered according to Hertz theory must be extended by the concentration of the mass flow.

According to the extended Hertz theory, the influencing parameters on the acoustic energy can be divided into four groups. These groups result from the material-dependent properties, from the properties of the mass flow and from the properties of the oscillator and the sensor. The first group includes the particle size distribution, the modulus of elasticity and the density of the granules. The second group consists of the velocity and concentration of the mass flow. The third group includes the modulus of elasticity of the oscillator and the frequency range and sensitivity of the sensor. Some of the relevant influencing factors are explained in more detail below.

4.1 Particle size

Grain size is a parameter used to describe granules for quality control and monitoring production processes. It is a very difficult task to express the particle size quantitatively, as particles possess asymmetrical profiles, and their size cannot be determined easily. Due to the complexity of the direct determination of the particle size, this property is

measured indirectly. This is done with defining an equivalent diameter, where the size of the particle is referred to be the same as a spherical shaped particle. This property can either be the volume, surface area, length, or physical or chemical properties [32].

In process engineering, particles with sizes ranging between 10^{-8} m and 0.1 m are measured. Different methods are used depending on the particle size. The most important methods are sieve analysis, sedimentation analysis, scattered light analysis, microscopic analysis and laser diffraction spectroscopy. Of the methods mentioned, sieve analysis is the most common method. It is used for dry grains with a particle size of more than 63 µm. For sieve analysis, the particle size is defined as the mesh size L of a test sieve through which the particle barely passes. In the context of the present thesis, grain sizes are determined by sieve analysis [33].

4.2 Particle size distribution

Particle Size Distribution (PSD) is a curve or function, which contains all the information on a collection of particles at a given point in time [34]. PSD expresses what particle size exist in what fractions compared to all the particles in the sample particle group to be measured. PSD is either shown as a frequency distribution, which can be explained using a Probability Density Function (PDF), or a cumulative form of the frequency distribution, also known as the Cumulative Probability Density Function (CDF).

For defining the PDF, initially the range of observed particle sizes needs to be divided into separate classes. The frequency distribution indicates in percentage what portion of particles can be found in a corresponding particle size class [34]. The density size distribution q_0 (x) is defined in Equation (4-6):

$$q_0(x) = \frac{dN}{N}\frac{1}{dx} \tag{4-6}$$

Where N is the number of total particles, dN is the number of particles having diameters between x and x + dx. The CDF or $Q_0(x)$ on the other hand, can be calculated through the integration of $q_0(x)$ over the range 0 to x according to Equation (4-7) [34]:

$$Q_0(x) = \int_0^x q_0(x)\, dx \tag{4-7}$$

The size distributions are on a number basis, where the subscript s indicates the basis of the expression. For number, length, area and mass the respective subscripts are 0,

1, 2 and 3. It is also possible to transform the density distribution $q_r(x)$ into another basis distribution $q_s(x)$ by Equation (4-8):

$$q_s(x) = \frac{x^{s-r} q_r(x) dx}{\int_0^{\infty} x^{s-r} q_r(x) dx} \tag{4-8}$$

For the presentation of PSD, mainly the acquired data is plotted, either $q_r(x)$ or $Q_r(x)$ in a graph. The $Q_r(x)$ representation with a logarithmic abscissa is more often used in industrial applications. Graph 4.1 shows an example of a cumulative particle size distribution [34, 35, 32].

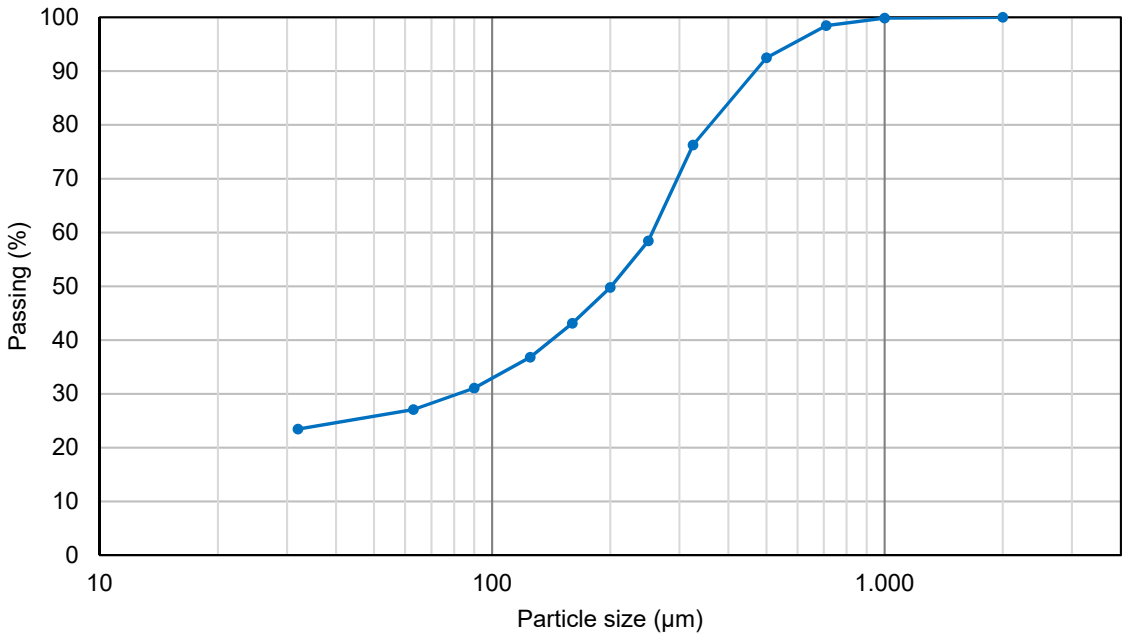

Graph 4.1: Example of the PSD format used in most industrial applications

4.3 Influence of the particle size distribution

The hypothesis seems simple if the grains are all the same size but have different density. This ideal case will almost never occur in industrial processes. The granules do not consist of one mono grain. They always have a grain size distribution. Therefore, it must be investigated which deviation between the grain sizes would still be tolerable for an online measurement. This calculation is carried out based on the extended Hertz theory. The calculation is intended to show at which grain diameter of gypsum and anhydrite the pulse or the energy of the collision is equal, if the velocity is assumed to be constant. Gypsum has a modulus of elasticity of 35.3 GPa and a Poisson's ratio of 0.338, where anhydrite has a modulus of elasticity of 63.8 GPa and a Poisson's ratio

of 0.315 [36]. A carbide rod is assumed as the oscillator. The tungsten carbide has a Poisson's ratio of 0.31 and a modulus of elasticity of 650 GPa. The properties of gypsum, anhydrite and the oscillator are presented in Table 4.1.

Table 4.1: Densities, Poisson's coefficients, and the moduli of elasticity of gypsum, anhydrite and hard metal

	Density (kg/m³)	Poisson's Coefficient	Modulus of Elasticity (GPa)
Gypsum	2,320	0.338	35.3
Anhydrite	2,930	0.315	63.8
Hardmetal	15,630	0.31	650

With Equation (4-9):

$$F_{A/G} = (\alpha_{A/G} + \alpha_{St})^{-0.4} \cdot \rho_{A/G}^{0.6} \cdot v^{1.2} \cdot \left(\frac{d_{A/G}}{2} \right)^2 \qquad (4\text{-}9)$$

with:

$F_{A/G}$	maximum impact force (kgm/s²)
$\alpha_{A/G}$	specific constant of anhydrite or gypsum (ms²/kg)
α_{St}	specific constant of oscillator (ms²/kg)
$\rho_{A/G}$	density of anhydrite or gypsum (kg/m³)
v	velocity of particles (m/s)
$d_{A/G}$	particle diameter of anhydrite or gypsum (m)

Where α_n is determined according to Equation (4-10):

$$\alpha_G = \frac{1-\mu_G}{E_G} = 0.01875 \left[\frac{1}{GPa}\right]$$
$$\alpha_A = \frac{1-\mu_A}{E_A} = 0.01074 \left[\frac{1}{GPa}\right] \quad (4\text{-}10)$$
$$\alpha_{St} = \frac{1-\mu_{St}}{E_{St}} = 0.001106 \left[\frac{1}{GPa}\right]$$

with: α_n specific constant of anhydrite, gypsum and oscillator (ms^2/kg)

μ_n Poisson's constants of anhydrite, gypsum and oscillator

E_n modulus of elasticity of anhydrite, gypsum and oscillator (kg/ms^2)

if $F_A = F_G$ Equation (4-11) can be written as followed:

$$(\alpha_A + \alpha_{St})^{-0.4} \cdot \rho_A^{0.6} \cdot v^{1.2} \cdot \left(\frac{d_A}{2}\right)^2 = (\alpha_G + \alpha_{St})^{-0.4} \cdot \rho_G^{0.6} \cdot v^{1.2} \cdot \left(\frac{d_G}{2}\right)^2 \quad (4\text{-}11)$$

According to the calculations, a gypsum grain would have to have a diameter 19 % larger than an anhydrite particle so that its acoustic energy of collision is identical to that of the anhydrite particle, which thus can be defined as the tolerance. Theoretically, the deviation of the grain classes must in any case be smaller 19 %. For the practical application, a deviation of 18 % may still be tolerable.

4.4 Influence of speed and concentration

The influence of the velocity and concentration of particles in a flow on the acoustic energy is investigated by the mechanical approach of dimensional analysis. It is assumed that the acoustic energy is proportional to the flow energy. When an oscillator is held in a flow, the force acting on the oscillator depends on the area of the oscillator and the velocity and mass concentration or bulk density of the mass flow.

To determine the relationship between several variables acting in a physical process, mathematical-functional equations are established in experimental investigations. If there are many variables, the establishment of mathematical-functional equations becomes complex, so that a direct determination of the relationships between the

parameters is usually difficult. One way to determine the relationship between the variables is to perform a dimensional analysis.

Here, the relationship is not established between individual variables, but between dimensionless similarity numbers. The mathematical basis of the dimensional analysis is based on the general similarity theory, the so-called "Buckingham Theorem" according to which Equation (4-12) with the basic form [37]:

$$f (y_1, y_2, y_3, ...y_n) = 0 \quad (4\text{-}12)$$

can be converted into the dimensionless form, see Equation (4-13):

$$\pi_1 = f (\pi_2, \pi_3, ...\pi_N) \quad (4\text{-}13)$$

The number of dimensionless parameters N is equal to the number of variables n involved in the process, deducted from the number of orthogonal basic physical parameters m involved. The Equation (4-14) applies:

$$N = n - m \quad (4\text{-}14)$$

A system can contain the dimensions {L, M, T, I, Θ, A, J} based on the physical quantities: length, mass, time, current, temperature, amount of matter and light intensity, all physical processes can be described.

The result of the dimensional analysis provides the following relationship between the influencing factors listed in Equation (4-15):

$$F = f (A * c * v^2) \quad (4\text{-}15)$$

with:

F	flow force (N)
A	oscillator area (m²)
c	mass concentration (kg/m³)
v	mass flow velocity (m/s)

Where F is the flow force, c represents the mass concentration, A denotes the Area of the oscillator, and v stands for the mass flow velocity.

The calculated force is a value that can change during the drilling process. The area of the oscillator can be assumed to be constant. In practice an oscillator with a certain dimension is chosen. This remains unchanged. However, the speed and concentration can change during the drilling process. Provided that the volume of compressed air, which exits the drill head to transport cuttings upwards, remains unchanged, the parameters speed and concentration of the cuttings depend on the drilling speed. At a low drilling speed, less cuttings are produced. The concentration of the cuttings in the annulus between the drill pipe and the borehole wall decreases. At the same time the velocity of the cuttings increases because the mass to be transported decreases per time unit. On the other hand, a high drilling speed leads to an increase in the concentration of the cuttings and to a decrease in the velocity of the mass flow. Based on this fact, the software to be developed must also consider the machine data. The online analysis of the cuttings will only be possible if the drilling speed is continuously recorded as an additional parameter. The acoustic signals must be normalized based on the speed before they are processed further.

4.5 Basics of data acquisition and data processing

This chapter explains the basic concepts on which this thesis is based. Data acquisition and analysis, dimensional reduction of data, and data classification are topics that are covered in the following sections.

4.5.1 Data acquisition and analysis

The word Sensor comes from the Latin word Sensorium. This word originates from the Latin word Sensus which means sense. In a technical sense, a sensor can be described as an entity which converts chemical or physical entities and their alterations into an electrical signal and their alterations [38]. These electrical entities and their alterations are then sent to other computational units for further calculations.

When choosing a sensor, it is important to consider the way and the amount of energy the sensor needs. If the sensor cannot acquire the necessary energy for operation from the environment, an auxiliary power source is necessary. An example of a sensor needing external power is a potentiometer, and an example of a sensor not needing external power would be a thermometer. Additionally, every sensor can operate over

a pre-specified range, where this measuring range represents the range of the ingoing signals, which can be mapped on to the outgoing signals [38]. Depending on the application this range needs to be considered carefully so the sensor is not damaged permanently due to a narrow operation range. The next aspect which needs to be considered is the resolution of the sensor. This quantity is a measure of the accuracy of a sensor, meaning it represents the minimum detectable signal fluctuation of the signal from the sensor. Another crucial factor characterizing a sensor is its linearity. The sensor linearity is the range in which the correlation between ingoing signal and outgoing signal is linear. In most cases this range is comparatively small compared to the whole range of measurement of the sensor. Examples of an ideal and a real sensor linearity can be seen in Graph 4.2.

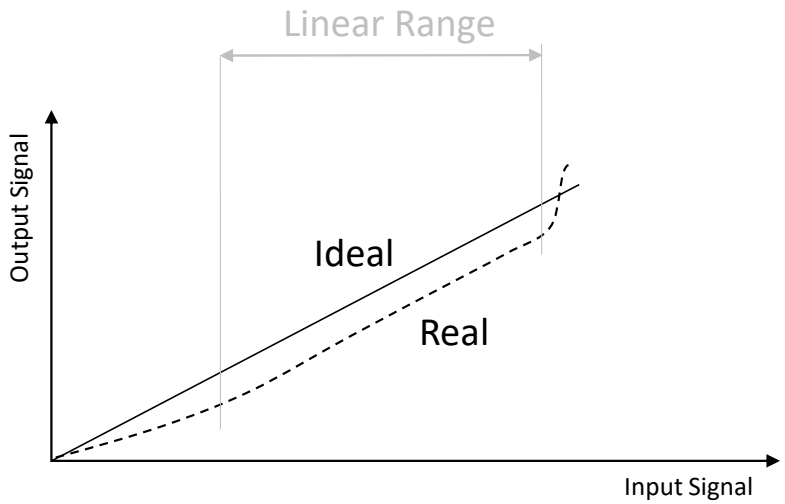

Graph 4.2: Illustration of an ideal and a real sensor [38]

Simple sensors, integrated sensors and intelligent sensors are typical categories in which sensors are classified into. These can be seen in Figure 4.1.

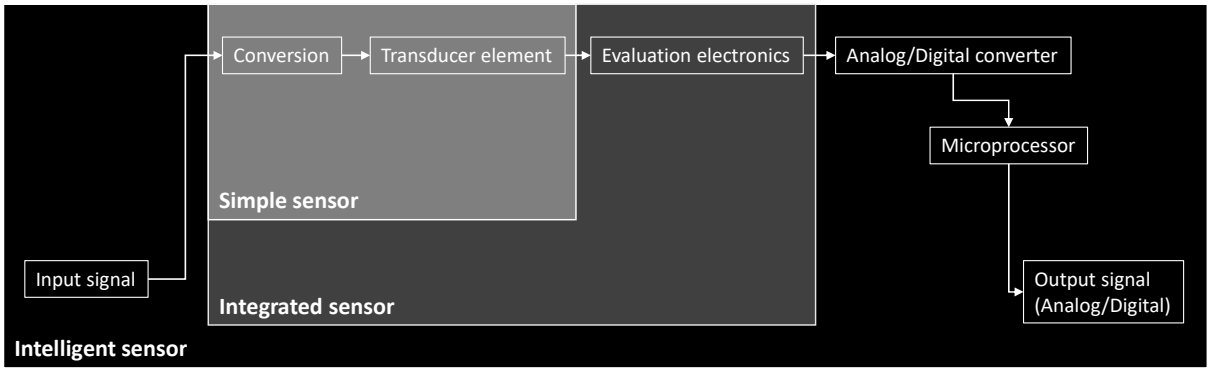

Figure 4.1: Schematic overview of the different integration level of sensors [38]

As the name of the simple sensor suggests, this is the most basic setup for a sensor. This type of sensor can convert the process variable into a transitional variable where a direct relationship between the two exist. Secondly, the simple sensor type can convert the measured entity into a proportional electrical unit such as voltage, current or resistance [39, 30]. The integrated sensor extends the capabilities of the simple sensor with capabilities such as having noise filtering or being able to compensate the zero-point fluctuations. Additionally, this type of sensor can linearize the incoming signal and standardize the outgoing signal [30, 39]. Intelligent sensors are the most capable type of sensors whose capabilities go even beyond those of the integrated sensors. In addition to data acquisition capabilities, they possess an analogue to digital converter with a subsequent data processing unit, the microprocessor. The microprocessor allows not only the monitoring and logging of the measurement data, but also can transmit an alarm condition. This occurs when a critical threshold is reached, so the system can be put in an emergency state or shut down. The sensor can also transmit multiple outgoing signals at once and the transfer features of the sensor if necessary. In addition to these capabilities, some other prerequisites are also needed if the intelligent sensor is in an autonomous multi-sensor system. These prerequisites are compensation, information processing, communications and integration and can be read in detail in [30].

If one assumes that the measured physical property by a sensor is E, the position in space to which the measured physical property refers to is r, the time instant at which the physical property was measured is t, the value of the measured physical property is y, and the uncertainty of the measurement due to errors is Δy, the sensor observation can be expressed according to Equation (4-16):

$$\text{Observation} = f(E, r, t, y, \Delta y) \tag{4-16}$$

If the data of the sensor are to be used in a multi-sensor system, which in most modern industrial applications is the case, the timing needs to be considered. Any possible communication and computational schedule can be used with the different interfaces for information communication [40]. In distributed systems, scheduling can be either time triggered, where the scheduling of all communication and processing activities are initiated at pre-determined time intervals, or event triggered, where communication and processing activities are initiated with the occurrence of a significant state change [30].

4.5.2 Data dimensionality reduction

With the prediction that by the year 2020, about 1.7 megabytes (MB) of new information will be created every second for every human being on the planet, it is obvious that novel methods for data acquisition, storage and manipulation need to be used [41]. With such large amounts of data being produced by modern hardware, a group of algorithms called dimensionality reduction have become popular. Dimension reduction is a collection of statistical methods that reduces the dimension of data while preserving relevant information, where dimensions are the number of different data types which exist. The so-called curse of dimensionality states that even with a large number of observations, high dimensional spaces are naturally sparse. Therefore, it is useful to reduce the data dimensions in a way, by which only the relevant information is left for further processing. How and by which degree data is reduced, depends on the dimension reduction technique used. These techniques transform the set of variables to a smaller set of either the original or new variables, the new variables being linear combinations or even nonlinear functions of the original variables [41]. If the number of dimensions of the new data set is relatively small (usually up to about 3), data visualization becomes possible, often making data modeling much easier. Dealing with high dimensionality can be difficult for machine learning algorithms. High dimensionality increases the complexity of the calculation and increases the risk of overfitting. Some of the techniques commonly used for dimensionality reduction of data are shown in Table 4.2.

Table 4.2: Some of the commonly used techniques for dimensionality reduction of data [42, 43, 44, 45, 46, 47]

Dimensionally Reduction Technique	
Principle Component Analysis (PCA) A chose linear transformation so the projected components achieve maximum variance.	**Factor Analysis (FA)** Similar to PCA but it uses a factor loading matrix
Linear Discriminant Analysis (LDA) A chosen linear transformation so that the projected components for each class are maximally separated from the projected components of the other class	**Independent Component Analysis (ICA)** A chosen linear transformation for maximized independence of projected projects.
Canonical Correlation Analysis (CCA) N linear transformations are chosen for N classes, so that the projected components of each class correlate maximally.	**Non-negative Matrix Factorization (NMF)** A method which finds only factors with non-negative elements.

Every dimensionality reduction method has its advantages and disadvantages [44]. Due to the popularity of PCA and FA only these two will be explained.

Let V_{val} be a vector expressed in Equation (4-17) with the values:

$$V_{val} = (v_1, v_2 , \dots , v_n) \tag{4-17}$$

A quite simple unobserved variable model, also known as a latent model, for each element of V_{val} can be written according to Equation (4-18):

$$v_i = Wh_i + \mu_{of} + \epsilon \tag{4-18}$$

Where h_i is an arbitrary vector, μ_{of} is an arbitrary offset, and ϵ represents the noise which can be modelled as a Gaussian normal distribution with mean 0 and covariance ψ. If h_i is given, then for determining elements of M, the following implies the following probabilistic interpretation can be made, see Equation (4-19):

$$p(v_i|h_i) = N(Wh_i + \mu + \epsilon,\psi) \tag{4-19}$$

However, for a complete probabilistic model a prior latent distribution for h_i is necessary. The simplest assumption of h $N(0,I)$ leads to Equation (4-20):

$$p(v_i) = N (\mu , WW^T + \psi) \tag{4-20}$$

If additional assumptions are made for the structure of the error covariance ψ, the probabilistic models of PCA and FA are achieved. For a probability-based PCA the error covariance can be expressed according to Equation (4-21):

$$\psi = \sigma^2 I \tag{4-21}$$

Whereas for FA the error covariance is expressed by Equation (4-22):

$$\psi = \text{diag} (\psi_1,\psi_2,\dots,\psi_n) \tag{4-22}$$

4.6 Data classification and regression

For being able to differentiate between gypsum and anhydrite, Methods for data classification can be used. Nowadays, classification methods are perhaps some of the most used techniques around the world. Many modern applications have integrated statistical classification methods. Famous Identification applications such as Google Lens or PlantSnap, which can be found on the Google Play Store or Apple's App Store, are based on statistical classification methods. Although most of these applications are based on complex neural networks, other techniques such as Ensemble classifiers,

Support Vector Machines for classification or Naive Bayes Classifiers are also powerful methods which have been used in many industrial applications. Although in most cases complex classification algorithms perform better than more simple ones, it is important to note that the degree of human understanding also depends on the model, which is used. It is possible for an engineer to understand the whole classification processes of a linear logistic classifier, however for the same person it is as simple or perhaps not possible at all to understand and identify problems which occur in a multi-layer neuronal network which is being used for classification. For the classification in this work the Random Forests and PCA based methods are used.

4.6.1 Statistical data analysis

In statistical data processing, data analysis by histogram and probability plot is often used. The shape of the distribution curve gives information about the general distribution of the data, especially the identification of frequencies within the data range. A distinction is made between symmetrical normal distributions or left-skewed or right-skewed forms. Rarely can the populations of the data groups be determined from a histogram. Particularly, if the data consists of different groups that are close to each other and overlap, a histogram does not provide a way to determine the populations.

In such cases, statistical data analysis by probability plot is used to determine the populations in data sets. This method is especially useful for the analysis of data sets that are suspected to consist of different populations or even subpopulations. This method is used for example in data analysis in geochemistry and mineral exploration [48, 49].

4.6.2 Principal component regression

As the name suggest, Principal Component Regression (PCR) is based on PCA, which has been discussed in the dimensionality reduction section before. PCR is usually used when a dataset contains many features and some of them strongly correlate. Per definition, principal components, latent variables or factors are defined as not directly measurable, implicit, orthogonal variables. Through the use of these principle components complex information can be condensed to only a few orthogonal pieces of information, and used for further analysis

As the classification between different substances with different densities and the determination of the ore grade is the aim of this work, three matrices can be defined. For the first matrix called X of size z * n, each row represents a single sample, and each column represents a pre-calculated feature for the given sample. This data can still be refined through a dimensionality reduction algorithm. In this case PCA is used, although LDA, FA and other dimensionality reduction algorithms were also possible. The resulting matrix after the k component PCA transformation of matrix X was called matrix P. The third matrix, which the algorithm should be able to calculate from the input data in the future, is the result matrix Y. The result matrix Y has a size z * m where each row represents a single sample, and each column represents a quality characteristic of the given sample. A schematic overview of the process is shown in Figure 4.2.

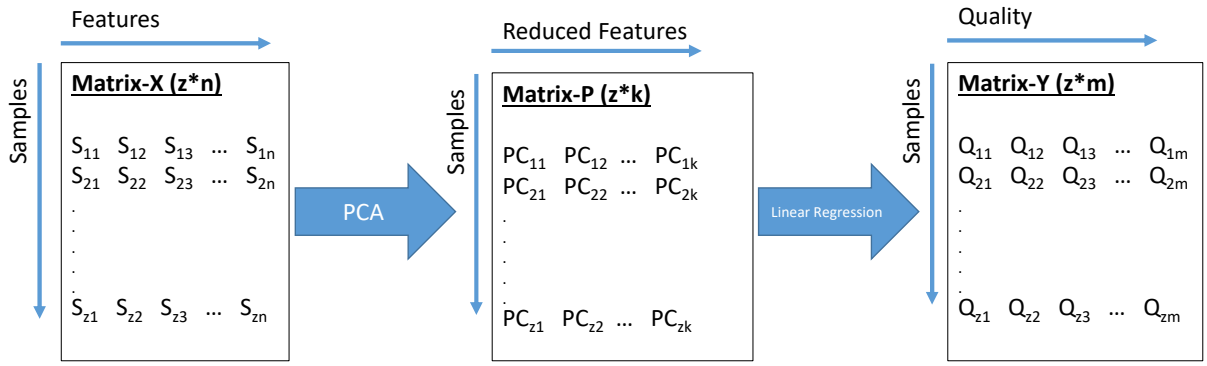

Figure 4.2: Schematic overview of the data classification method PCR

4.6.3 Random forest classifier and regressor

The concept of the random forest model was initially introduced by Breiman in 2001 [50]. The first implementation of this method was done by him personally in FORTRAN. As from the name of the algorithm can be derived, random forests are a pool of decision trees established on random algorithms. Each tree in the algorithm is a Classification and Regression Decision Tree also known as CART. For a random forest model, the user initially adjusts multiple parameters, such as the number of trees, and thereafter a diverse set of trees is built through randomness in the creation process. The random forest classifier and the random forest regressor both are categorized as ensemble methods due to their nature of a collection of decision trees. When a prediction is made with a pre-trained random forest model, each individual tree predicts the results. Later, a majority voting for classification or an averaging for regression tasks is done and the result is presented to the user [50]. Random forest methods have gained a lot of

popularity due to their good predictions out of the box, meaning that even without initial parameter cross validation they can deliver plausible results [44].

4.6.4 Neural network

In computer science community's discussions about neural networks have started as early as the 1950s. As the training of neural networks required high computational power, it was not until the 1980s where it become useful and popular for many applications [51]. Advantages of neural networks are, that they can perform many tasks depending on their structure and implementation. Famous models such as the VGG16, VGG19, ResNet, Inception, and Xception all perform feature extraction and classification, and can achieve very high accuracy for object identification in images

As the name of the model indicates, a neural network is a network of neurons. Neural networks usually consist of three different types of layers, where each layer contains a predefined number of neurons. The first layer in the neural network is the input layer, the second to the second last layer are the so-called hidden layers, and the last layer is called the output layer. Each neuron is a mathematical unit which performs certain mathematical operations on differently weighted incoming data from the previous node and passes it to the next node. The exceptions here are the input layer and output layer, which respectively do not have layers before or after them. The most used node today is the Rectified Linear Unit (ReLU) [52]. The mathematical function of a neuron is called the activation function. Before ReLU became a popular choice, the sigmoid function and the tanh function where mostly used. Additionally, many more activation functions exist which can be found in machine learning libraries such as PyTorch, Theano and Tensorflow [53].

Neural networks are mostly associated with the term deep learning. Deep learning is the ability of a model to learn representations from data that puts an emphasis on learning successive layers of increasingly meaningful representations [51]. Modern deep learning models have tens or sometimes even hundreds of successive layers of representations, such as the VGG16 with sixteen layers or the VGG19 model with 19 layers. These representations, which all depend on the weights and biases of the connections between the neurons, are all learned automatically from training data [51].

Figure 4.3 shows a simple setup of a dense or fully connected neural network. The input of the model is the Matrix X, and the output of the model is the matrix Y. in such

a network all nodes are connected to each other, and each connection possess a weight matrix Wand a bias vector b, which are optimized through an optimizer such as the Adam Optimizer. The goal of the optimization or training step is to minimize a predefined loss function. This loss statement is mostly the sum of all elements of the mean squared error result vector, as can be seen below [44].

$$\text{loss} = \sum_{n=1}^{N} \left(y_{real_j} - y_{model_j} \right)^2 \tag{4-23}$$

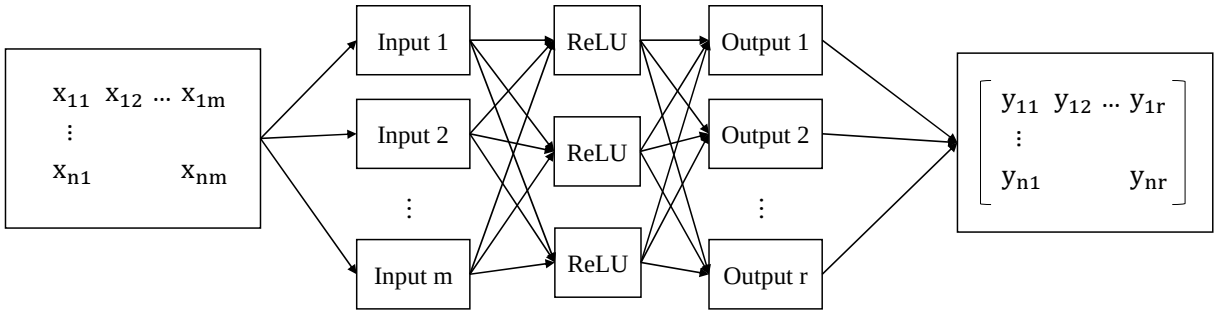

Figure 4.3: Simple dense neural network schematic with a 3-node ReLU hidden layer, an output layer with r output neurons, and an input layer with m input neurons

If a set of data is continually being generated in fixed periods of time, the data is called a time-series data. Time-series data can be found in many different applications such as stock market or weather trend predictions, as well as the online characterization of gypsum and anhydrite. For these types of data, instead of the fully connected neural networks with ReLU nodes, recurrent cells such as the Long-Term Short-Term Memory (LSTM) neurons are used. The different between these types of computational units and simple neurons such as ReLU is that the output of the recurrent cell is fed back into itself multiple times [53].

5 Design of the laboratory analyser

The laboratory equipment must be designed in such a way that the research hypothesis can be validated. For this purpose, it is necessary to investigate the influence of the defined four groups of technical parameters on the acoustic signal properties. As already explained, these groups result from the material-dependent properties, from the properties of the mass flow and from the properties of the oscillator and the sensor.

Overall, the laboratory analyser is intended to simulate as far as possible the process of cuttings flow during the drilling of blast holes in the mine. If the research hypothesis is confirmed in the laboratory, in the final stage of the development the cuttings, which are produced during the drilling, should collide continuously as mass flow with an oscillator. The impulses generated during the collision are registered by an acoustic sensor. The simulation of the continuous mass flow of the drill cuttings and their collision with the oscillator requires a test device with a disperser. If samples are continuously dispersed dry and collide with an oscillator, the prerequisite for the simulation is given. For the detection of different influencing parameters, the laboratory device should have the necessary possibility to vary parameters. Based on the described requirements, the laboratory device shown in Figure 5.1 was designed. The laboratory device is assembled as follows.

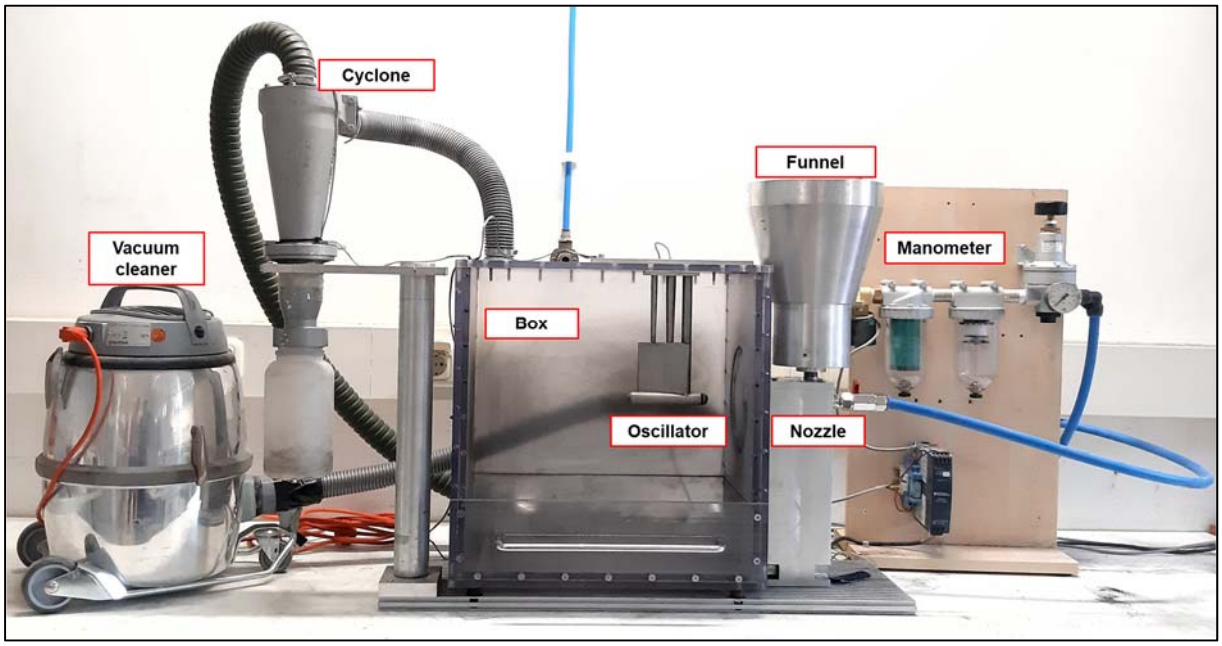

Figure 5.1: Setup of the laboratory analyser

It consists of a funnel for receiving the samples. The inner part of the nozzle is made of ceramic for wear protection. The nozzle allows the flow of grain sizes up to 2.5 mm diameter. The nozzle has three connections. The rear opening is for connection to the compressed air line. The upper connection is connected to the funnel. Here the sample flows into the nozzle. The front port is for the material flow after dispersion. The dispersed sample flows out of the front opening. The nozzle is connected to the box into which the dispersed sample flows. The box contains the oscillator. The position of the oscillator is designed so that the flow of the dispersed sample hits it directly. a sensor is integrated in the oscillator. The box has a drawer to remove the sedimented material after dispersion. A drainpipe is installed above the box. This pipe is connected to a cyclone, which in turn is connected to a vacuum cleaner. The cyclone is used to clean the fine dust before the air enters the vacuum cleaner. The main parameters of dispersion, the speed of the material after acceleration, the flow rate and finally the suction power of the nozzle will be controlled by adjusting the inlet pressure. For this purpose, a finely adjustable manometer is installed between the compressed air line and the nozzle.

For each test, the material is placed in the funnel-shaped container. When the vacuum cleaner is switched on, the nozzle inlet pressure valve is opened. The pressure is always set before the start of the test. The sample is drawn into the nozzle by vacuum and dispersed into the box. The oscillator is located about 20 cm from the exit point of the nozzle. The sample collides with the oscillator during the entire dispersion time. The impulses are picked up by a sensor and transmitted and processed by the electrical unit. The following sections describe the main components of the laboratory analyser and discuss their characteristics. The selection of the components was partly based on dimensioning.

5.1 The accelerometer

The first step in the data acquisition and processing tool chain is the accelerometer. As the name suggests an accelerometer is a tool that measures the rate of change of velocity of a body in its own instantaneous rest frame and not the absolute or coordinate acceleration [54]. Accelerometers find use in a wide range of application such as in the inertial navigation systems for aircraft, almost all modern phones and tablets, and in drones for flight stabilization. In addition to these cases where the

accelerometer is used for orientation measurements, accelerometers can be used for machine health monitoring such as for rotating machines.

Throughout the course of this thesis, an Integrated Electronics Piezoelectric (IEPE) accelerometer is used. The word piezoelectric finds its roots in the Greek word piezein, which means to squeeze or press. An accelerometer that makes use of the piezo-electric effect of certain materials to measure dynamic changes in acceleration is called a piezoelectric accelerometer. As with all transducers, piezoelectric accelerometers convert the mechanical energy they experience into electrical energy and thus provide an electrical signal in response to the acceleration being measured [55].

Using the general sensing method upon which all accelerometers are based, acceleration acts upon a seismic mass that is restrained by a spring or suspended on a cantilever beam and converts a physical force into an electrical signal. A preload ring or stud applies a force to the sensing element assembly to make a rigid structure and insure linear behavior. Under acceleration, the seismic mass causes stress on the sensing crystals which results in a proportional electrical output. The output is collected on electrodes and transmitted by wires connected to the microelectronic circuitry in IEPE accelerometers [56]. This electrical output then can be used for further data analysis. A general setup of a piezoelectric accelerometer can be seen in Figure 5.2.

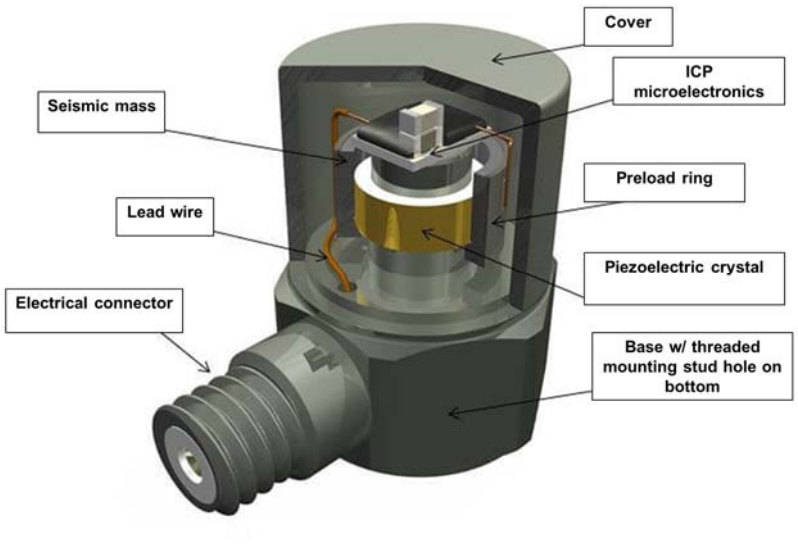

Figure 5.2: Basic diagram of a piezoelectric accelerometer [56]

5.2 The analog/digital converter

After the analog signal has been created by the accelerometer, it needs to be converted to a digital signal for further data processing through a computer. The

electronics unit which converts the analog electric signal to a digital electric signal is called an A/D Converter or ADC. In more precise terms, an ADC converts a continuous-time and continuous-amplitude signal to a discrete-time and discrete-amplitude signal. As this conversion involves quantization of the input signal it automatically introduces a small amount of error or noise. Furthermore, this process is done periodically instead of continuously. In each period the ADC samples the input and limits the allowable bandwidth of the input signal.

The performance of an ADC can be characterized by the two factors. The first factor which can be mentioned is the sampling rate. In signal processing, the sampling rate is the rate at which the reduction of a continuous-time signal to a discrete-time signal is done. The second factor is the Signal-to-Noise Ratio (SNR). This characteristic by itself is influenced by many factors, including the resolution, linearity, accuracy, aliasing and jitter. The SNR of an ADC is often summarized in terms of its effective number of bits (ENOB), the number of bits of each measure it returns that are on average not noise. An ideal ADC has an ENOB equal to its resolution. According to the Nyquist-Shannon sampling theorem, the required sampling rate for a sensor can be estimated before the application in the design phase of a system and needs to be at least twice the bandwidth of the signal to be measured. The functional block diagram of a modern ADC from Analog Devices can be seen in Figure 5.3.

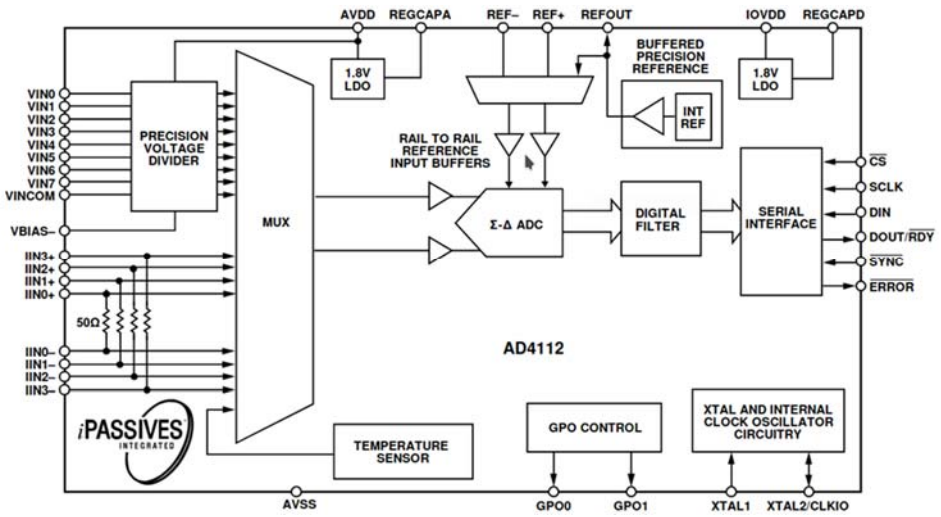

Figure 5.3: Functional block diagram of the AD4112 ADC from analog devices [57]

5.3 Venturi nozzle

The laboratory analyser described in chapter 5 was designed to simulate the mass flow during the drilling process. This device should contain a nozzle for the dispersion of

the samples. For this purpose, a nozzle working according to the Venturi principle was selected. The design of the nozzle is shown schematically in Figure 5.4.

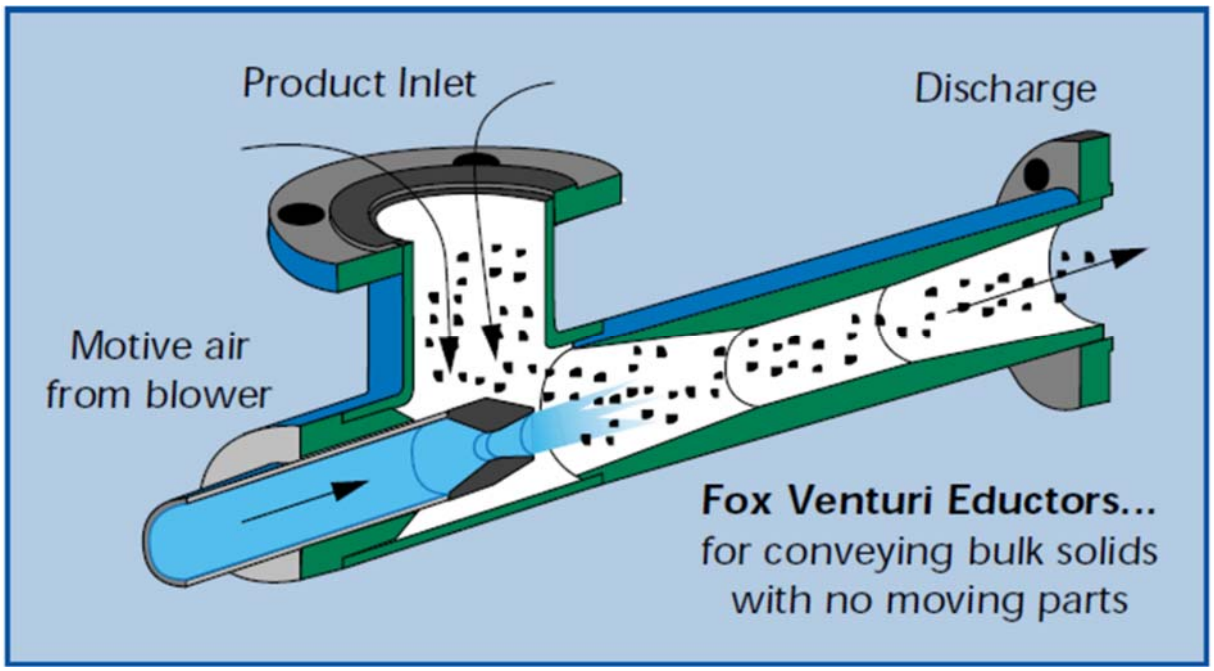

Figure 5.4: Schematic overview of the structure of a Venturi nozzle [58]

The physical processes in a Venturi nozzle are based on continuity equations for stationary flows. According to the principle of mass constancy, the mass flowing through a pipe remains constant. The mass flow entering a pipe is equal to the mass flow leaving the pipe. This property is described by the principle of mass conservation. If a mass flow m_1 with a velocity v_1 and the density ρ_1 flows into a pipe with the cross-section A_1 and a mass flow m_2 with a velocity v_2 and the density ρ_2 flows into a pipe with the cross-section A_2, the principle of mass conservation applies and is expressed by Equation (5-1):

$$A_1 \cdot v_1 \cdot \rho_1 = A_2 \cdot v_2 \cdot \rho_2 \qquad (5\text{-}1)$$

with:

A_1	entry cross section (m²)
v_1	entry velocity (m/s)
ρ_1	material density at the entry point (kg/m³)
A_2	outlet cross section (m²)

	v_2	outlet velocity (m/s)
	ρ_2	material density at the outlet point (kg/m³)

Where A_1 represents the entry cross section, A_2 represents the outlet cross section v_1 and v_2 respectively stand for the entry velocity and the outlet velocity, and ρ_1 and ρ_2 respectively denote the material density at the entry point and at the outlet section. For incompressible flows, the density "ρ" can be assumed as constant. It applies in Equation (5-2):

$$A_1 \cdot v_1 = A_2 \cdot v_2 \tag{5-2}$$

Provided that the fluid in the pipe flows without friction and no energy is supplied to or removed from it, the continuity equation can be extended by assuming the Bernoulli equation as follows, Equation (5-3):

$$\frac{v_1^2}{2} + g \cdot h_1 + \frac{p_1}{\rho} = \frac{v_2^2}{2} + g \cdot h_2 + \frac{p_2}{\rho} \tag{5-3}$$

with:	h_1	height of the entry point (m)
	p_1	pressure of the entry point (Pa)
	h_2	height of the discharge point (m)
	p_2	pressure of the outlet point (Pa)

Where A_1 represents the entry cross section, A_2 represents the outlet cross section v_1 and v_2 respectively stand for the entry velocity and the outlet velocity, and ρ_1 and ρ_2 respectively denote the material density at the entry point and at the outlet section. For incompressible flows, the density "ρ" can be assumed as constant. It applies:

Multiplying the equation with "ρ" leads to Equation (5-4):

$$\frac{v_1^2 \cdot \rho}{2} + \rho \cdot g \cdot h_1 + p_1 = \frac{v_2^2 \cdot \rho}{2} + \rho \cdot g \cdot h_2 + p_2 \tag{5-4}$$

Assuming a horizontal flow, the potential energy is not considered. This results in Equation (5-5):

$$\frac{v_1^2 \cdot \rho}{2} + p_1 = \frac{v_2^2 \cdot \rho}{2} + p_2 \qquad (5\text{-}5)$$

The following applies with reference to the preservation of mass expressed in Equation (5-6):

$$v_1 = \frac{A_2}{A_1} \cdot v_2 \qquad (5\text{-}6)$$

Where Δp is determined by Equation (5-7):

$$\Delta p = \frac{1}{2} \cdot v_2^2 \cdot \rho - \frac{1}{2} \cdot \left[\frac{A_2}{A_1} \cdot v_2\right]^2 \cdot \rho \qquad (5\text{-}7)$$

with: Δp suction pressure (Pa)

Where Equation (5-7) can be transformed to Equation (5-8) respectively (5-9):

$$\Delta p = \frac{1}{2} \cdot v_2^2 \cdot \rho \cdot \left[1 - \left(\frac{A_2}{A_1}\right)^2\right] \qquad (5\text{-}8)$$

where:

$$v_2 = \sqrt{\frac{2 \cdot \Delta p}{\rho \cdot \left[1 - \left(\frac{A_2}{A_1} \right)^2 \right]}} \tag{5-9}$$

Thus, the mass flow through the Venturi nozzle can be calculated by Equation (5-10) respectively (5-11):

$$\dot{m} = \rho \cdot A_2 \cdot v_2 \tag{5-10}$$

with: $\dot{m}$ mass flow (kg/s)

where:

$$\dot{m} = \rho \cdot A_2 \cdot \sqrt{\frac{2 \cdot \Delta p}{\rho \cdot \left[1 - \left(\frac{A_2}{A_1} \right)^2 \right]}} \tag{5-11}$$

The mass flow in a Venturi nozzle thus depends on the diameter of the nozzle at the inlet and at the outlet as well as the pressure difference and density of the fluid.

A series of tests were carried out to dimension the mass flow for the laboratory tests. For this purpose, the suction pressure Δp for different inlet pressures and different diameters of the compressed air supply line were carried out. In addition, the tests were carried out with two different pressure regulators in order to find an optimal combination of the devices for the laboratory tests.

Depending on the diameter of the compressed air pipe, the Venturi nozzle generated a differential pressure or suction pressure Δp of 140 to 280 mbar. The tests show that the influence of the diameter of the pipe depends on the choice of the compressed air regulator. The influence can be significantly reduced if the regulator is selected correctly. According to the results of the tests, the suction pressure increases linearly and relatively quickly with increasing inlet pressure up to a pressure of 1.5 bar. From a pressure of 1.5 bar, the suction pressure increases only insignificantly. With a pressure of 4 bar a suction pressure of 400 mbar could be reached. The results of the tests are shown in Graph 5.1 to Graph 5.3.

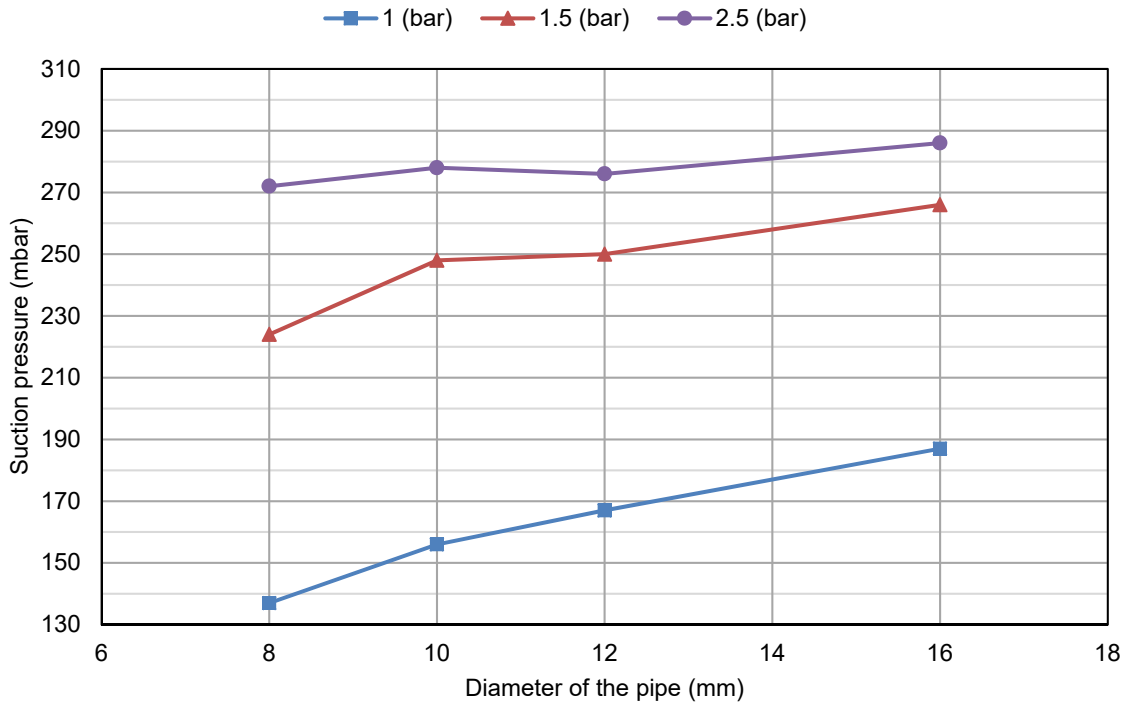

Graph 5.1: Influence of the air pressure and diameter of the air pipe on the suction pressure of the nozzle (pressure regulator type A)

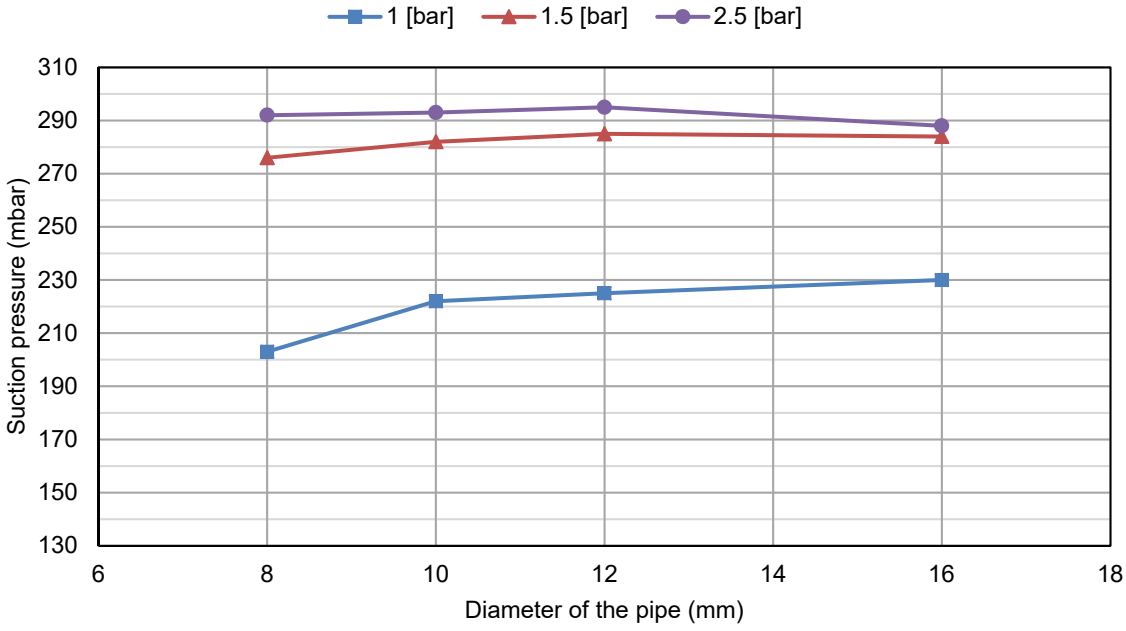

Graph 5.2: Influence of the air pressure and diameter of the air pipe on the suction pressure of the nozzle (pressure regulator type B)

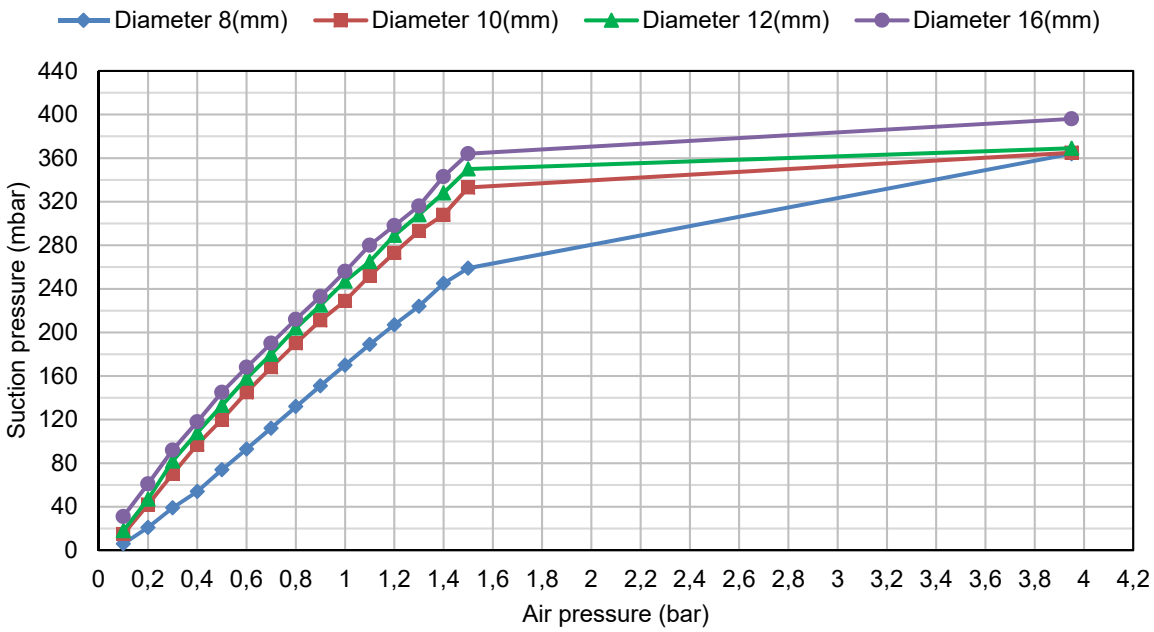

Graph 5.3: Relationship between the compressed air and the suction pressure for different pipe diameter

Another important requirement for the selection of the Venturi nozzle is a high wear resistance. The mineral samples can have Mohs hardness of up to 7. In combination with a high speed the samples are very abrasive. Therefore, a Venturi nozzle with a ceramic inner component was chosen for the laboratory analyser. In addition, a Venturi nozzle was chosen whose design and function resembles that of a spray gun. With the help of this component it is possible to pick up and accelerate large quantities of material with a very high suction force, even with small amounts of compressed air.

The selected Venturi nozzle consists of two parts. In the first part there is an injection nozzle. The accelerated air enters a chamber which has a much larger diameter than the injector nozzle. In this area a vacuum or suction pressure is created due to the Venturi effect. The chamber is open at this point. The sample is fed through this opening to the Venturi nozzle. The suction pressure draws the sample into the chamber. The second part of the nozzle is connected to this section. The relaxed air, which has a high velocity, mixes with the sample and enters a second Venturi nozzle. The mixture of air and sample is accelerated at the end of the second nozzle.

The following parameters of the Venturi nozzle are used to calculate the volume flow and mass flow. The dimensions of the nozzle and the dimensions of the relevant parts are shown in Figure 5.5 and Table 5.1.

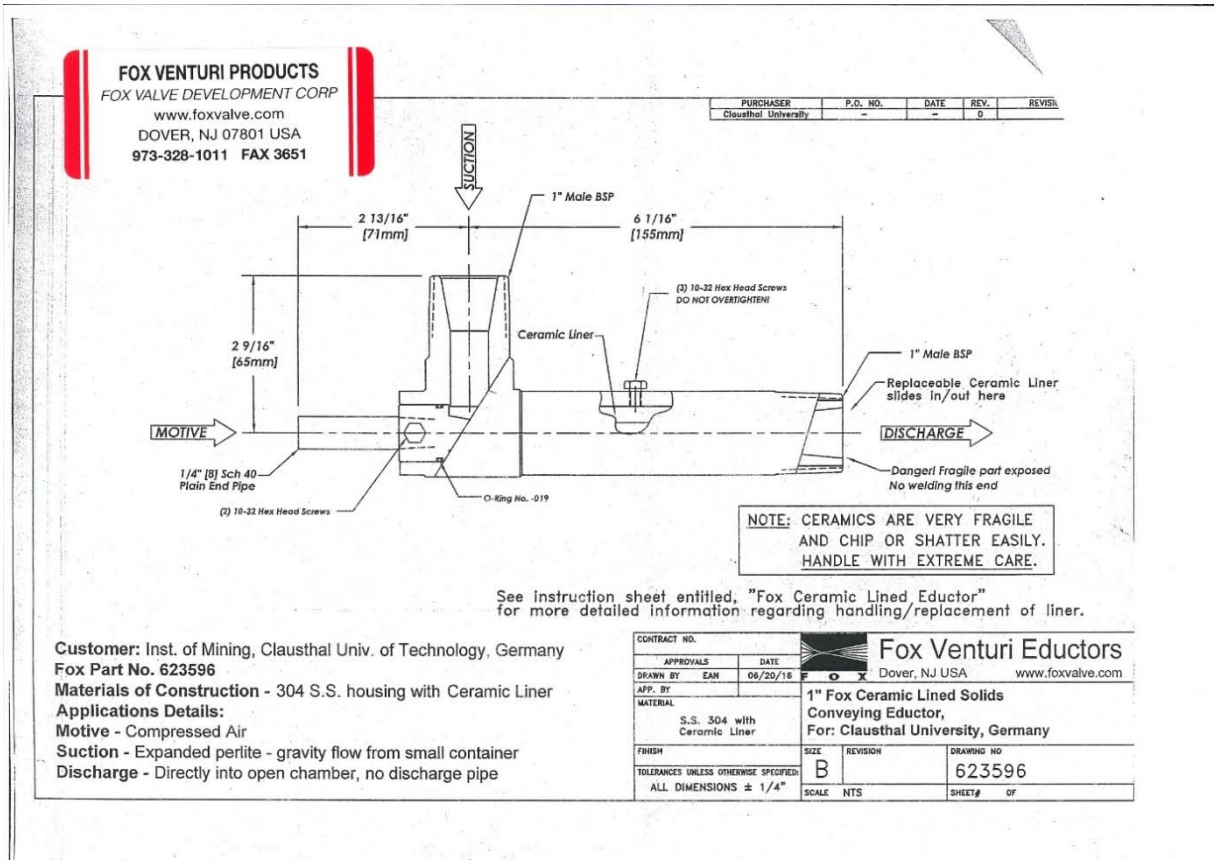

Figure 5.5: Information sheet about the used Venturi nozzle from Fox Venturi Educators [58]

Table 5.1: Dimension of the nozzle

Section	Diameter (cm)	Area (cm^2)
A: Motive	1.10	0.95
B: Suction	2.10	3.46
C: Venturi	0.88	0.61
D: Discharge	2.10	3.46

The negative pressure (vacuum) can be varied by the pressure of the air supplied to the nozzle, as explained above. Considering the dimensions of the respective cross-sections of the nozzle, the volume flow or mass flow can be calculated. If the air has a pressure of 0.7 bar, the nozzle generates a differential pressure of 186 mbar. The following calculations show that in this case the nozzle generates a mass flow of 18.86 g/s or a volume flow of 0.2281 m^3/s.

To determine the mass concentration during dispersion, the selected Venturi nozzle was connected to the laboratory analyser. Different differential pressures were generated by regulating the compressed air. After the differential pressure was adjusted, tests were carried out. During the tests, one kilogram of gypsum with a particle size of less than 250 µm was always fed to the nozzle and the time for

dispersion was measured. The nozzle needs between 53 and 69 seconds for 1 kg of gypsum depending on the pressure difference. Considering the above calculations, a pressure difference of 186 mbar results in a mass concentration of 82 g of sample per standard cubic meter of air. The results of the laboratory tests are shown in Graph 5.4.

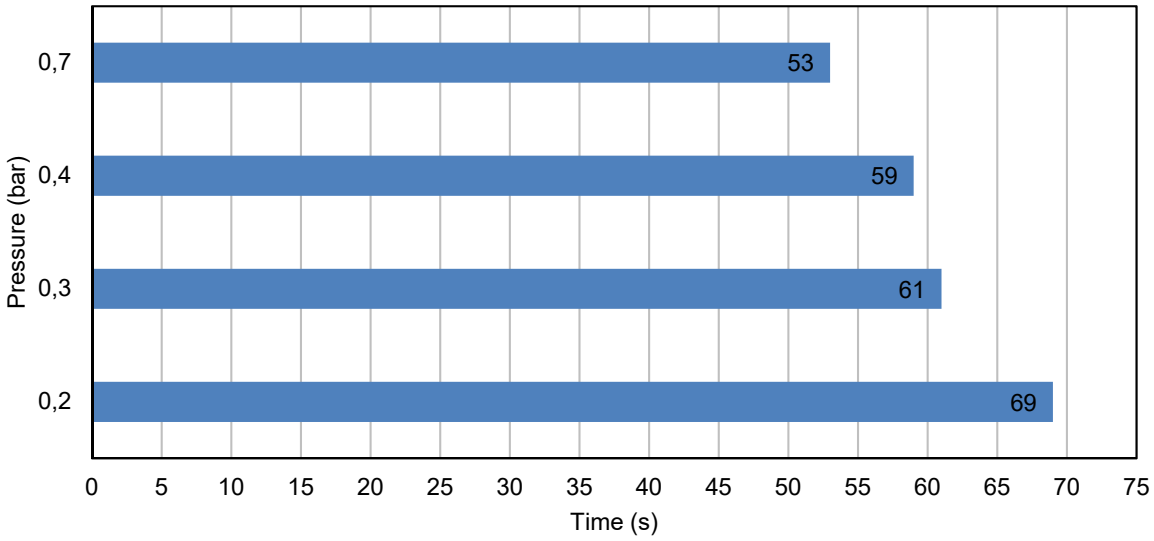

Graph 5.4: Results of the laboratory tests

5.4 Selection of the oscillator

Experience shows that the signal quality, especially the signal to noise ratio, depends on the shape of the oscillator and its composition. In order to select the optimal shape of the oscillator, laboratory tests were carried out in advance. Investigations for the development of an online particle size analyser have shown that the hemispherical oscillators provide good signal quality. To verify this, experiments were carried out with two different oscillators. In the first case a tungsten carbide pin was used as oscillator. This is mounted in such a way that the sample hits the pin along the longitudinal axis after dispersion. The sensor is attached to the cross-section of the pin. The flow direction or pulse direction and sensor axis form an angle of 90 degrees. It is assumed that the shock waves reflect several times before reaching the sensor. In the second case the sensor is located behind a hemispherical oscillator. The flow direction and the sensor axis are the same. Both versions are designed to be mounted on the top cover of the box. These variants are shown in Figure 5.6.

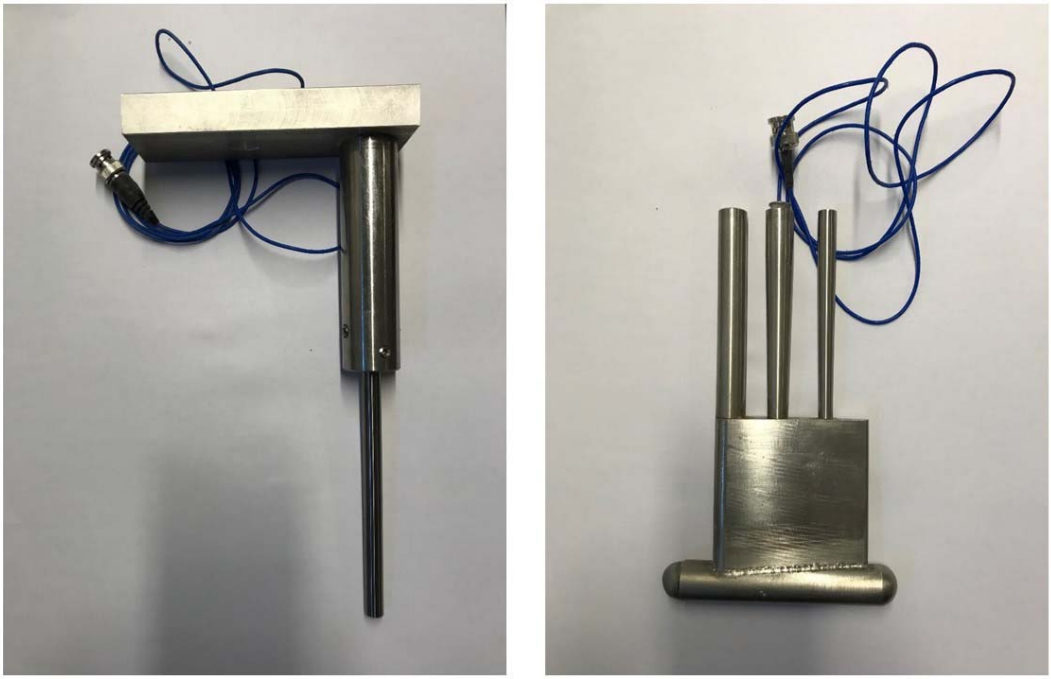

Figure 5.6: Structure of the oscillators pin (left) and semi-sphere (right)

The results of the tests are shown in Graph 5.5 to Graph 5.8 as an example of a test run with cuttings. The signals resulting from the collision between the cuttings and the elongated oscillator (pin) are relatively weak. The signals resulting from the collision between the cuttings and the spherical oscillator are higher by a factor of ten. The frequency analysis of the signals shows that the signals from the spherical oscillator are more energetic over the entire frequency spectrum. Furthermore, no resonance oscillation can be detected with this type. Additionally, it can be stated that signal to noise ratio of this type of oscillator is very high and simplifies the signal processing. The elongated oscillator shows an interference of the oscillation by resonance at 12 kHz and 20 kHz or 24 kHz. Based on the results of the investigation, a spherical oscillator should be chosen for the laboratory tests. The analysis of the signals generated by the collision of samples with such an oscillator allows a better differentiation of the samples depending on their density.

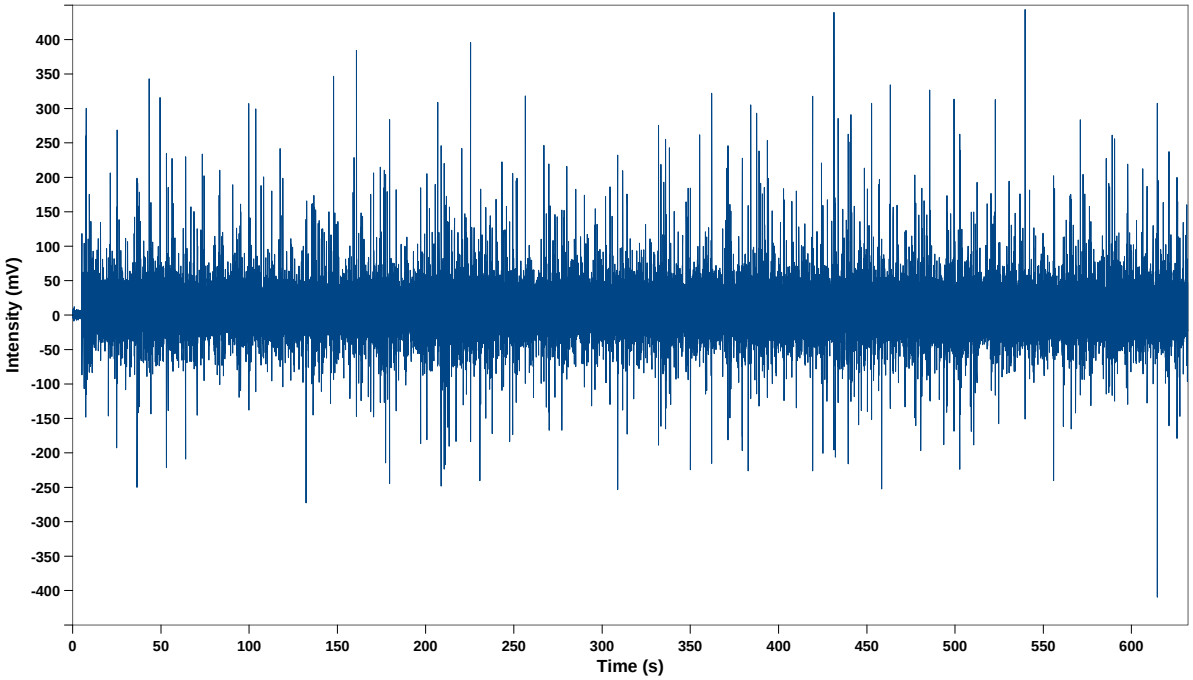

Graph 5.5: Raw signal for spherical oscillator

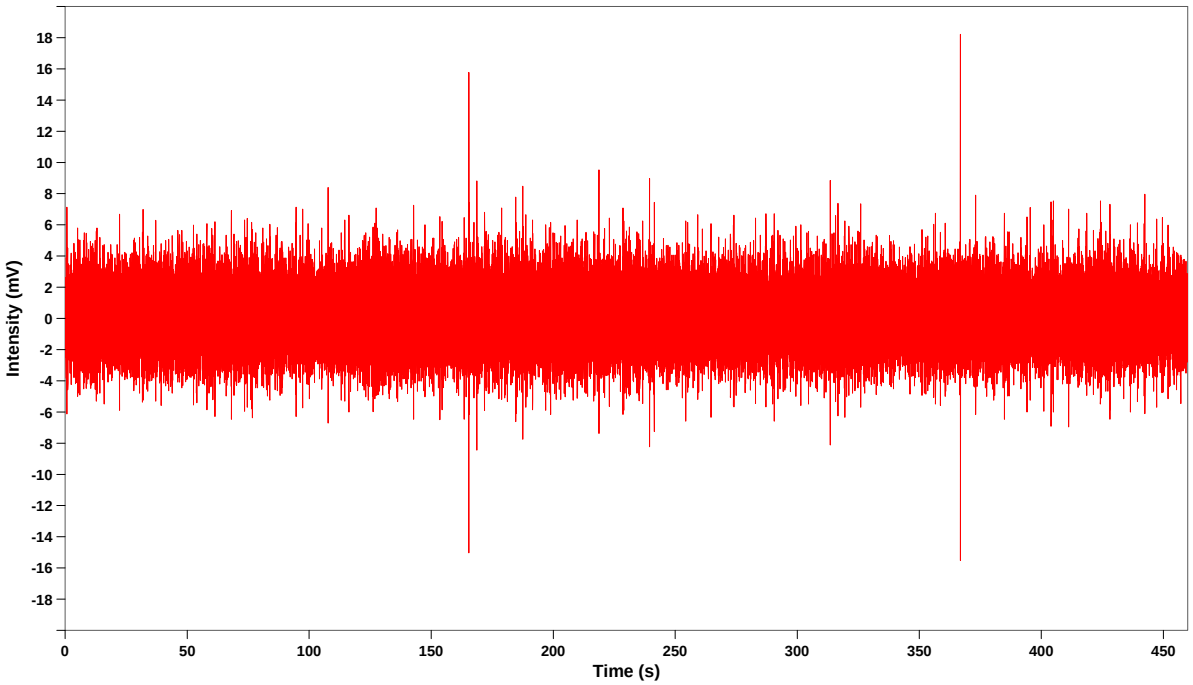

Graph 5.6: Raw signal path for pin-shaped oscillator

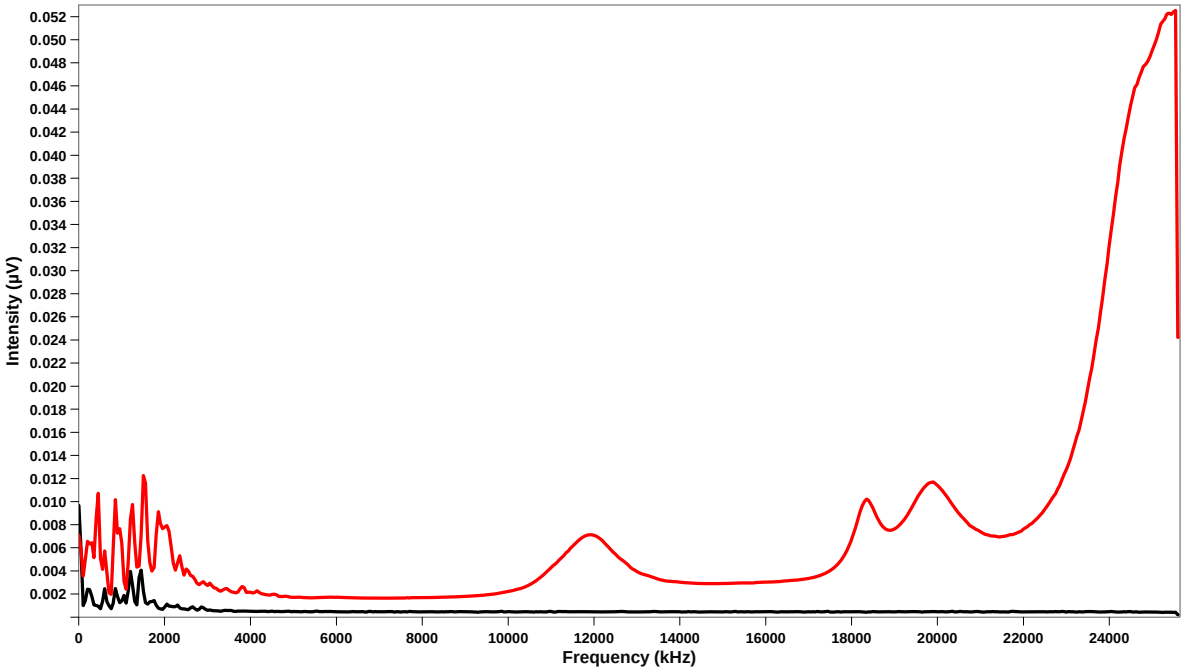

Graph 5.7: Spectral analysis of signals for pin-shaped oscillator

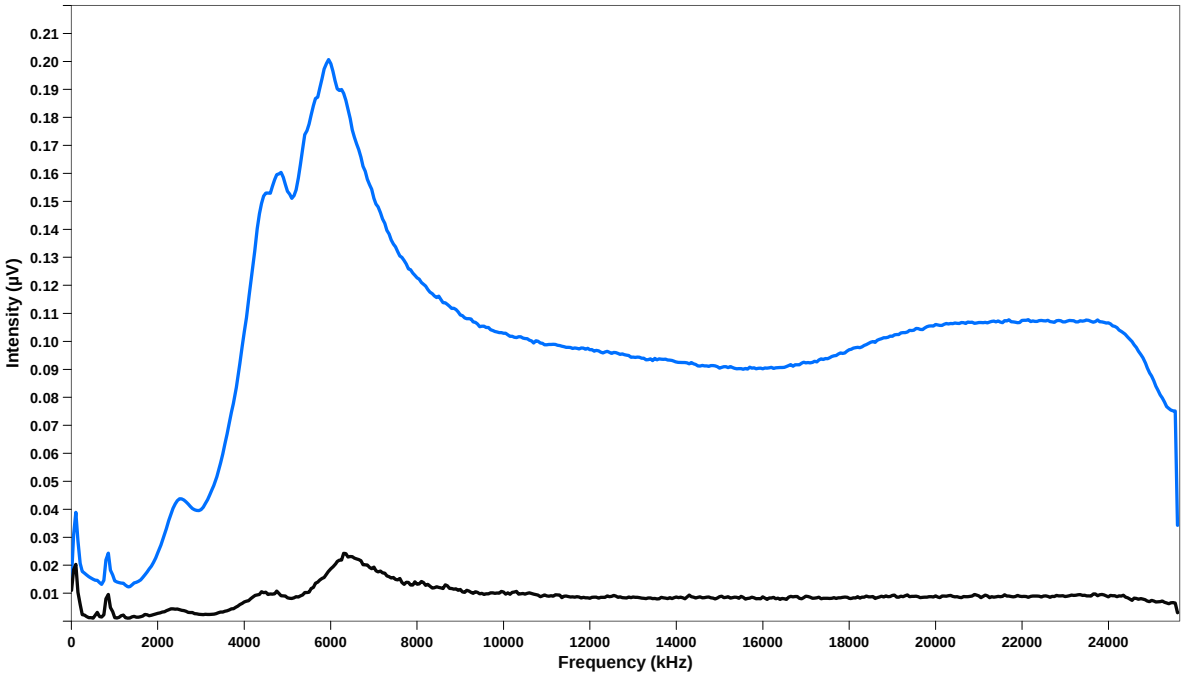

Graph 5.8: Spectral analysis of signals for spherical oscillator

5.5 Selection of the data classification algorithm

The signal processing is performed with the data from the accelerometer. During laboratory tests the flow parameters are kept constant. For the field tests, the machine data are added to the data of the accelerometer and processed.

After the acquired time series data is obtained, it is processed by frequency domain and time domain methods. Initially the raw signal is filtered using a band-pass filter.

This is necessary to be able to only select the frequencies where the sensor operates linearly as well as filtering out unnecessary signals and noise. Even after this step the acquired raw digital signals are usually very large in size and one is not able to efficiently use these data without high computing capabilities. Thus, time series data is usually divided into fixed periods of time, where for each period certain statistical characteristics are calculated which represents the data. Each one of these characteristics is called a feature. Many features based on time series data analysis based have been suggested.

In addition, a fast Fourier transformation (FFT) is performed on the selected signal periods and the results are used additionally. Furthermore, as mentioned above, additional data from the machine are combined with the properties of the acoustic data and used for further analysis and result prediction. Two algorithms are developed for the prediction of the ore grade. One algorithm based on multivariate data analysis PCR and one algorithm based on statistical probability.

6 Basic verification of the hypothesis

The developed laboratory analyser is used for all laboratory tests. Based on the objectives of the research, a basic validation of the hypothesis is first carried out. For this purpose, gypsum and anhydrite samples are examined. The samples were taken from pure gypsum and anhydrite. The samples were separated by pre-screening to a grain size of less than 180 µm. The samples were dispersed with the laboratory analyser by means of a Venturi nozzle as described above and collided with the oscillator. The waves created by the collision of the particles with the oscillator were recorded by the accelerometer. The raw signals generated from gypsum and anhydrite differed in intensity and frequency spectrum. At certain frequencies they showed up to 100 % differences in intensity. As was assumed in the hypothesis, the anhydrite grains generate a much stronger impulse than the gypsum grains when they collide with the oscillator. The difference in the signal intensity will be attributed to the fact that the cuttings, which consist of gypsum or anhydrite, give different pulse to the sensor due to the different density. The results of this analysis are shown in Graph 6.1.

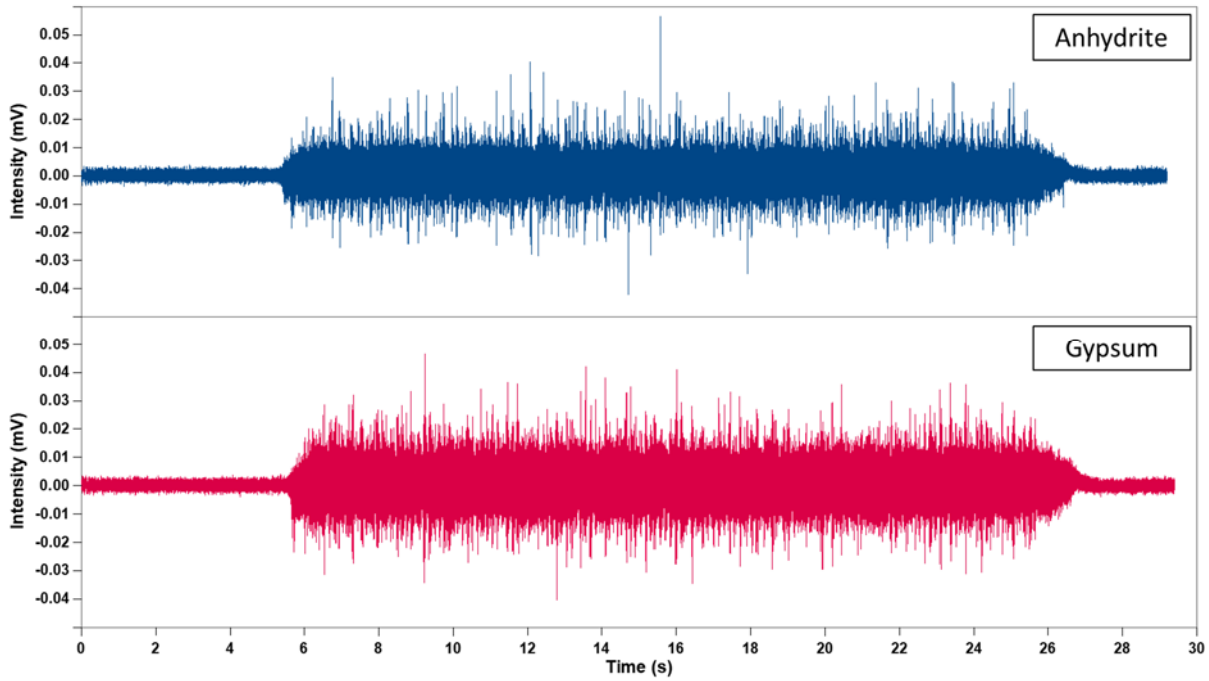

Graph 6.1: Signal intensity for gypsum and anhydrite (fraction 0 - 180 µm)

7 Determination of the influence of grain size

For the determination of the influence of the particle size, the samples were divided into five different grain classes. The grain classes were chosen very narrowly so that an almost uniform grain size was achieved. The range of grain sizes in one class is only 30 µm. The respective classes were then analysed up to 50 times. The frequency analysis of the raw signals shows that the signal intensity seems to be a function of the particle size. With constant particle size, the signals of the gypsum showed only half the intensity of the anhydrite signals. Conversely, it can be concluded from this that an online detection of the gypsum and anhydrite, is still possible even if they are not present in the same particle sizes. It should also be noted that the online detection of gypsum and anhydrite does not require the generation of very narrow particle size classes. For particle size classes 32 - 63 µm, 63 - 90 µm and 90 - 125 µm detection of gypsum and anhydrite is possible when using the frequencies starting from 10 kHz, see Graph 7.1 and Graph 7.2. Graph 7.3 documents the signal characteristics or gypsum and anhydrite as examples.

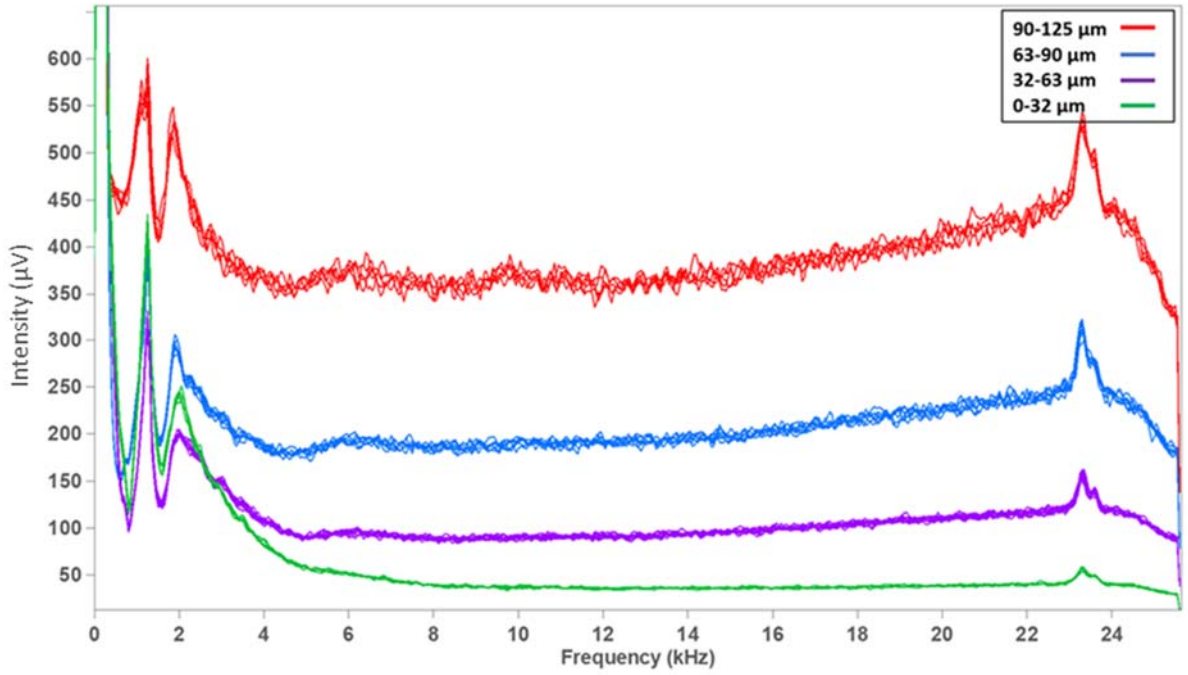

Graph 7.1: Frequency spectrum and signal intensity of anhydrite samples for different particle size classes

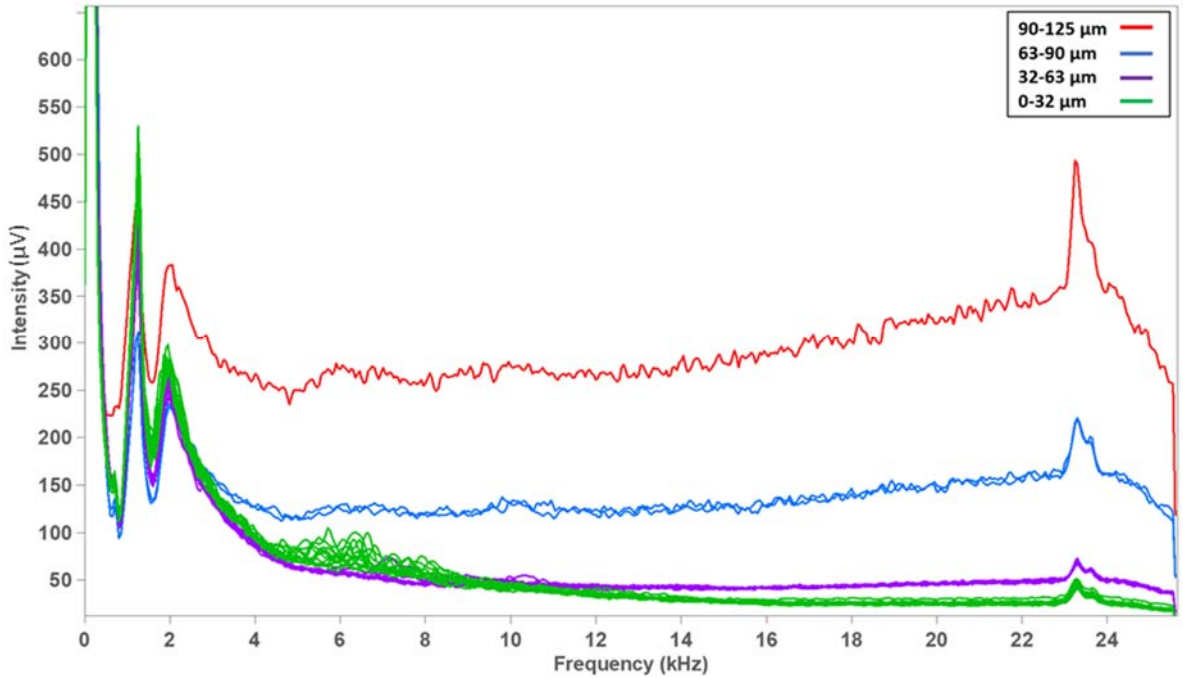

Graph 7.2: Frequency spectrum and signal intensity of the gypsum samples for different particle size classes

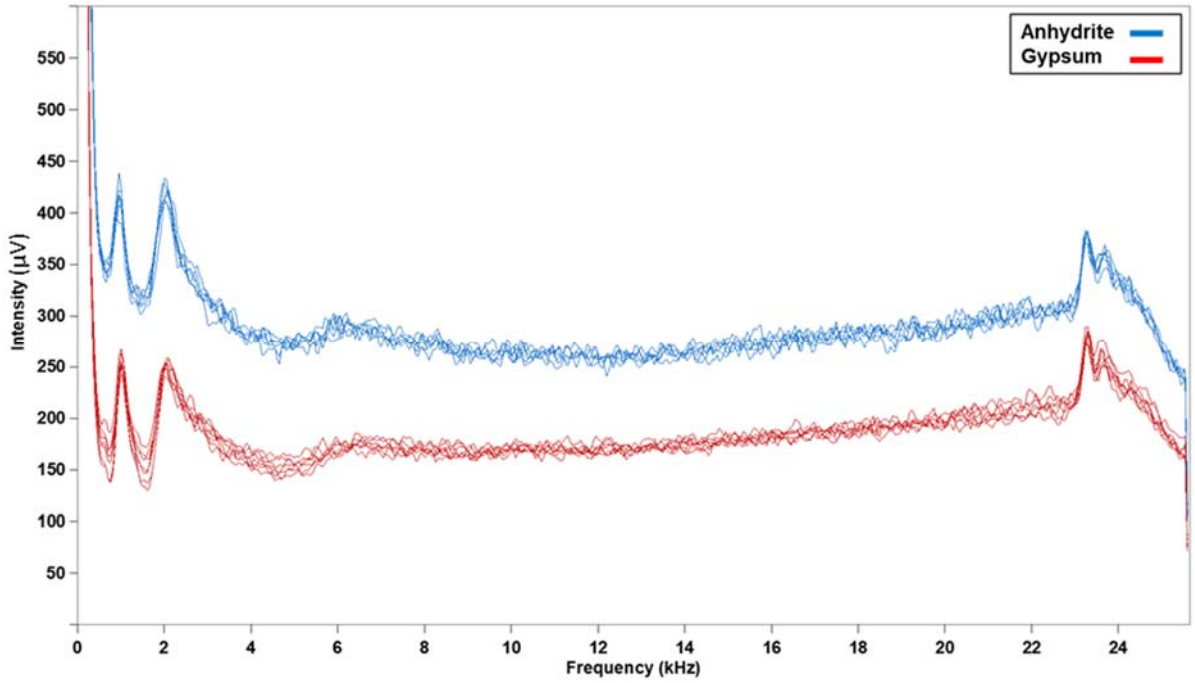

Graph 7.3: Frequency spectrum and signal intensity of the anhydrite and gypsum samples of the particle size class 63 - 90 µm

To determine the repeatability of the results, the samples were examined several times and the results were evaluated. The repeatability of the results could be proven for all particle size classes. A comparison of the signal intensities for gypsum and anhydrite as a function of the particle size class shows that the intensity of the signals generated by anhydrite are by a factor of 1.31 to 2.23 greater than the amplitude of the signals

generated by gypsum. Graph 7.4 shows the intensity ratio between anhydrite and gypsum.

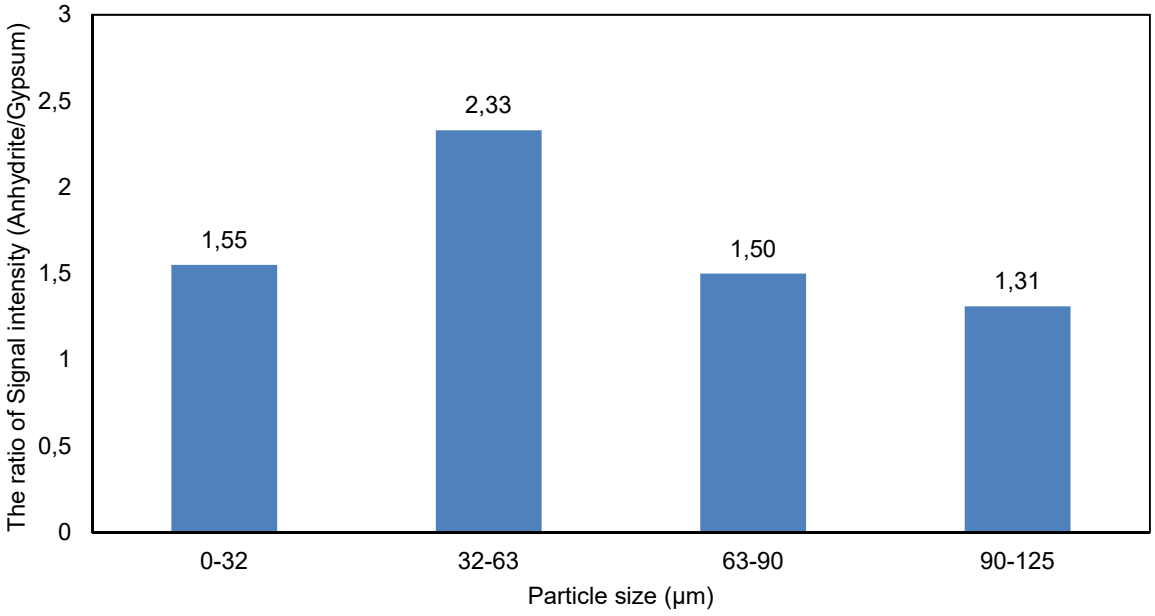

Graph 7.4: The ratio of signal intensity between anhydrite and gypsum for different particle sizes

8 Determination of the influence of particle size distribution

During the investigation step described above, very narrow particle size ranges were selected and investigated to determine the influence of particle size on the signal properties. It was shown that for all grain classes the signal intensity of gypsum and anhydrite differs significantly. Within the scope of the extended investigations the influence of the grain size distribution on the signal properties was investigated. This investigation is important because in practice it may be very difficult to prepare the drill dust in a narrowly limited grain spectrum for the analysis.

For this purpose, gypsum and anhydrite samples were taken from a mine again. These samples were first crushed in the mine and examined for their crystal water properties. The anhydrite samples had 0.21 % water of crystallization, while the gypsum samples had 20.03 % water of crystallization. This corresponds to a purity of 97 % for gypsum samples and a purity of 2 % for anhydrite samples. Screening of the samples showed that the anhydrite samples were coarser than the gypsum samples. The particle size distribution of gypsum and anhydrite after crushing in the mine is shown in Graph 8.1.

According to the hypothesis, the collision of an anhydrite grain leads to a higher signal intensity than a gypsum grain of the same diameter, if the velocity of the grain remains constant. This principle has been confirmed in previous experiments even for narrow grain ranges.

The screening results of the crushed samples show that the gypsum is finer than anhydrite in all fractions. In this respect it is to be expected that the signal intensity of anhydrite is automatically higher because the anhydrite grains are larger than the gypsum grains. With such a material condition, the desired influence cannot be determined.

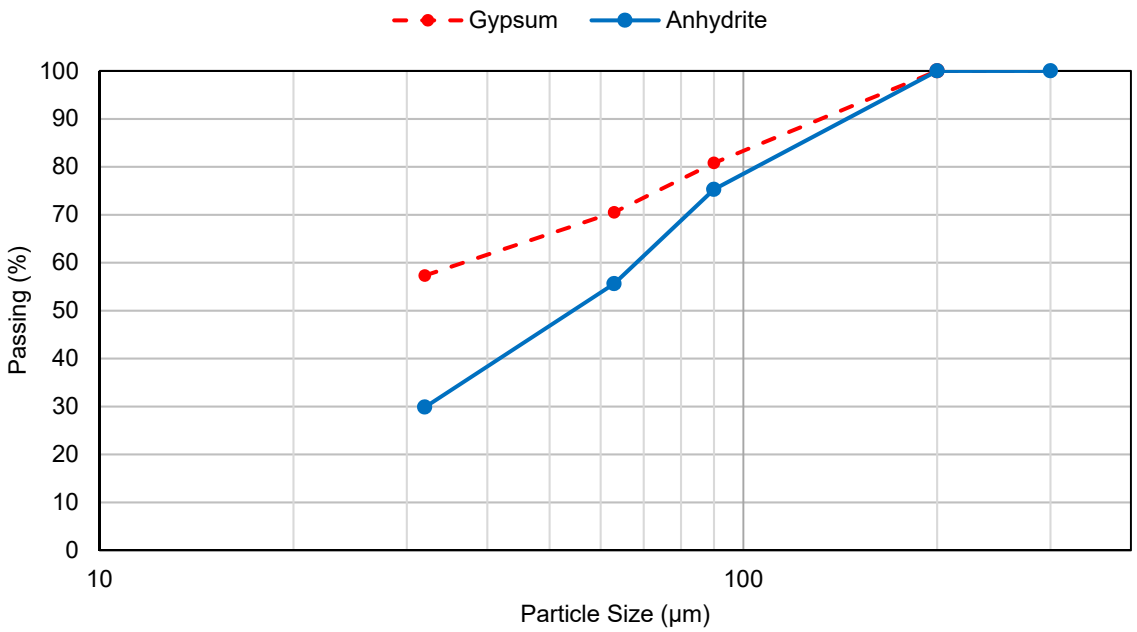

Graph 8.1: Particle size distribution of the investigated samples

To obtain samples with approximately the same grain size distribution, the anhydrite samples were subjected to a two-stage milling. The first, ten-minute stage led to a considerable reduction in the particle size of the anhydrite particles. Especially the grain fraction larger than 90 µm had almost the same grain size distribution as gypsum samples. After a further twenty-minute milling the anhydrite sample became even finer than the gypsum samples for fractions larger than 63 µm, see Graph 8.2.

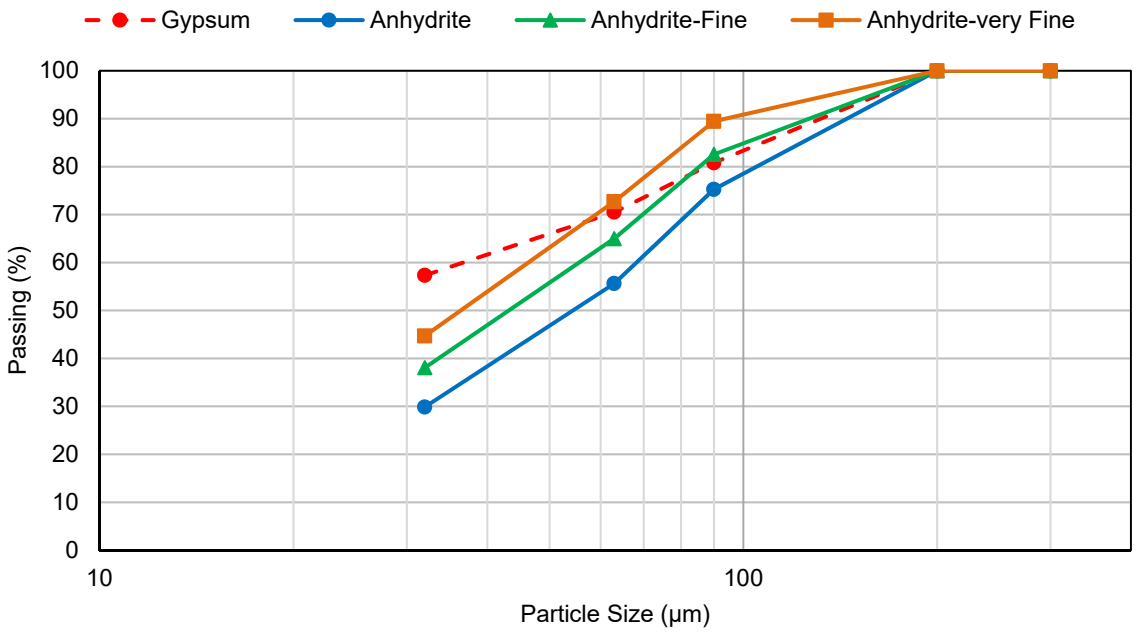

Graph 8.2: Sieve analysis of gypsum and anhydrite samples. Anhydrite was crushed in two steps

The results of this stage are shown in Graph 8.3. In all tests the signal of the anhydrite has a higher amplitude than the signals of Gypsum up to a frequency of 14 kHz. The difference between the amplitudes of gypsum and anhydrite is reduced with the fineness of the anhydrite grains. Because the curves of the particle size distributions of gypsum and fine or very fine anhydrite intersect, it is very difficult to derive a clear statement from these results. In the sample from the first milling stage, the anhydrite is coarser than gypsum up to a particle size of 90 µm. Above 90 µm the grain sizes of gypsum and anhydrite are equal. In the sample from the second grinding stage, the grain size of anhydrite below 80 µm is larger than gypsum. Above 80 µm, anhydrite is finer than gypsum. To avoid misinterpretation, the samples were screened again at 60 µm and tested. The result of this test is shown in Graph 8.4. Although the anhydrite in the grain fraction is finer than gypsum, the amplitudes of the signals from anhydrite are 18 % higher than gypsum. Overall, these test series show that the influence of the particle size distribution on the measuring accuracy is very large.

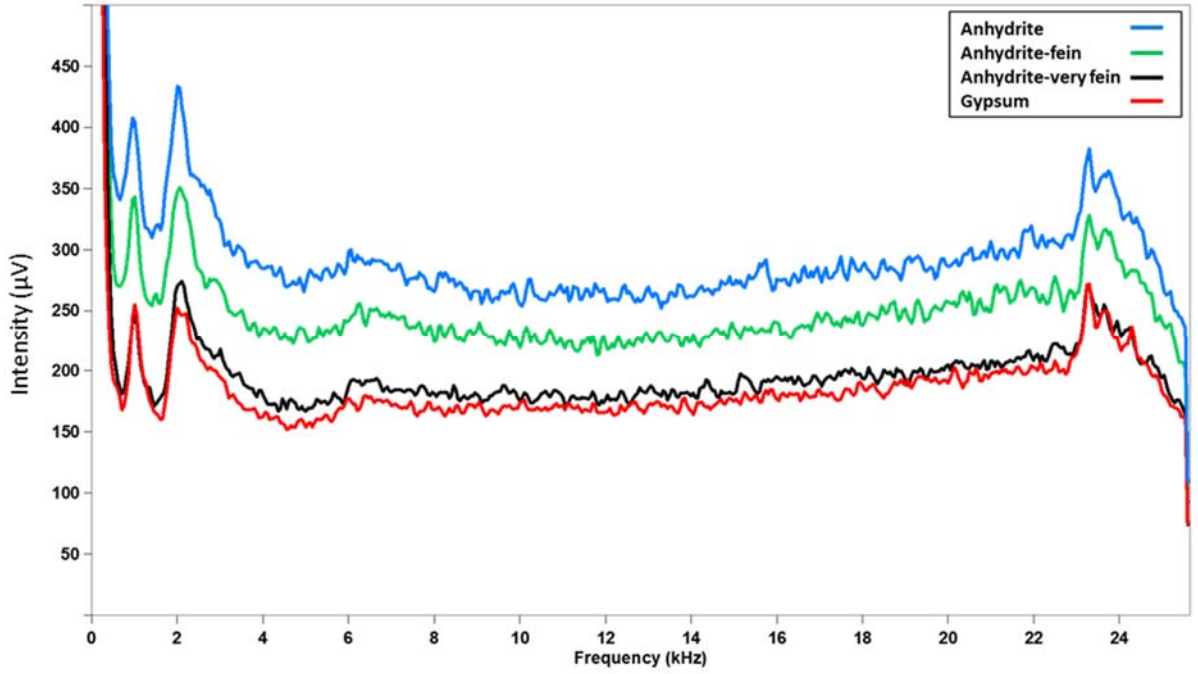

Graph 8.3: Frequency spectrum and signal intensity of gypsum and anhydrite samples with different particle size

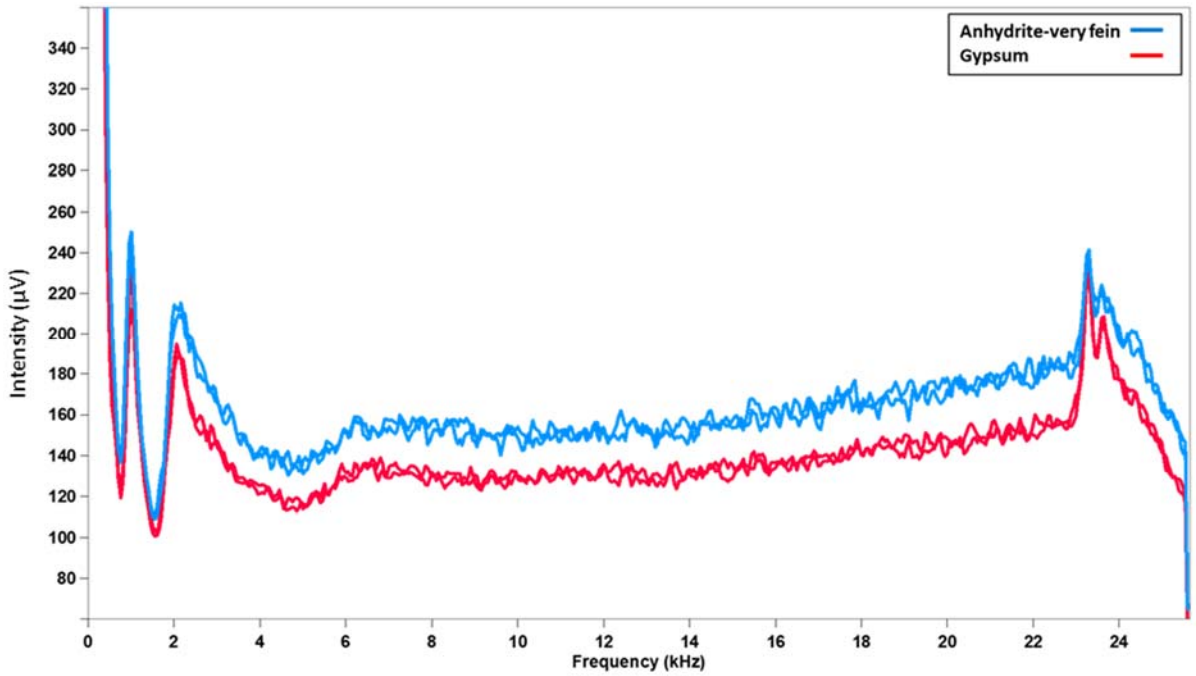

Graph 8.4: Frequency spectrum and signal intensity of gypsum and anhydrite samples with a grain size < 60 µm

9 Determination of the Influence of moisture

To determine the influence of the moisture of the samples numerous tests were carried out with the respective samples. The determination of the influence of moisture is particularly relevant for the practical application of the method. In the near-surface part of the deposit the water content of the ore is relatively high due to infiltration of surface water. In the deeper part of the deposit the moisture usually decreases. Below the groundwater level, the humidity rises again due to the saturation of the rock. In general, the cuttings moisture changes depending on the location of the drill in the mine. In this test group, the samples with different moisture were dispersed at different speeds. On the one hand, the influence of the change of the degree of moisture on the signal properties was to be investigated, on the other hand, the influence of the velocity on the signal intensity was to be determined for different moisture contents.

In this test series the samples were dispersed according to the procedure described in chapter 6. To find the optimum nozzle setting, the inlet pressure was varied. Experiments were carried out with inlet pressures of 0.4 bar, 0.6 bar, 0.8 bar and 1 bar. To determine the influence of moisture, partial quantities of the drill dust samples were dried before dispersion. These samples were stored for about 24 hours at 40 °C in a drying cabinet. The moisture of the samples was about 4.5 %.

The results of these tests show that the signal intensities of undried samples are stronger than those of dried samples. This is because the moisture of the samples acts like a damper during the collision. The kinetic energy is partly consumed as deformation energy of the particles. The frequency analysis of the signal shows that the moisture leads to a frequency shift. The signal pick between 6 kHz and 7 kHz shifts in the higher frequency range. This property of the signal to exhibit a frequency shift depending on the moisture of the sample is a measurable indicator that can be used for signal interpretation. The higher the water content of the sample, the more there is a frequency shift. This frequency shift can be used for a calibration. Thus, the water content of the sample is determined during the measuring process by the frequency analysis. This allows a normalization of the signal for a more precise determination of the ore grade. A further result of this test series is that the influence of moisture on the signal property is frequency dependent. The difference in signal intensity is relatively small between a few Hz and 4 kHz. Between 4 kHz and 7 kHz the difference reaches its highest value. Between 9 kHz and 24 kHz the difference in intensity is average. It is

noteworthy that for a frequency band between 8 kHz and 8.5 kHz the signal intensities are almost equal. This means that in this frequency band the moisture has no influence on the signal intensity. This result is also particularly important for the use of the online analyser in the practice. By filtering the signal, the influence of the water content on the analysis can be reduced to a minimum. Graph 9.1 shows the spectral lines for all experiments where the intensity of the signals increases with decreasing humidity.

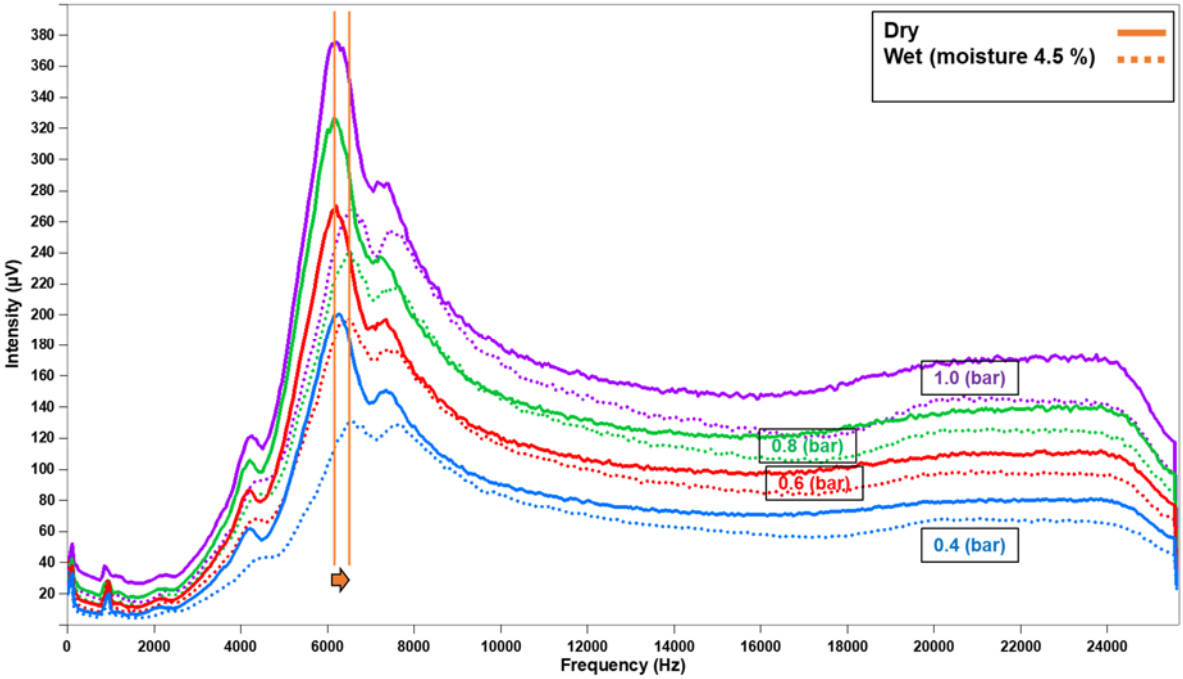

Graph 9.1: Comparison of the intensities of the mixed sample before and after drying over all frequencies

10 Online detection of gypsum and dolomite

The previous investigations were carried out with gypsum and anhydrite. In the sedimentary sequence of evaporates, gypsum, anhydrite and dolomite occur more frequently together. For quality control in mining it is important to be able to distinguish these minerals online. In a stratified deposit the layer boundaries often change due to tectonics. Small-scale folding and disturbances change the spatial position of the interfaces between the respective sediments. The geological formation preconditions also led to the formation of local lenticular or stock-like formations within the deposit. This change makes quality control in mining very difficult.

For the practical application of the online analyser it is therefore important to distinguish between gypsum and dolomite. Dolomite has a density of about 2.84 g/cm^3. The density of gypsum and dolomite differ by 0.52 g/cm^3. Based on the results of the examination of gypsum and anhydrite it is expected that a distinction between gypsum and dolomite is also possible. For this purpose, drill dust samples from a mine were selected for the laboratory tests.

For the laboratory tests samples were taken from a mine. The gypsum sample has a crystal water content of 19.37 % and a degree of purity of 92.56 %. The dolomite sample has a purity of 2.23 %. These samples were subjected to intensive crushing with the aim of creating equal conditions in terms of grain size distribution. The grain size distributions of these material can be seen in Graph 10.1 below.

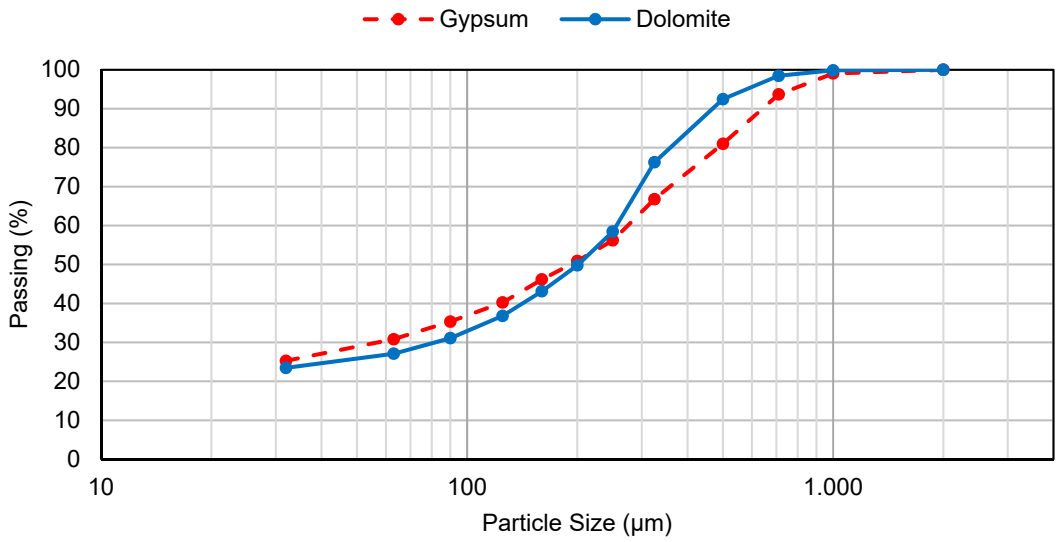

Graph 10.1: Particle size distribution of the investigated samples

After carrying out various online measurements for various grain fractions of the respective samples and recording their signal intensities, the results were subsequently compared. All investigations for samples smaller than 335 µm showed a clearly measurable difference in signal intensity as a function of purity. It should be noted that the signal intensity increased with decreasing purity and crystal water content. The results of the laboratory test for samples with a particle size between 250 and 355 µm are shown in Graph 10.2.

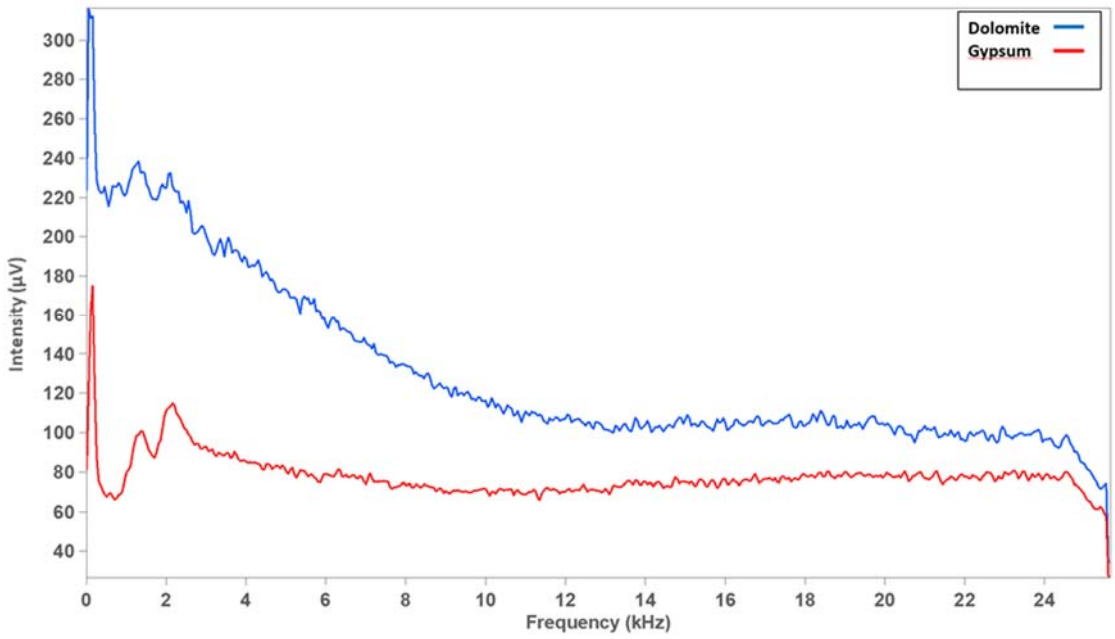

Graph 10.2: Frequency spectrum and signal intensity of the fraction 250 - 355 µm for all samples

The signal analysis shows that in the whole frequency spectrum the signals resulting from the collision of dolomite are up to 250 % more intense than the signal intensities of the gypsum samples. This investigation step also confirms the hypothesis of the research. It is possible to make a material differentiation on basis of density when the cuttings collide with an oscillator and the signals are recorded and analysed.

11 Investigations to classify the drill cuttings

The previous investigations show that a distinction between gypsum and anhydrite or gypsum and dolomite is possible for a wide particle size distribution. However, it was calculated in chapter 4.3 that, due to the material properties of gypsum and anhydrite, the deviation of the grain sizes in all grain fractions must be less than 16 %, so that a detection of the materials based on the pulse is still possible. It is assumed that this condition is present in the drilling process. Nevertheless, based on the results obtained so far, the online analysis will be the more accurate the more similar the particle size distributions of gypsum and anhydrite are. In this respect, the possibility of pre-classifying the cuttings will be included in the investigations. The following aspects had to be considered when selecting a classifier, considering the technical requirements and conditions of the field:

- Good selectivity
- Low wear
- Minimum space requirement

After thorough research, a so-called zigzag classifier was selected for the task. This is a countercurrent classifier in free fall with a zigzag-shaped channel. Figure 11.1 shows the device selected for initial laboratory tests. The classifier consists of an input hopper, a dosing device in the form of a vibrating channel, the zigzag-shaped channel, coarse grain container, fine grain container as well as a flow machine (vacuum cleaner) and a cyclone. The vacuum cleaner generates an air flow. The fresh air is sucked in by the lower, open part of the zigzag separator. It flows upwards in the separator chamber and passes through the cyclone in the upper part of the separator and ends up in the vacuum cleaner, where it is finally filtered. The material to be classified is filled into the upper hopper. When the classifier is switched on, the material is fed to the classifier via a vibrating chute. The material moves downwards in a zigzag shape through the separator chamber against gravity. The fine particles are carried upwards by the air flow of the vacuum cleaner and separated in the cyclone, while the coarse material falls downwards and is collected there. The adjustment of the separator or the separation cut is carried out via the control of the vacuum cleaner.

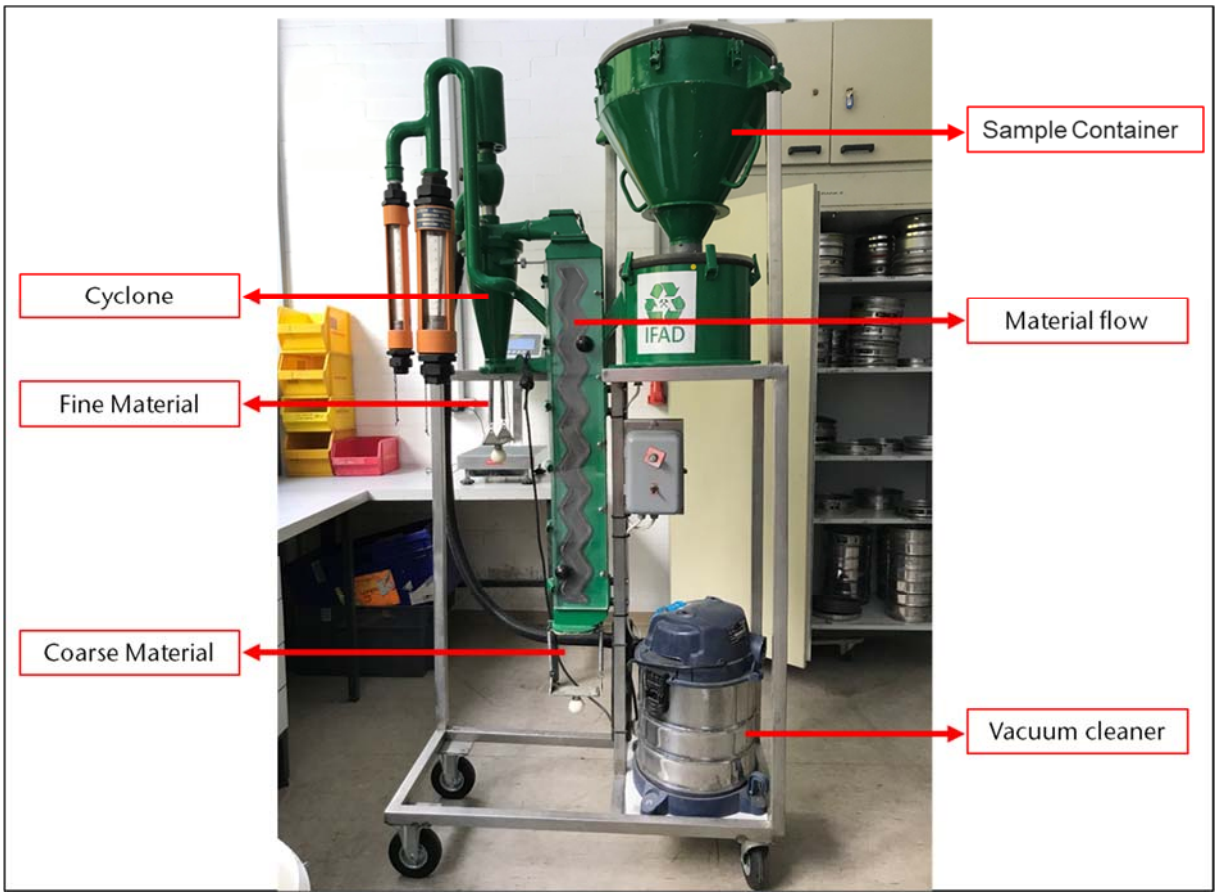

Figure 11.1: Experimental apparatus for classification, zigzag separator

For the investigations, the samples from two mines were first sieved. The grain class 0 - 2000 µm was selected for the classification by means of separator. This grain class corresponds approximately to the grain size distribution of the drill dust. In a first test series an air velocity of 4.17 m/s with an air volume flow of 24 m³/h was adjusted. The separator has two throughput stages of 16 kg/h and 40 kg/h due to its dimensions. At a throughput rate of 16 kg/h, the Samples were classified. These tests were repeated several times for 4 kg sample. The results of three tests with sample from the first mine are shown in Graph 11.1. The orange grading curve corresponds to the grain size distribution of the feed material. With the selected setting, the fines contain approximately 100 % grain size with less than 700 µm and 50 % less than 125 µm. The classification of 4 kg of sample took 6 minutes. Per minute 660 g were classified. Considering the classification results for the grain size classes smaller than 700 µm and smaller than 125 µm, the classifier can prepare between 600 g per minute or 330 g sample in the mentioned classes for online measurement.

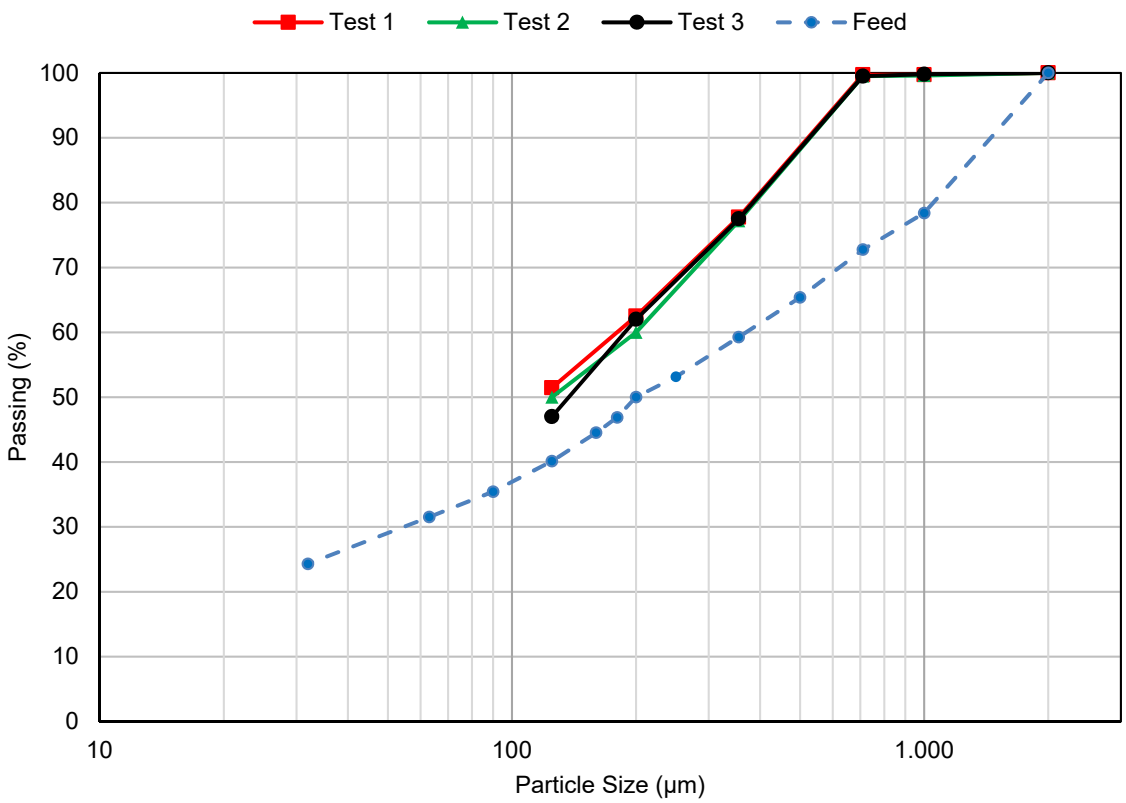

Graph 11.1: Results of the classification of the sample from first mine

Graph 11.2 shows the results of the same investigation series for the samples from the second mine. With the same setting, the fines contain approximately 100 % grain size with less than 1,000 µm and in average 60 % less than 125 µm. The classification of 4 kg of sample took 15 minutes. Per minute 266 grams were classified. Considering the classification results for the grain size classes smaller than 700 µm and smaller than 125 µm, the classifier can prepare between 160 g/min to 250 g/min samples in the mentioned classes for online measurement.

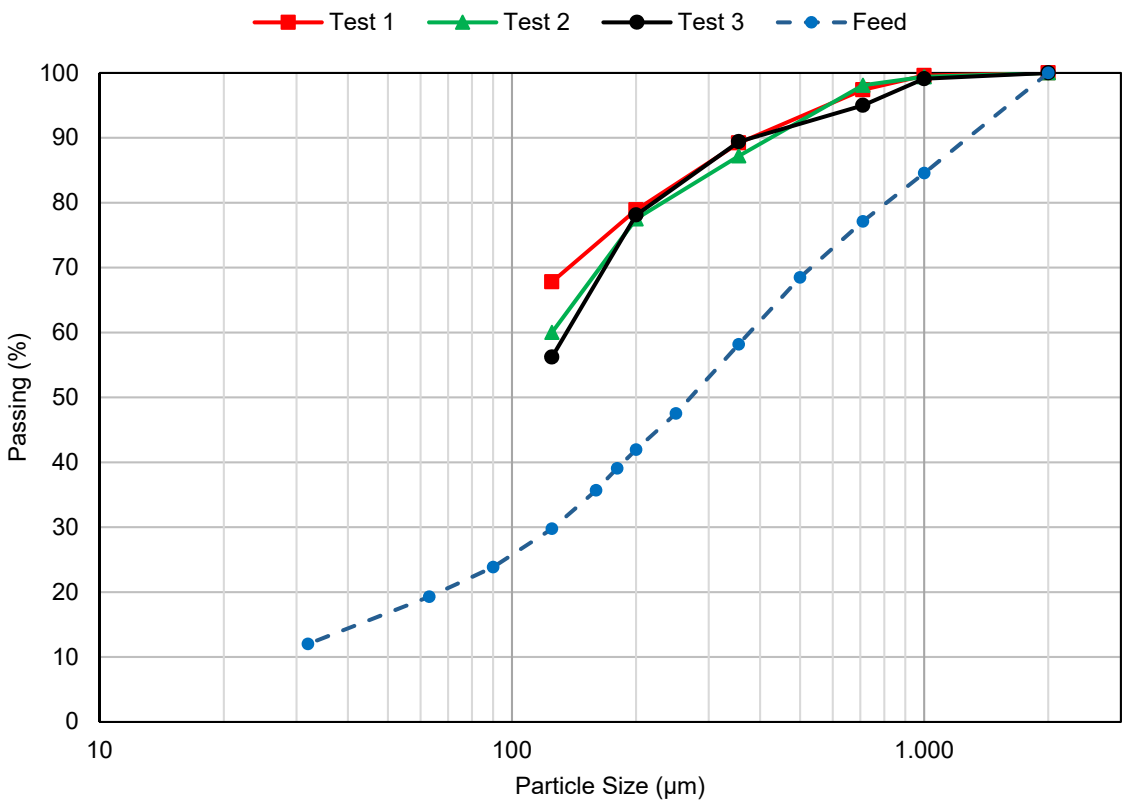

Graph 11.2: Results of sample classification from second mine

In a second series of investigations a throughput rate of 40 kg/h was used, the samples were classified with air flow of 24 m³/h and an air velocity of 4.17 m/s. The results of the investigations show that the separation rate decreases considerably at higher throughput rates. While at a throughput of 16 kg/h approx. 60 % of the fines are smaller than 125 µm, at a throughput of 40 kg/h the proportion of these grains drops to 30 %. As a result, for practical application, where around 12 kg of drilling dust is produced in around 60 seconds during the drilling of a borehole, only a partial flow of the cuttings must be fed to such a classifier. The results of this analyses are shown in Graph 11.3.

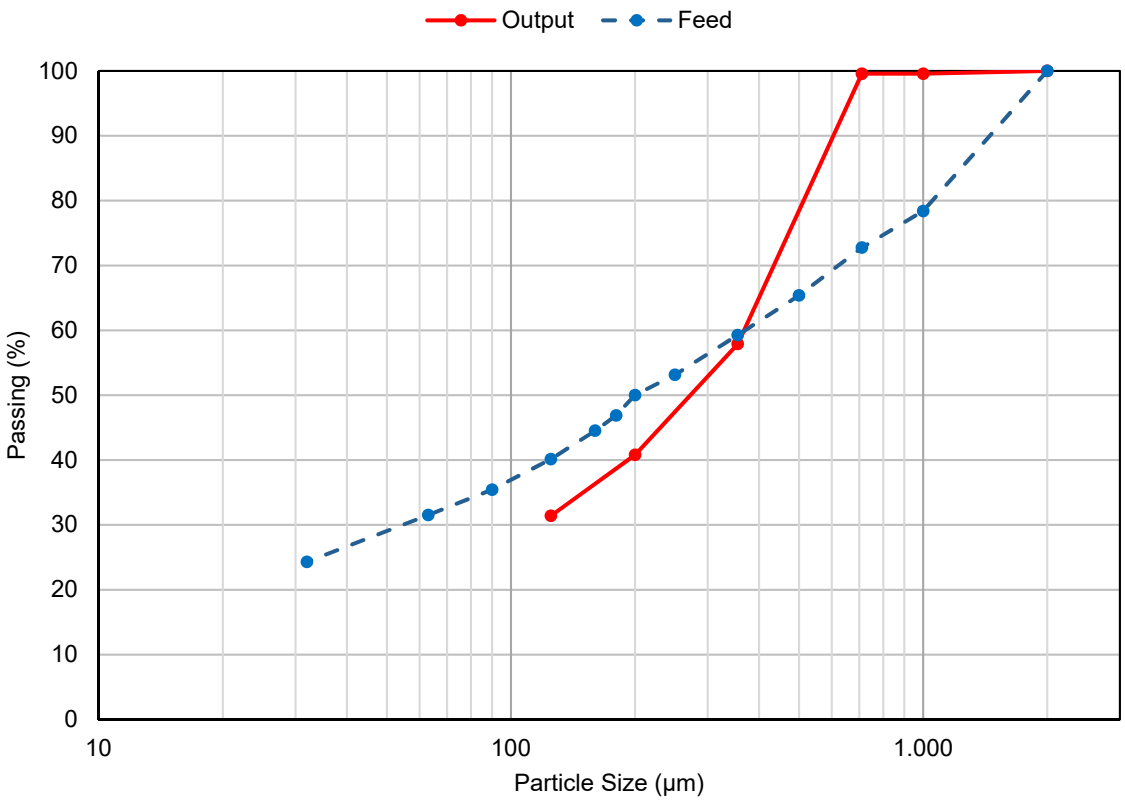

Graph 11.3: Results of sample classification for an hourly feed of 40 kg

12 Moisture influence on the classification of cutting

The previous investigations were carried out with dry samples. In the mine it can be assumed, as already mentioned, that cuttings are wet. To investigate the influence of the moisture content on the classification, samples were taken from a mine. The samples have a moisture content of 4.5 %. To determine the particle size distribution of the samples, they were screened before classification. The results of the grain size analysis of the samples are shown in Graph 12.1. The samples were tested in the classifier. The classifier was adjusted with the parameters. The test results show that the moisture content has an influence on the classification. The separation cut off is within 1,000 µm. About 97 % of the sample has a grain size smaller than 1,000 µm. The percentage of grains smaller than 125 mm is 38 %. The comparison of the classification of dry and wet samples shows that the percentage of grains smaller than 125 mm in the wet samples is 25 % lower than in the dry samples. Nevertheless, it is possible to classify the drill cuttings during drilling to prepare the samples for online quality analysis. Graph 12.2 shows the result of the classification.

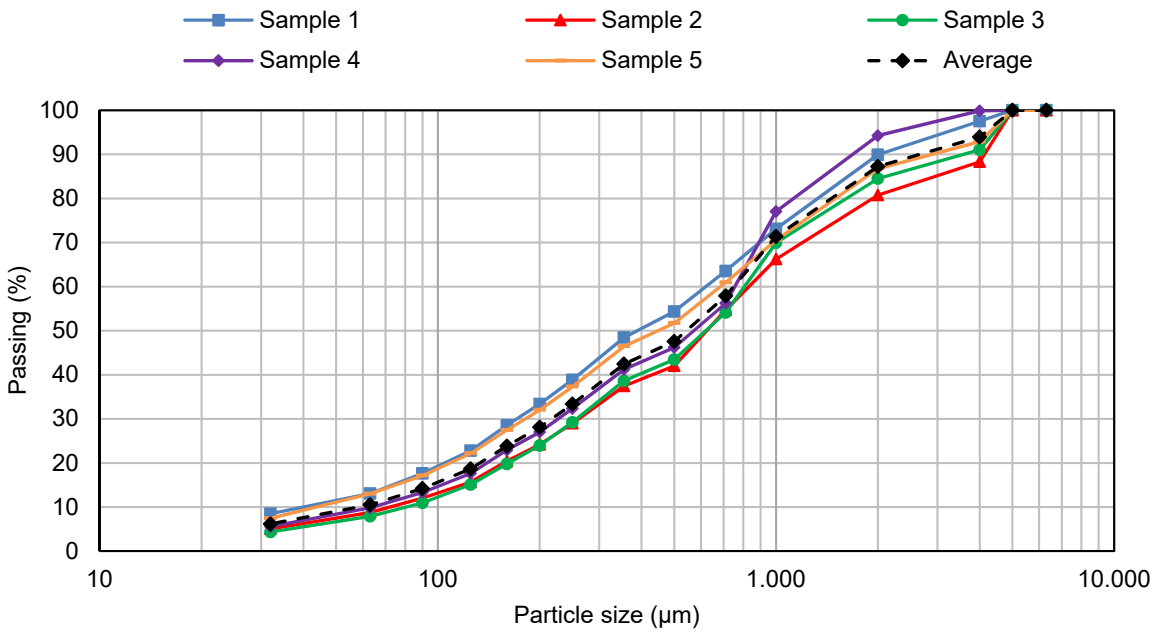

Graph 12.1: Particle size distribution of samples

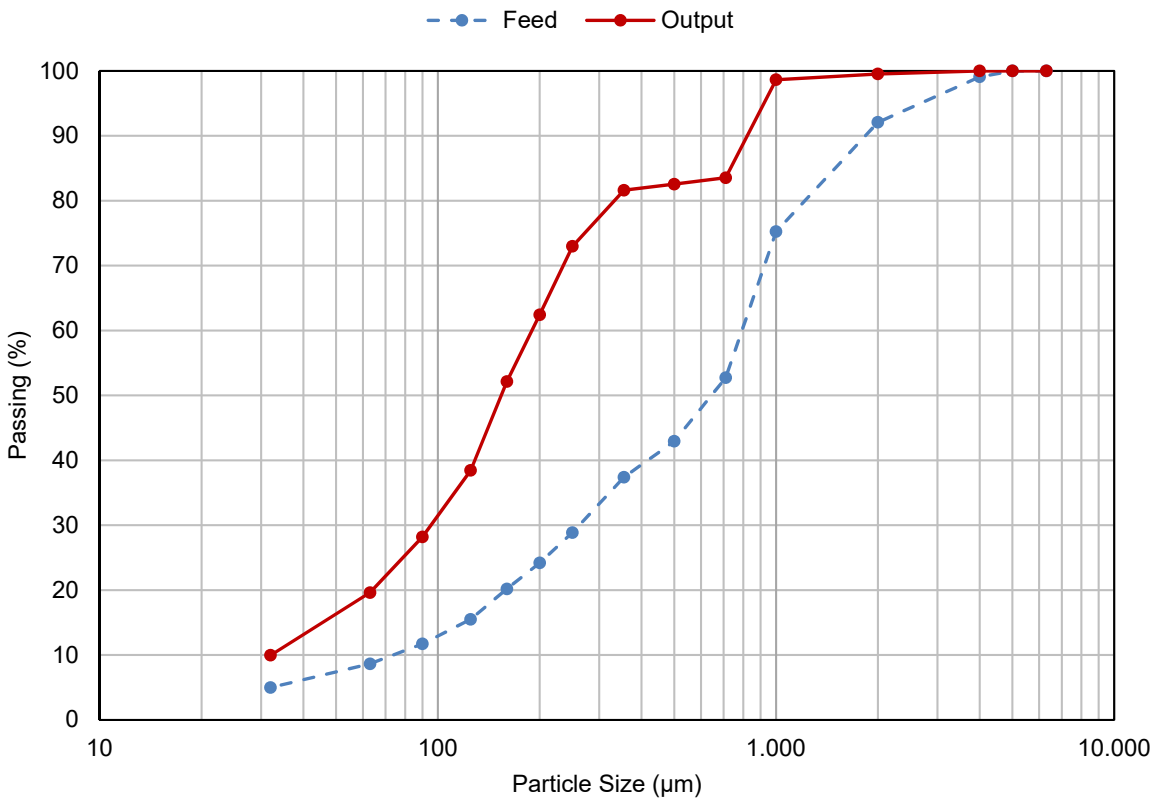

Graph 12.2: Result of the classification of the samples at a separation cut-off of 0 - 355 µm

13 Quantitative analysis of samples

The results so far have shown that online detection of gypsum and anhydrite or gypsum and dolomite is possible based on the developed method. A prerequisite for the online analysis is that the particle size distribution of the samples remains approximately the same. The analysis would give incorrect results if the diameter of the gypsum grains in all classes is more than 16 % larger than that of the anhydrite grains or the diameter of the anhydrite grains in all classes is less than 85 % of the diameter of the gypsum grains. In practice, if all the anhydrite grains are larger in diameter than the gypsum grains, no misanalysis will occur.

It is assumed that during the drilling process the cuttings from anhydrite will be relatively coarser than cuttings from gypsum. The relatively higher hardness of the anhydrite would cause this effect. On the Mohs hardness scale, gypsum has a value of 2 and is characterized by an elasticity modulus of 35.5 GPa and an axial compressive strength of 12 -15 N/mm². Anhydrite is characterized by a Mohs hardness of 3 to 3.5, a modulus of elasticity of 63.8 GPa and an axial compressive strength of 72 - 133 N/mm². During drilling tests in the laboratory, it has been noted that the properties of anhydrite lead to coarser drill cuttings than drilling gypsum. The samples taken from the mine for the test series were first crushed in the laboratory. With the same crusher setting and crushing time, the anhydrite samples always produced coarser output material. To achieve the same particle size distribution as in the gypsum samples, the anhydrite samples were crushed in a multi-stage process.

Based on these results, further laboratory work was focused on investigating the possibility of a quantitative online analysis of samples using the developed method. For this purpose, both gypsum and anhydrite samples were taken from the mine. The samples were first crushed in the laboratory. The milling was continued until the grain size of the samples was less than 1,000 µm. The aim of the milling process was to produce an equal particle size distribution for the gypsum and anhydrite samples. The grain size distribution of the samples is shown in Graph 13.1.

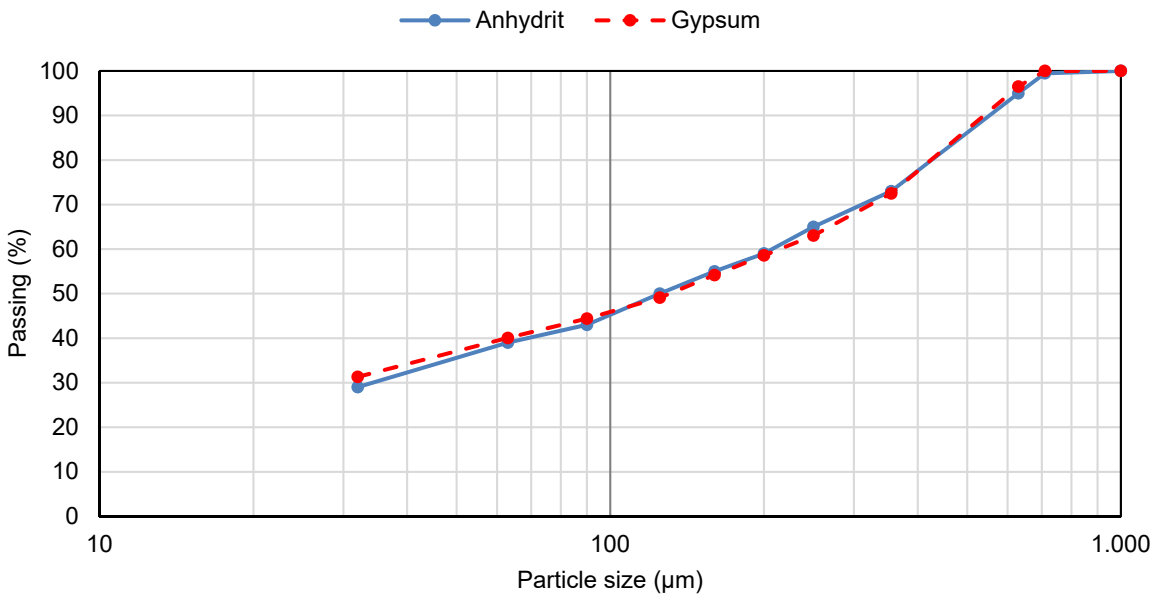

Graph 13.1: Particle size distribution of gypsum and anhydrite samples

The gypsum and anhydrite samples were then homogenized and analysed. The gypsum sample showed a purity of 84.55 %. The anhydrite sample demonstrated a purity of 3.12 %. From the homogenized samples 21 composite samples were prepared. Two of the samples consisted of 100 % gypsum (purity 84.55 %) and anhydrite (purity 3.12 %). The remaining 19 samples were composite of gypsum and anhydrite with the stated purity. The mixing ratio was adjusted in 5 % steps. For all composites the purity was calculated and verified by chemical analysis. The results of the sample preparation are shown in Table 13.1.

Table 13.1: Mixing ratio of the samples and their purity

Sample	Anhydrite (%)	Gypsum (%)	Purity (%)
A0	0	100	84.55
A5	5	95	81.06
A10	10	90	77.78
A15	15	85	74.02
A20	20	80	70.07
A25	25	75	66.31
A30	30	70	61.16
A35	35	65	57.44
A40	40	60	52.98
A45	45	55	49.08
A50	50	50	44.74
A55	55	45	40.25
A60	60	40	36.16
A65	65	35	32.22
A70	70	30	27.91
A75	75	25	24.27
A80	80	20	20.36
A85	85	15	15.86
A90	90	10	11.52
A95	95	5	7.52
A100	100	0	3.12

The gypsum and anhydrite samples and some mixed samples were additionally examined by X-ray diffraction. The results are shown in the Figure 13.1. The impurities are mainly anhydrite. The samples also contain a small amount of dolomite.

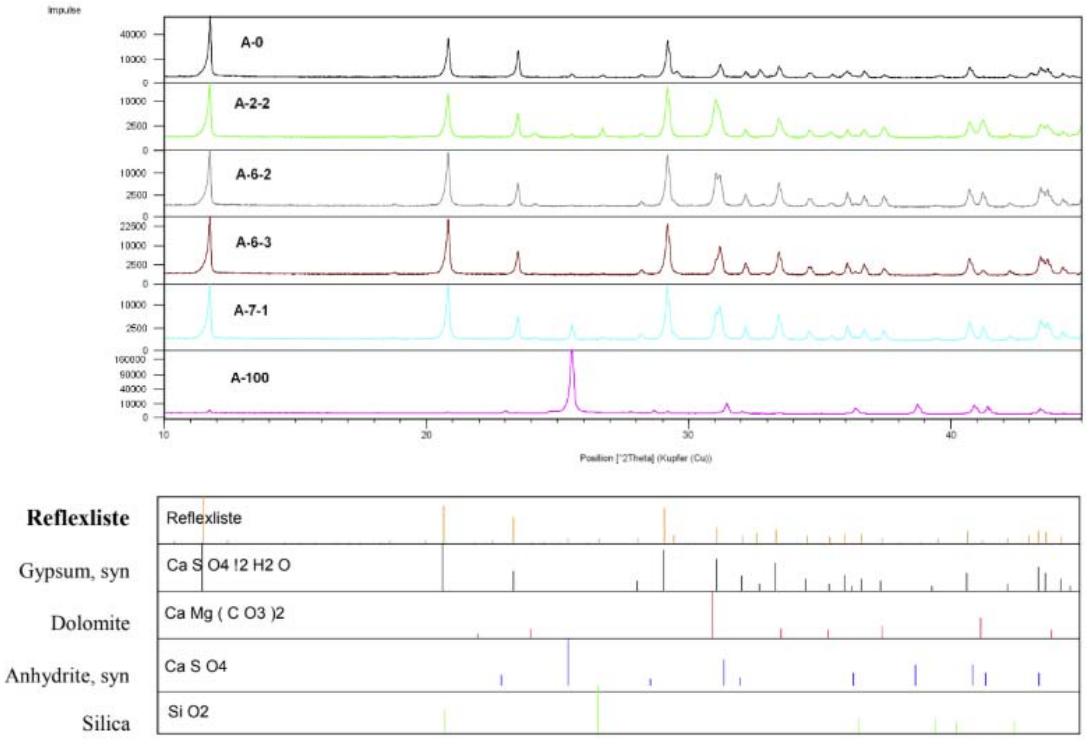

Figure 13.1: Results of X-ray diffractometry. Samples A0 and A100 correspond to "pure" gypsum and anhydrite samples from the open pit.

The samples produced in this way were then tested with the laboratory equipment. Each sample was examined 5 times. A total of 105 tests were performed. The signals were recorded and subsequently analysed. Graph 13.2 shows an example of a time signal for one of the 105 tests. Graph 13.3 shows the results of the FFT analysis for all samples.

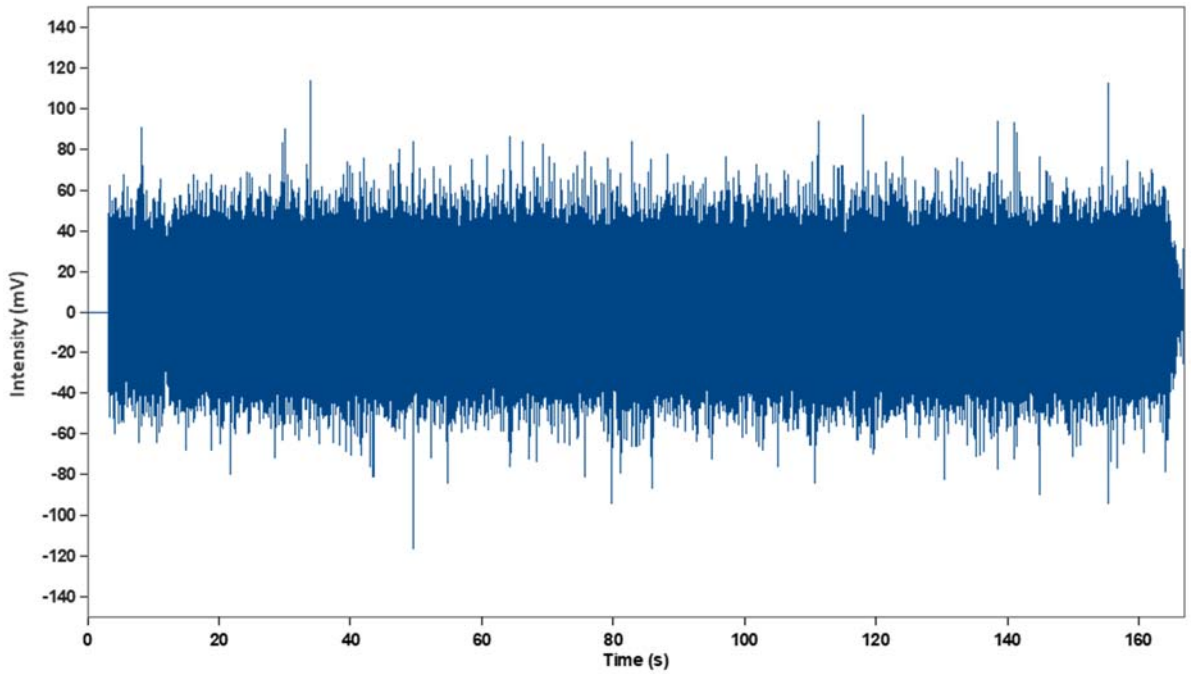

Graph 13.2: Time dependent intensity of the unfiltered signal

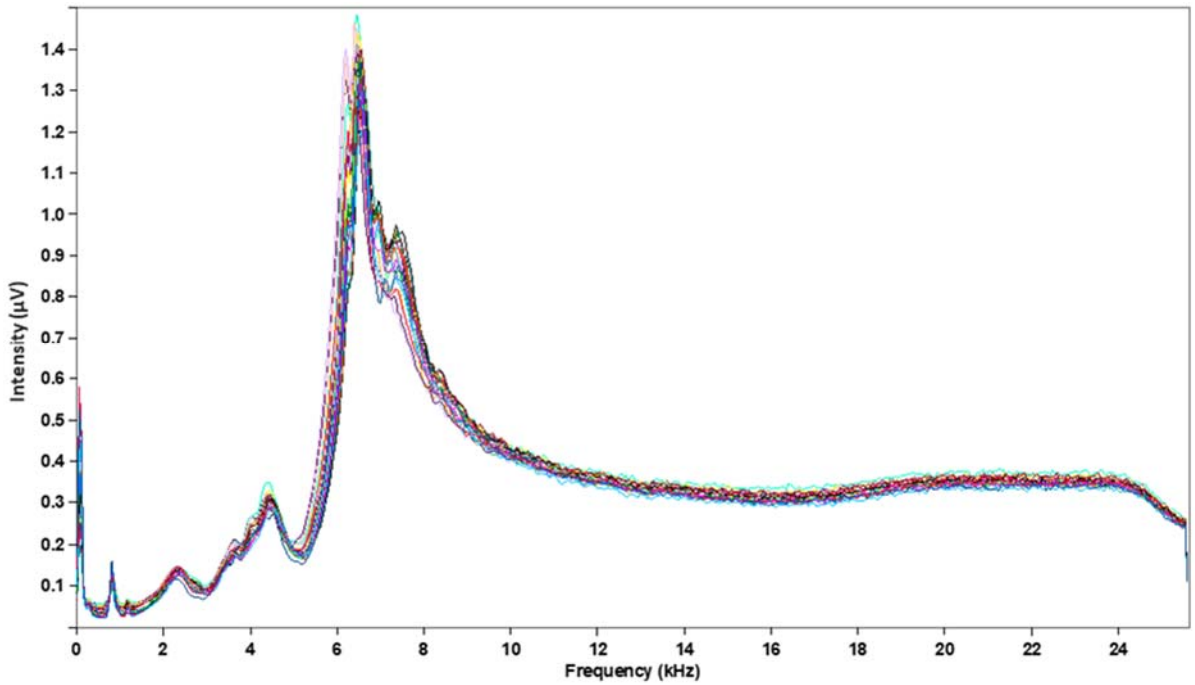

Graph 13.3: Frequency analysis of the signals from all samples

The signal evaluation was carried out according to the methods described in chapter 6.5. The time signals were processed in different stages after filtering. In a first step the signal intensities of the respective experiments were determined after the FFT analysis of the time signal. The results demonstrate a linear relationship between the purity of the samples and the signal intensity. In other words, the signal intensity increases with increasing amount of anhydrite in a sample. The signal intensity of the sample with a purity of 3.12 % is 67 % higher than the sample with a purity of 84.55 %. The linearity can be described by the following ratio. An average change in the degree of purity of 1 % results in a change in signal intensity of 0.8 %. The results of the data analysis are shown in Graph 13.4.

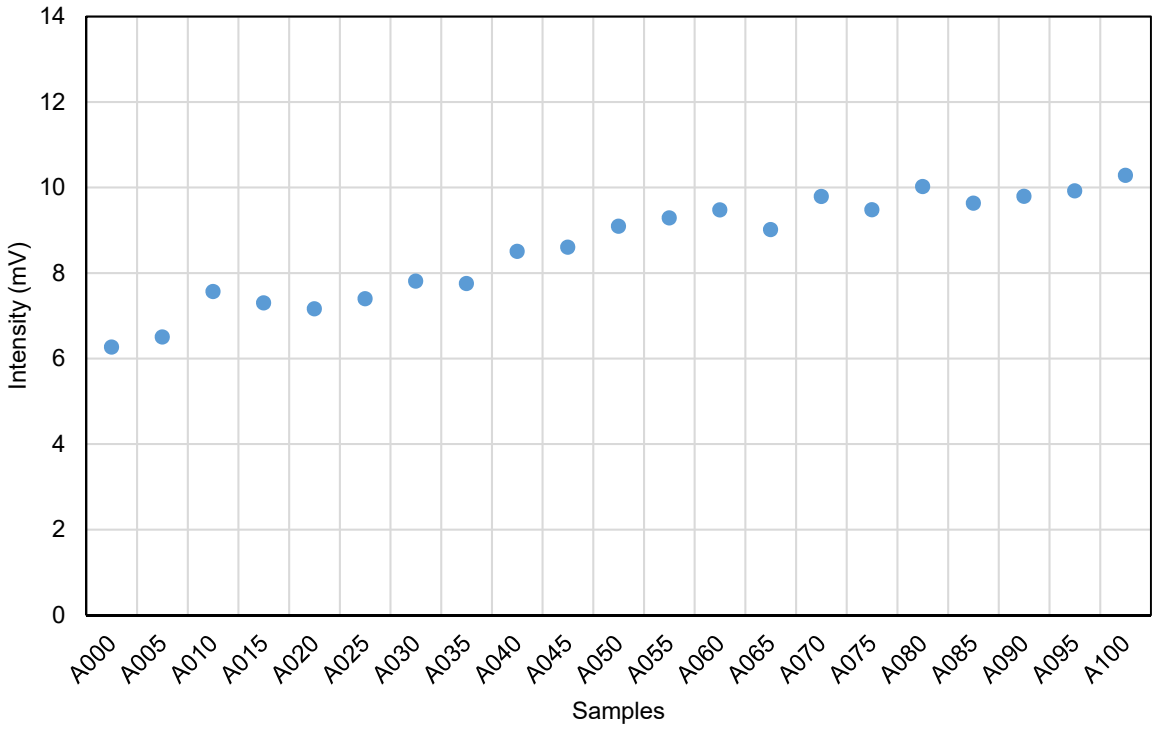

Graph 13.4: Relationship between signal intensity and purity

The slight fluctuations in the values or the deviation of the values from the mathematical functional equation are due to the abrupt change in the purity of the respective composites. This is because of the fact, that the difference in the degree of purity of prepared composites is not the same. The first evaluation confirmed the results of the previous test and shows a basic possibility of quantitative online analysis of ore grade. In an initial approximation, the intensity of the signal can be used as an indicator for determining the degree of purity of the gypsum.

In a second step of signal analysis, the distribution of signal intensities of all samples was displayed as a histogram. The intensity varied between about 4.5 mV and 39.6 mV. The histogram is positive skewed. The low intensities contain noise signals, which are generated when the samples are dispersed by a Venturi nozzle. The deflections with high intensity result from variable environmental conditions or is caused by the collision of single coarse grains with the oscillator. The mean value of the signal intensity demonstrated a value of about 8, the histogram is shown in Graph 13.5.

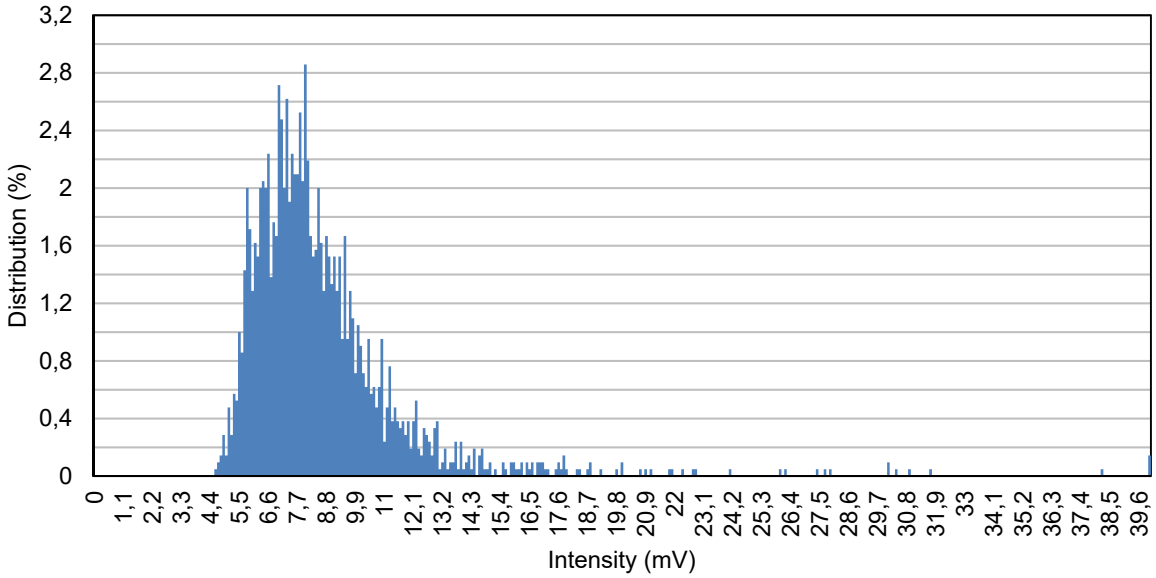

Graph 13.5: Distribution of the signal intensities

As expected, signal populations dependent on the quantity of samples cannot be derived from the histogram. To determine the populations, the probability plot was created for the respective signals of the experiments carried out. Graph 13.6 shows the Probability Plot for all samples. As expected, the individual populations are not normally distributed. The influence of noise is visible in the low intensity range. The same can be observed for outliers in the higher intensity range. The Probability Plot shows that with a probability of 80 % to 90 % a relatively good differentiation of the individual populations in the intensity range from 8 mV to 14 mV is possible. The samples A0, A05 and A10 with a purity of 84.55 %, 81.06 % and 77.78 % respectively can be clearly distinguished. The same applies to samples A100, A95 and A90 with a purity of 3.12 %, 7.52 % and 11.52 % respectively. For all other samples, the signal

intensity can be assigned at 80 % and 90 % probability. However, it appears that this sometimes results in an error of up to 10 % in the analysis results.

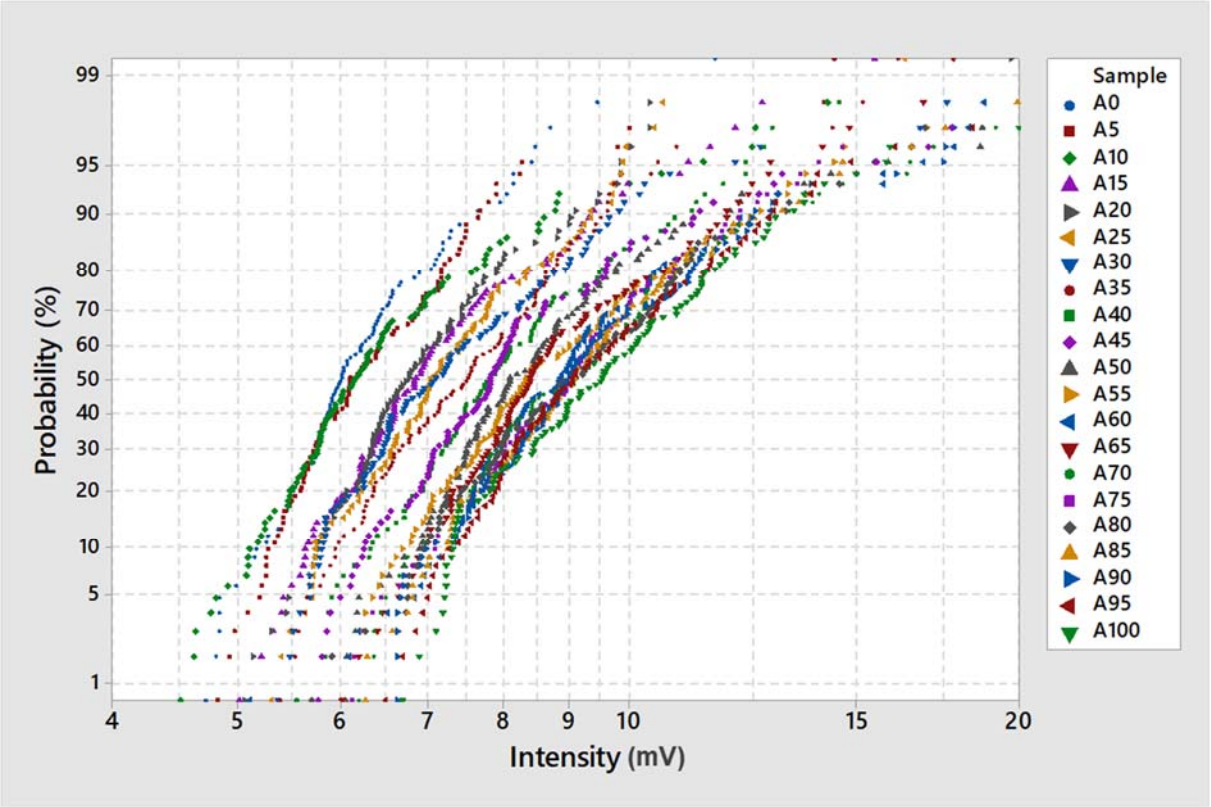

Graph 13.6: Probability plot of the signal intensities of the samples

Due to the lack of clarity in the probability distribution of the signal intensities of the individual samples, the samples were combined into groups. From the 21 samples 8 groups were formed, which are characterized by different degrees of purity. The raw signals of these groups were again subjected to signal processing. Based on the data of the respective groups, the probability distribution was calculated and plotted in a probability plot. The results of these calculations are shown in Graph 13.7. The Figure shows the course of the probability curve for a probability of 30 %. The cut off of 30 % probability was chosen to eliminate the noise component of the signals.

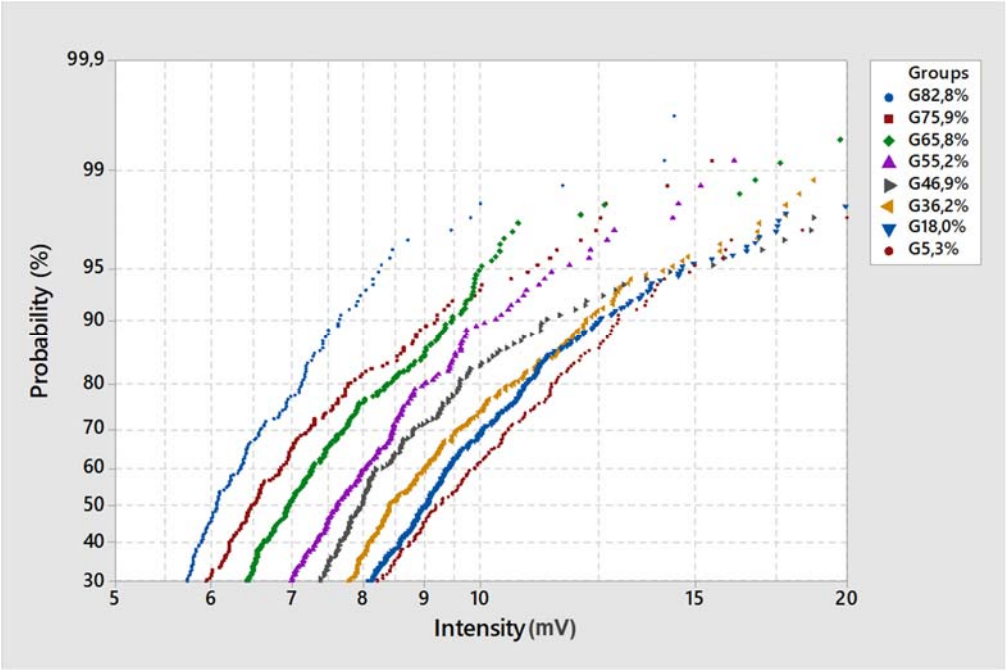

Graph 13.7: Probability plot of the groups at a cut-off of 30 % probability

It is noticeable by the new probability plots that a clear quantitative differentiation of groups with different degrees of purity is possible. For further investigations, the progression of the probability curves was interpolated at a cut off probability of 30 %. The single points were replaced by an adjusted continuous curve. The mathematical functions of the probability plots are the basis for a validation of the results. They are part of the algorithm for online analysis of the ore grade, see Graph 13.8.

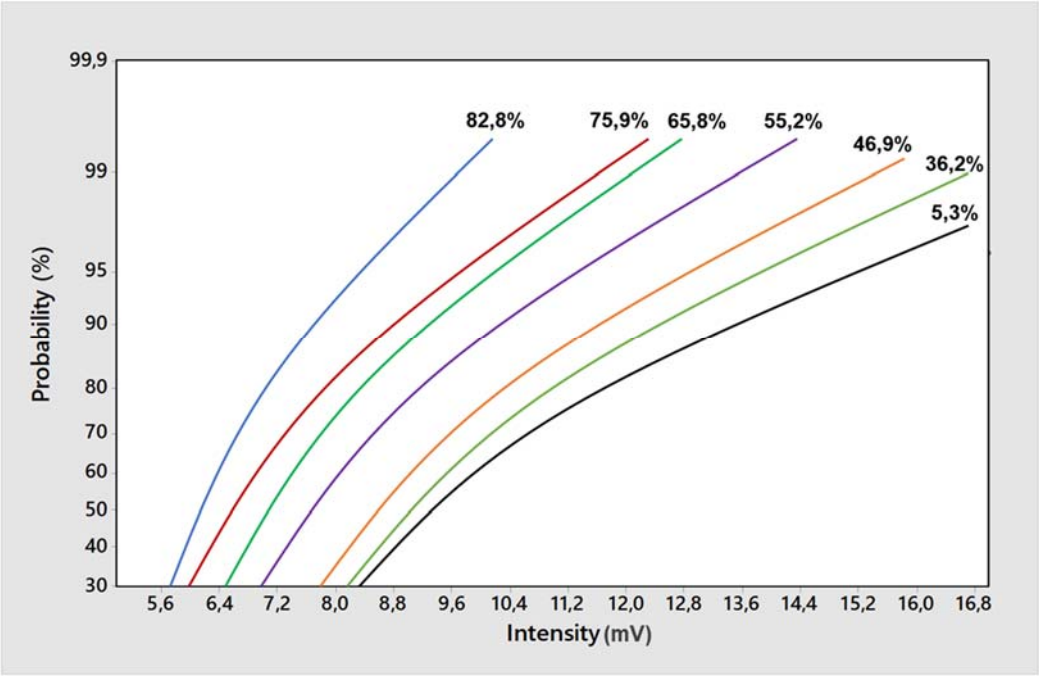

Graph 13.8: Interpolated probability plots at a cut-off of 30 % probability

The validation should confirm the accuracy and repeatability of this method of online analysis. For the validation 15 additional samples were prepared from the crushed gypsum and anhydrite samples. The prepared composites have a degree of purity between 27.5 % and 81.9 %. The purity of the samples is shown in Table 13.2.

Table 13.2: The purity of the samples for validation

Sample	Purity-Laboratory (%)
1	43.83
2	47.72
3	57.73
4	45.02
5	37.93
6	34.48
7	33.29
8	30.74
9	23.84
10	76.63
11	72.90
12	65.02
13	81.92
14	79.09
15	27.55

For the validation, the samples were prepared randomly. The purity of the samples reflects real conditions in a mine. 15 samples were tested with laboratory equipment. The signals from each test were then further processed after filtering and FFT analysis. The probabilities were calculated from the determined signal intensities. Graph 13.9 shows the probability plots of the 15 samples. This graph shows the probability plot for the cut off of 30 % probability for each sample, the intensity at 80 % signal probability was selected and entered into the general probability plot already created. The results of the validation are shown in Graph 13.10. Graph 13.11 shows the comparison of the analysis results by laboratory and online method. Table 13.3 shows the results and the differences of the values in tabular form.

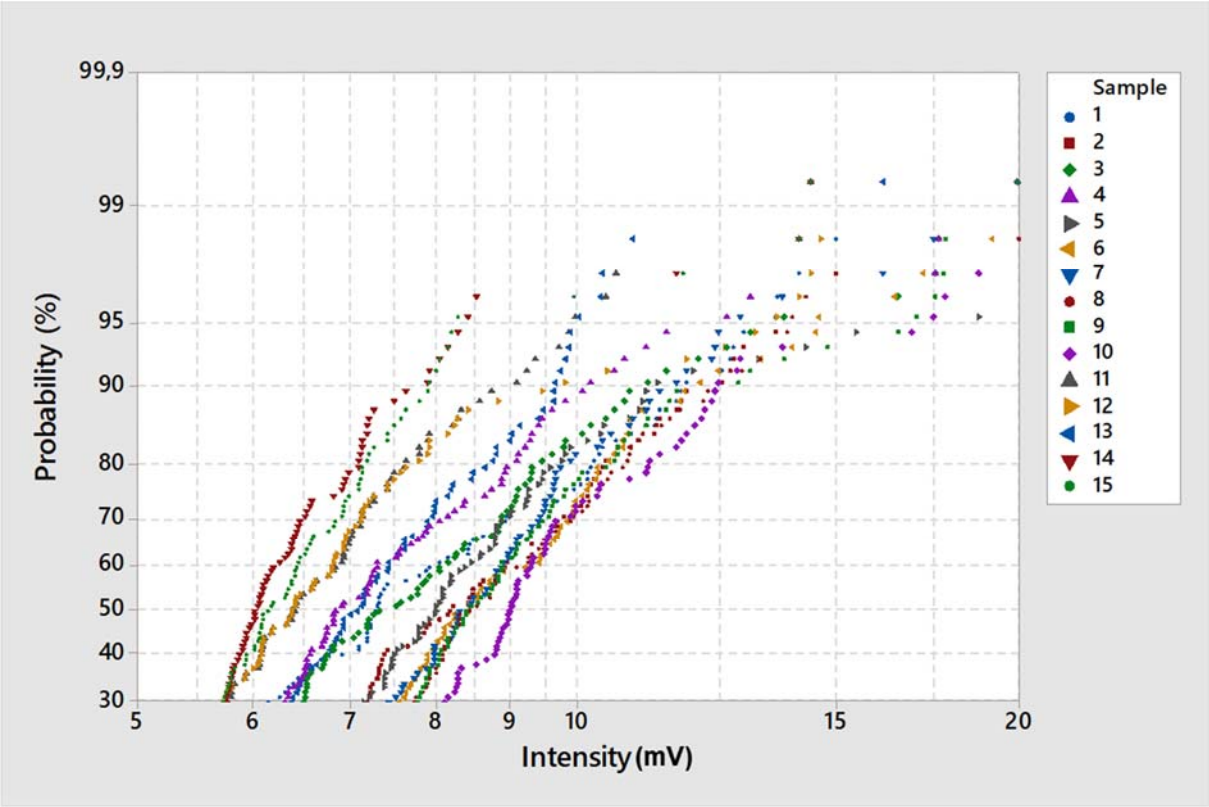

Graph 13.9: Probability plot of the groups at a cut-off of 30 % probability

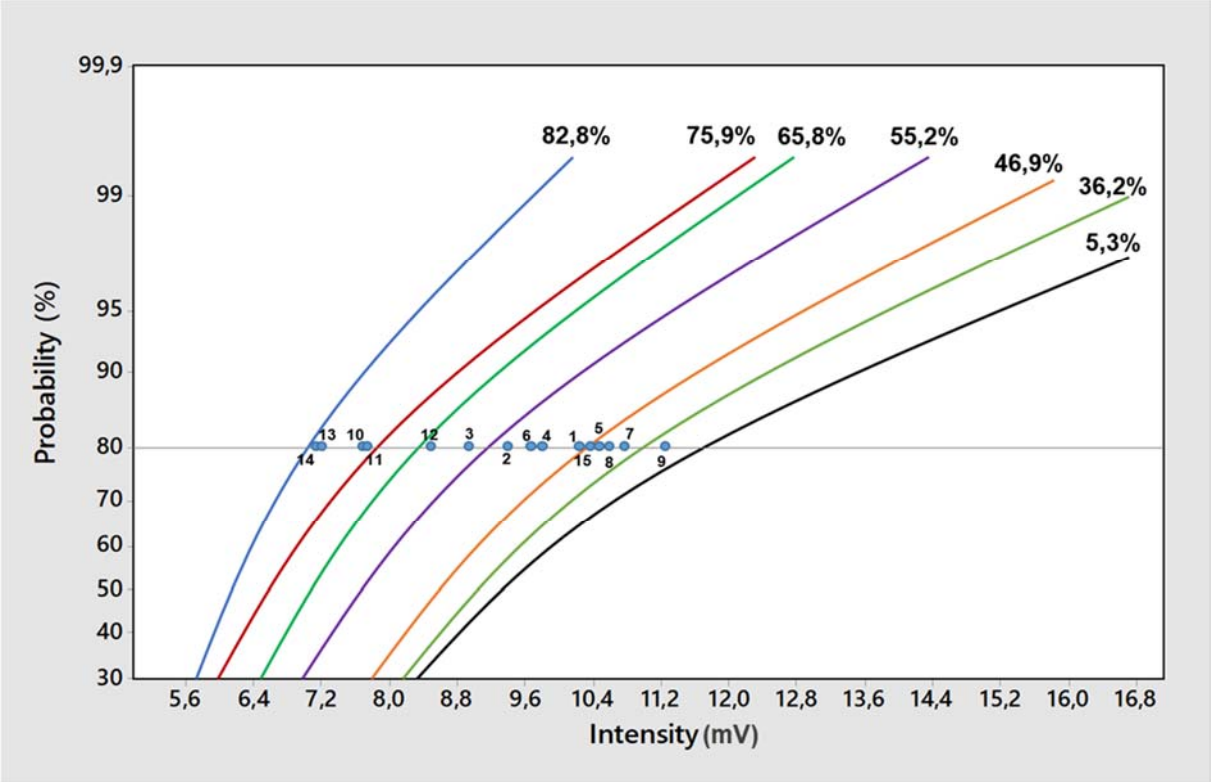

Graph 13.10: Intensity of the validation samples at a probability of 80 % shown in the calibration function

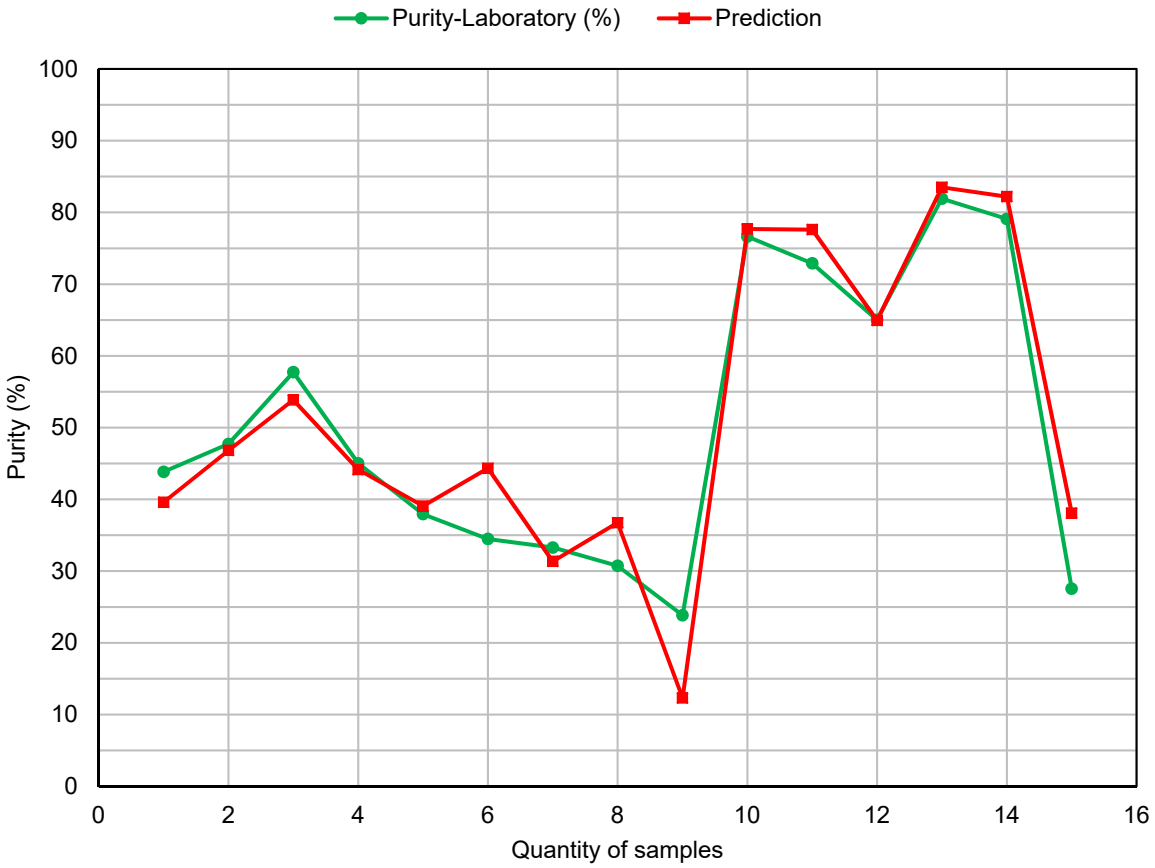

Graph 13.11. Comparison of the laboratory results with the results of the Probability Analysis

Table 13.3: Comparison of the laboratory results with the results of the Probability Analysis

Sample	Purity-Laboratory (%)	Purity-Online (%)	Deviation (Laboratory-Online) (%)
1	43.83	39.60	4.24
2	47.72	46.82	0.90
3	57.73	53.86	3.87
4	45.02	44.15	0.88
5	37.93	39.06	-1.13
6	34.48	44.32	-9.85
7	33.29	31.36	1.93
8	30.74	36.75	-6.01
9	23.84	12.32	11.52
10	76.63	77.70	-1.07
11	72.90	77.60	-4.70
12	65.02	64.95	0.07
13	81.92	83.50	-1.58
14	79.09	82.20	-3.11
15	27.55	38.08	-10.53

The validation shows that, based on the probability calculations, a relatively accurate prediction of the ore grade of the 15 samples is possible. The comparison of the results from the laboratory analysis and the online analysis shows a difference of 0.88 % to 11.52 %. The comparison of the deviation of the results of laboratory and online analysis depending on the degree of purity allows a better evaluation of the results.

The results of samples with a purity level higher than 50 % differ between 0.07 % and 4.7 % from the laboratory results. The difference between laboratory and online results of samples with a purity level lower than 50 % is higher. The deviation of these samples is between 0.88 % and 11.52 %.

For the practical application of the online method it is important that the deviation is lower, especially for parts of the deposit with a higher ore grade. Normally, deposit parts with a purity level of less than 50 % are relatively well known and are not mined.

As explained in chapter 4.6 different algorithms were chosen for the development of the online procedure. One algorithm is based on the statistical method of probability calculation and determination of ore grade dependent signal populations. The second algorithm is based on an established multivariate regression analysis. This method consists of the composition of two mathematical procedures of multi-variant data analysis. The algorithm includes the structure-covering method of principal component analysis for the determination of relevant factors and the method of principle component regression (PCR) for the calculation of regressions of independent variables.

For the input of the data into the online model, the raw signals recorded during the measurement were filtered in a first step. The filtered signals were evaluated in time intervals of 0.2 seconds. From the filtered signals 528 signal characteristics per time interval were extracted. The characteristics consist of frequency data and statistical values calculated from the signal waveform. With these data a matrix was created. A quality matrix was created from the results of the laboratory analyses of the 21 samples. The correlations between the respective matrices were calculated. Here, a correlation function is formed between each parameter of the first matrix and the second matrix. The correlation functions thus determined form solution matrix the basis of the calibration.

The solution matrix forms the basis of the system calibration. For the validation of the model the samples were tested with the laboratory equipment. The signals of the 15 samples with different ore grade were processed. The time signal of the samples was filtered and a spectral analysis was performed. After the spectral analysis, 528 properties were calculated from the signal. These are composed of frequency-dependent intensities, statistical values of the signal and machine parameters. A matrix was created from this data as explained above. Using the correlation matrix created in

the calibration stage, the online analysis was performed. The results of the online analysis were compared with the laboratory results. The results of the comparison of the respective methods are shown in Graph 13.2 and Table 13.4. The comparison of the results from the laboratory analysis and the online analysis shows a difference of 0.88 % to 19.77 %. The comparison of the deviation of the results from the laboratory and online analysis depending on the ore grade shows the same character as the results of the online method on basis of probability. The results of samples with a degree of purity of more than 50 % deviate between 0.84 % and 7.21 % from the laboratory results. For samples with a purity level of less than 50 %, the difference between laboratory and online results is higher. The deviation of these samples is between 1.97 % and 19 %.

The higher deviation of the results for samples with a purity level lower than 50 % seems to be characteristic. It occurs in both the online probability-based method and the online multivariate data analysis method. This phenomenon can be explained by the fact that when the anhydrite content is dominant, the signals resulting from the collision of gypsum with the oscillator are superimposed. This effect could especially occur with very fine gypsum grains. The signals resulting from the collision of the very fine gypsum with the oscillator are detected as noise.

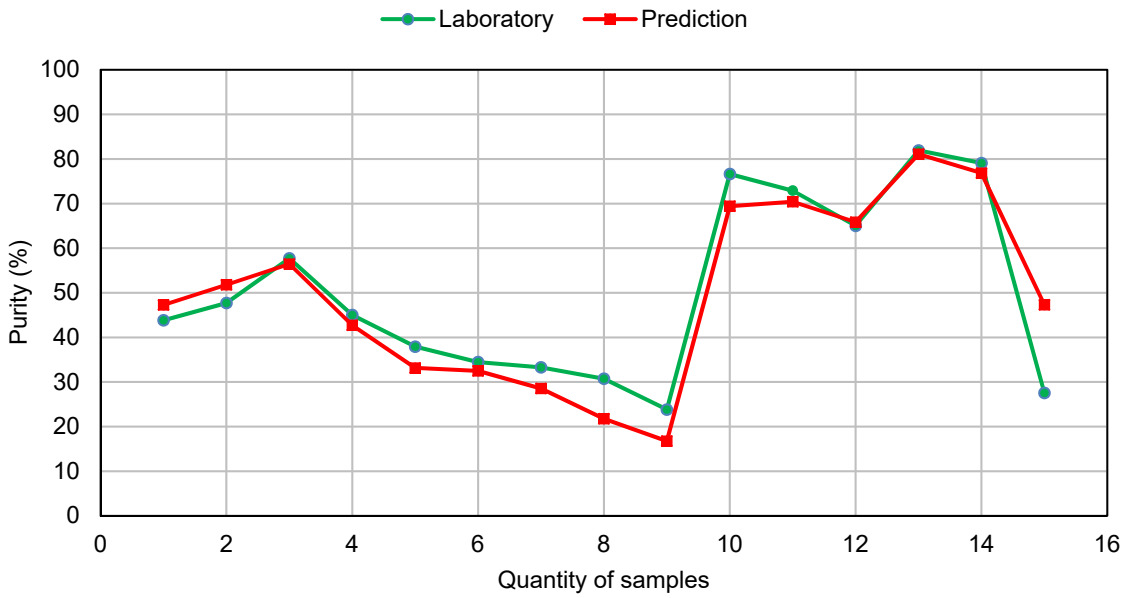

Graph 13.12: Comparison of the laboratory results with the results of the multivariate analysis

Table 13.4: Comparison of the laboratory results with the results of the multivariate analysis

Sample	Purity-Laboratory (%)	Purity-Online (%)	Deviation (Laboratory-Online)(%)
1	43.83	47.28	-3.44
2	47.72	51.80	-4.08
3	57.73	56.44	1.29
4	45.02	42.73	2.29
5	37.93	33.16	4.77
6	34.48	32.50	1.97
7	33.29	28.56	4.73
8	30.74	21.77	8.97
9	23.84	16.75	7.09
10	76.63	69.42	7.21
11	72.90	70.42	2.48
12	65.02	65.85	-0.84
13	81.92	81.08	0.84
14	79.09	76.83	2.26
15	27.55	47.32	-19.77

Table 13.5 shows the results of the laboratory tests and the results of the online methods. Both online methods are basically suitable for the quantitative analysis of samples. Although they show deviations in comparison to the laboratory results, the deviations are not high, especially for samples with a purity level of more than 50 %. This accuracy would be sufficient for online quality control in the mine. The comparison of the online methods shows that the results of the online analysis based on the probability algorithm differ less from the laboratory results.

Table 13.5: Comparison of the results of the laboratory analysis with the multivariate analysis and probability analysis

	Purity (%)				
Sample	Laboratory	Multi Correlation function	Deviation (Laboratory-MCF)	Probabilty	Deviation (Laboratory-Probability)
1	43.83	47.28	-3.44	39.60	4.24
2	47.72	51.80	-4.08	46.82	0.90
3	57.73	56.44	1.29	53.86	3.87
4	45.02	42.73	2.29	44.15	0.88
5	37.93	33.16	4.77	39.06	-1.13
6	34.48	32.50	1.97	44.32	-9.85
7	33.29	28.56	4.73	31.36	1.93
8	30.74	21.77	8.97	36.75	-6.01
9	23.84	16.75	7.09	12.32	11.52
10	76.63	69.42	7.21	77.70	-1.07
11	72.90	70.42	2.48	77.60	-4.70
12	65.02	65.85	-0.84	64.95	0.07
13	81.92	81.08	0.84	83.50	-1.58
14	79.09	76.83	2.26	82.20	-3.11
15	27.55	47.32	-19.77	38.08	-10.53

All laboratory tests confirm the hypothesis. By recording the signals generated by the collision between grains in a mass flow and an oscillator, it is possible to differentiate the materials online, provided that they have a difference in density. Furthermore, it was shown that the methods developed on the basis of the hypothesis also allow an online determination of the ore grade of a composite of substances if the mixture

consists of granules of different densities. The laboratory investigations were carried out with the aim to analyse the cuttings produced during drilling online. For this purpose, the laboratory device was designed in such a way that the flow of the cuttings is approximately simulated. The results of the laboratory tests have shown that the accuracy of the online analysis is sufficient for the application in the mine.

Based on the results of the laboratory investigations, the research was expanded and field tests were started. The field test was conducted in several stages. First, the basic principle and feasibility were validated. In two further test phases, the entire system was gradually optimized and tested.

14 Design of the online analyser for the field test

The design of the online analyser for the field test based on the experience with the laboratory device as well as the results of the laboratory tests. The system components for recording and processing the signals were chosen similarly to the electronics assembled for the laboratory device. In total the test system should have the following features:

- Continuous recording of the drill cuttings
- Classification of the drill cuttings
- Transporting the classified cuttings to a nozzle
- Dispersing the selected fraction during the drilling process
- Recording the measurement signals
- Electronic unit for signal processing
- Easy integration of the device into the drilling rig
- Low space requirement and compact design
- Possibility of connection to the power supply of the drilling rig

The implementation of the concept is basically simplified if the drilling rig itself has a classifier. This requirement is fulfilled by many modern drilling rigs, which are used especially in open-cast mining. With these drilling rigs, the cuttings are extracted directly after discharge to reduce environmental pollution and classified by dust collectors. The fine grain fraction of the cuttings is transported to a silo mounted on the vehicle. Depending on the type of machine, the coarse grain fraction is either separated in a cyclone or remains directly at the drilling site. The integration of the online analyser in such a device is relatively simple. Compressed air for dispersing and electricity for operating the electrical and electronic components are also supplied by the drilling machine. Additionally, an underground mine was selected for the basic validation of the developed system. The drilling equipment in this mine did not have all the features described above for an optimal test. However, the mine was located close to the research facility. Nevertheless, it was possible to test the basic suitability of the components there and, if necessary, to optimize them with little time expenditure. The machine intended for the test is shown in Figure 14.1.

Figure 14.1: The drill selected for the test

The main disadvantage of this drill is that it did not have a dust collector. Due to the construction of the drilling mast, it is not possible to install components in the front part of the mast. Therefore, the installation of an exhaust system was not possible there. Theoretically, a separate suction pipe could be installed next to the machine to collect the cuttings. The distance between the cabin and the front part of the mast was about 20 m. This variant was out of the question because the power supply of such a device cannot be extended. Furthermore, this drill rig had no data recording. Data such as drilling speed and bit load are not available for evaluation.

All in all, the concept in its optimal execution could not be implemented at this location. As a result, it was considered to modify the concept under consideration of the existing technical conditions in such a way that a first field application is possible. The analysis of the mass flow of cuttings during the drilling process shows that, due to the nature of the cuttings discharge, the material exits the borehole at high velocity. This process corresponds to a kind of dispersing. In this respect, the existing cuttings discharge could replace the dispersing system with limitations. In the realization of this modified and greatly simplified solution, the front bushing of the drill pipe guide, which is

attached to the outer end of the mast, was used as an oscillator. The sensor was placed behind the guide bush in a protected area. The connection between the sensor and the electronic unit is made via a likewise protected cable. The electronic unit was mounted in the area of the driver's cab. The solution is shown in Figure 14.2.

Figure 14.2: Position of the sensor in the field

14.1 Field test

The field tests were carried out at 5 different locations in the mine. At each location 6 drift face holes were drilled. The online measurement was performed during the entire drilling process. The drill cuttings produced during the drilling process were then collected. A representative subset of the drill dust was later examined in the laboratory with regard to the ore grade. The recorded signals were then processed. The tests were carried out without difficulty. The results were used to optimize the online analyser for further tests. In summary, the selected concept for the field test, including the measurement technology was confirmed. The test was carried out without interruption of the measurement and interruption of the drilling process. The signal acquisition and the transmission of the signals into the driver's cab was realized without any problems.

The data evaluation demonstrated that the developed signal processing unit and the algorithms allow an online determination of the ore grade during the drilling process. A first rough evaluation of the results showed that the deviation between the online measurement and the chemical analysis was less than 10 % in 90 % of the drillings. Only in 10 % of the drillings the deviation was greater than 10 %. This deviation was attributed to the type of sampling for laboratory analysis and to the variation of the machine parameters during the drilling process. These optimization approaches were considered for further field tests. The results are shown in Graph 14.1.

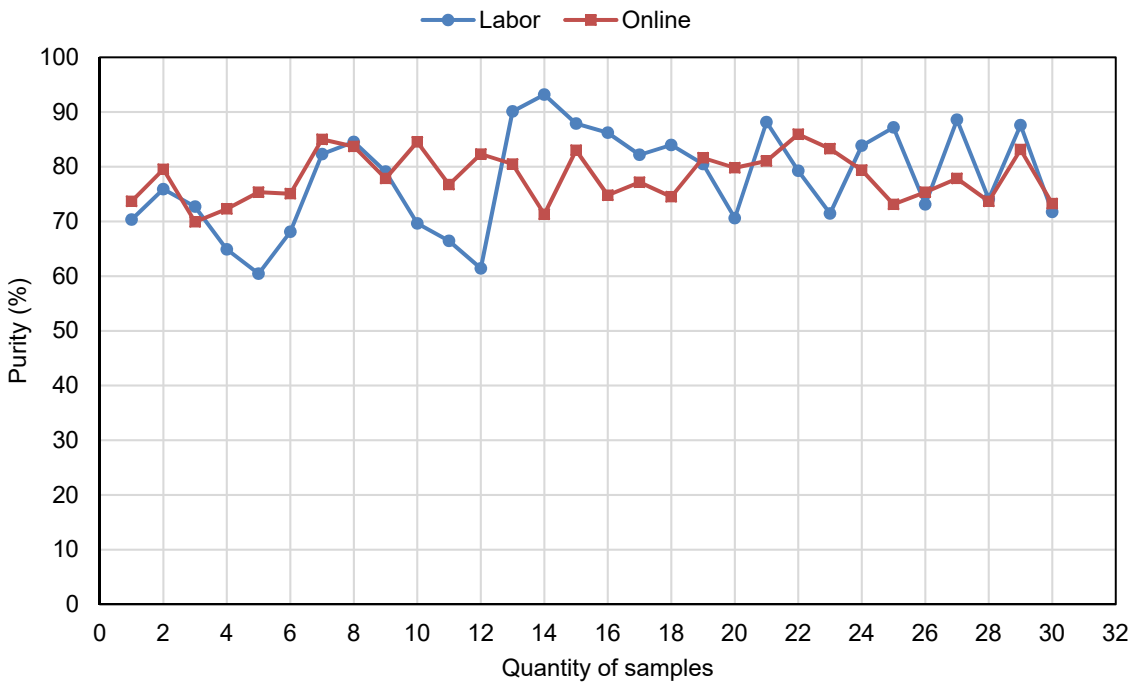

Graph 14.1: Results of the first field application

14.2 Extended field tests

In the first stage of the investigation, the basic feasibility of online analysis of the cuttings in the mine was demonstrated. The problem with this test series was that the drilling machine did not have a separator (classifier), nor did the machines record data such as drilling speed and bit load. For the second test stage, a drilling machine with these technical features was selected. The drilling machine was a wheeled drilling rig that was used in open pit and underground mining. Furthermore, the drill rig was equipped with a dust collector. The drill cuttings were then collected at the borehole by means of negative pressure. The cuttings ware later transported via a pipe to the dust collector. There the cuttings were collected and the air, which transports the cuttings

as a mass flow, was cleaned. At the end of the drilling process, the dust collector automatically opened. The drill cuttings discharged behind the drill rig and would fall to the ground. More than 90 % of the cuttings entered the dust collector. Only a small amount of the cuttings with a large grain remained on the surface at the drill hole. This resulted in a classification of the cuttings. The mass flow of the cuttings into the dust collector was similar to the mass flow of a Venturi nozzle. The basic requirements for the installation of the online analyser were automatically included in the drilling rig. The drilling rig with the dust collection system is shown in Figure 14.3.

Figure 14.3: Drilling rig with the dust collection system

The prerequisite for the integration of the online analyser into the drilling rig were given. The oscillator was mounted along the mass flow in the dust collector and the sensor mounted behind the oscillator. The installation of the oscillator with integrated sensor at the dust collector opposite the pipeline where the cuttings enter the dust collector creates the same technical condition as the designed laboratory analyser. Due to the negative pressure, the cuttings were accelerated and arrive at the exit point as a jet. The mass flow hit the oscillator in the dust collector, where the direction of the mass flow coincided with the piezoelectric axis of the sensor. The vibrations caused by the collision of the cuttings and the oscillator were transmitted relatively directly and over a short distance to the sensor. The sensor recorded the pulses and the acquired data

was sent to the signal processing unit and further processed with the help of the previously mentioned algorithms. The electronics for signal conversion and signal processing were located in the driver's cab and the electronic unit and the oscillator were connected with a cable. Figure 14.4 shows the dust collector and the position of the oscillator.

Figure 14.4: Oscillator in the dust collector

During drilling operations, the drilling unit automatically recorded the drilling depth and drilling speed as well as the bit load and the speed of the bit. The electronic unit of the online analyser as well as the algorithm were designed with the integration of the data of the machine into the software in mind. The machine data acquisition was performed every couple of seconds. After signal processing this data was used in combination with the data from the online analyser for material quality determination. Graph 14.2 shows the recoded machine data during drilling.

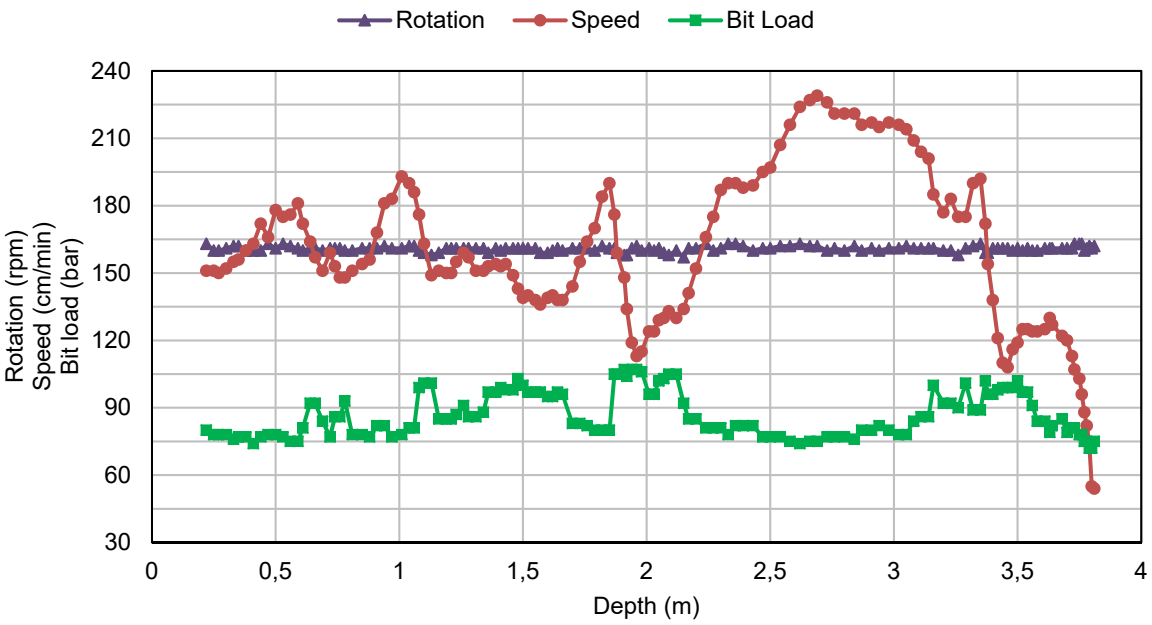

Graph 14.2: Machine data recorded during drilling

For the field test, the oscillator and electronics unit were mounted on the drill rig. The developed software for data evaluation, system calibration and data analysis were also installed on a mini computer integrated in the electronics box. An essential part of the software development process was the online acquisition of the machine data. Here the drilling speed, bit load and the speed of the bit during the drilling process, and the acoustic signals were acquired. The data was stored as a basis for later normalization of the signals and final evaluation. After the first test, in which the concept and feasibility of the online analyser was validated, the field test began. For this purpose, the drilling rig was driven onto a gypsum deposit. After the overburden was pushed off, 8 boreholes with a borehole depth of 4 m each were drilled there. At each of the 8 boreholes the drilling rig was stopped after a defined depth, the dust collector was opened and the cuttings collected in the dust collector were removed. The removed cuttings were homogenized and a part of them was taken for laboratory tests. The samples were packed in airtight containers. Part of each sample was retained for possible checks. A total of 24 samples were taken during this field test. These samples represented the average quality of the deposit in the drill intercept from which the samples were taken. Throughout the test phase, the sensor signals and machine data were recorded. Table 14.1 shows the drilling depths and purity line of samples.

Table 14.1: Description of the samples with drilling depth and purity

Borehole	Sample	From (m)	To (m)	Purity (%)
1	1	0.21	2.21	90.98
	2	2.27	3.15	46.02
2	3	0.22	3.81	84.10
3	4	0.22	1.98	78.51
	5	2.07	3.87	84.96
4	6	0.21	1.99	78.32
	7	2.06	2.98	95.67
	8	3.06	3.83	84.77
5	9	0.22	0.99	80.57
	10	1.08	2.00	79.99
	11	2.05	2.98	96.19
	12	3.06	3.73	88.50
6	13	0.21	0.98	68.48
	14	1.06	2.00	95.71
	15	2.07	2.98	95.95
	16	3.06	3.86	59.11
7	17	0.23	1.09	79.18
	18	1.16	1.98	78.61
	19	2.08	3.01	93.52
	20	3.08	3.55	81.86
8	21	0.22	1.02	82.00
	22	1.09	1.99	83.34
	23	2.08	2.97	94.85
	24	3.07	3.91	72.59

14.3 Evaluation of the field test data

To optimize the interpretation of the signal intensities, the samples were examined for their particle size distribution in addition to the chemical analysis. In Graph 14.3 the results of the Particle size analysis for three samples are exemplarily shown.

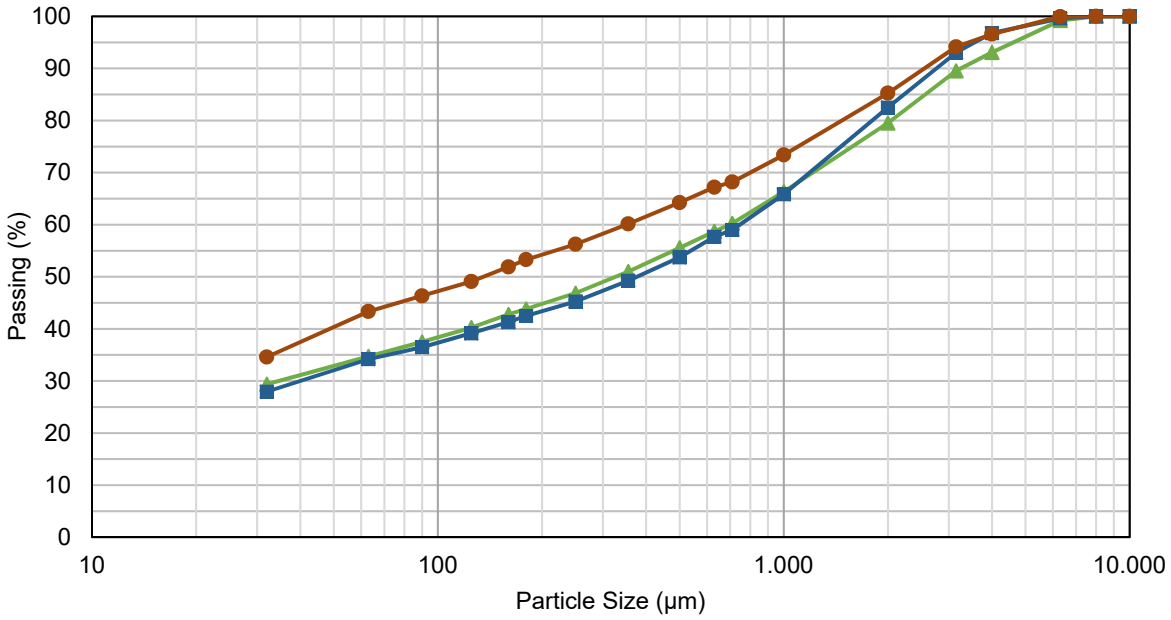

Graph 14.3: Particle size analysis of the samples

The samples showed a similar particle size distribution. The relatively equal grain spectrum of the samples showed that the dust collector of the drilling rig works almost constantly. About 50 % of the drill cuttings had a grain size smaller than 200 µm. 75 % to 80 % of the cuttings were smaller than 2000 µm. About 90 % of the cuttings were smaller than 3000 µm. For the signal evaluation it was important that only about 2 % of the cuttings were larger than 5000 µm. These particles generated high signal intensities. They were generated randomly and had no particular influence on the evaluation. In signal processing, these signal groups can be recognized as outliers and filtered out.

During the test the machine data was recorded every second and filtered for data analysis. This included the speed of the bit, the drilling speed and the bit load. Here, only data recorded during the drilling process was used. The results of the analysis were shown as an example for a drilling in Graph 14.2. The speed of the bit was approximately constant during the drilling process. The drilling speed varied considerably, fluctuating within the limits of 105 cm/min and 225 cm/min. The bit load was anti-proportional to the drilling speed and fluctuated between 75 bar and 107 bar. The correlation between bit load and drill speed is shown in Graph 14.4. The change in bit load and drill speed is an indicator for a change in the axial compression strength in the deposit.

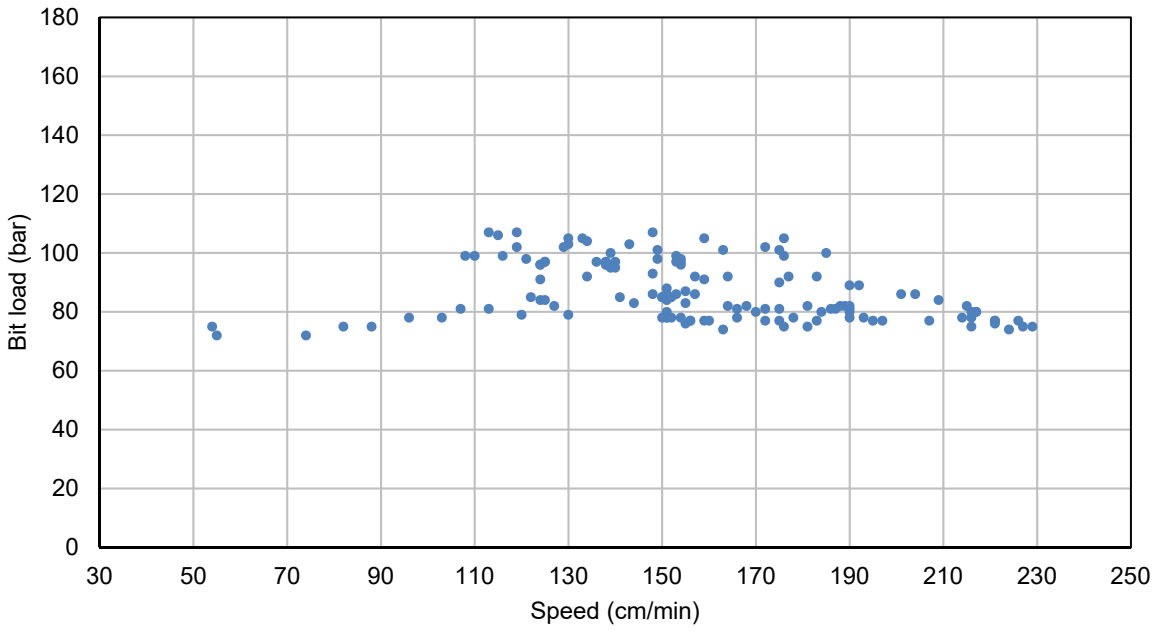

Graph 14.4: Correlation between bit load and drill speed

The laboratory tests have shown that the concentration of the grains in a mass flow has a significant influence on the signal intensity. This effect must be considered in the signal analysis. The change of the mass concentration during the drilling process can be described as follows: The borehole diameter remains constant during the entire drilling process. Thus, the volume of the rock, which is drilled through in a unit of time, is significantly dependent on the drilling speed. The cuttings are the result of the cutting process and are transported out of the borehole with compressed air. The volume of compressed air always remains constant. Thus, the concentration changes depending on the drilling speed. In this respect, a normalization of the intensity via the drilling speed is necessary for the signal processing. Graph 14.5 shows the normalized RMS values for all drillings in a time frequency of 0.2 seconds.

Some very strong intensities were filtered out of the standardized values. Such signals are either caused by a collision of a coarse grain that randomly hits the oscillator, or are generated by the dynamics of the machine. The adjusted intensities are between zero and 0.5. In Graph 14.6 the correlation between the degree of purity of the samples and the normalized RMS values is shown. The general correlation between sample quality and signal properties is shown. However, there is no linear dependency between the values as shown in the laboratory test. A very strong linearity was found in the laboratory test. This linearity probably does not occur in the field test because composite samples are present.

The samples were always taken after 0.5 m to 3 m drilling because of the nature of the drilling process. The drill cuttings from this drilling section were collected in the dust collector. This sample was then taken and chemically analysed. It cannot be expected that the average intensities of a drill section correlate linearly with the average quality of the borehole section.

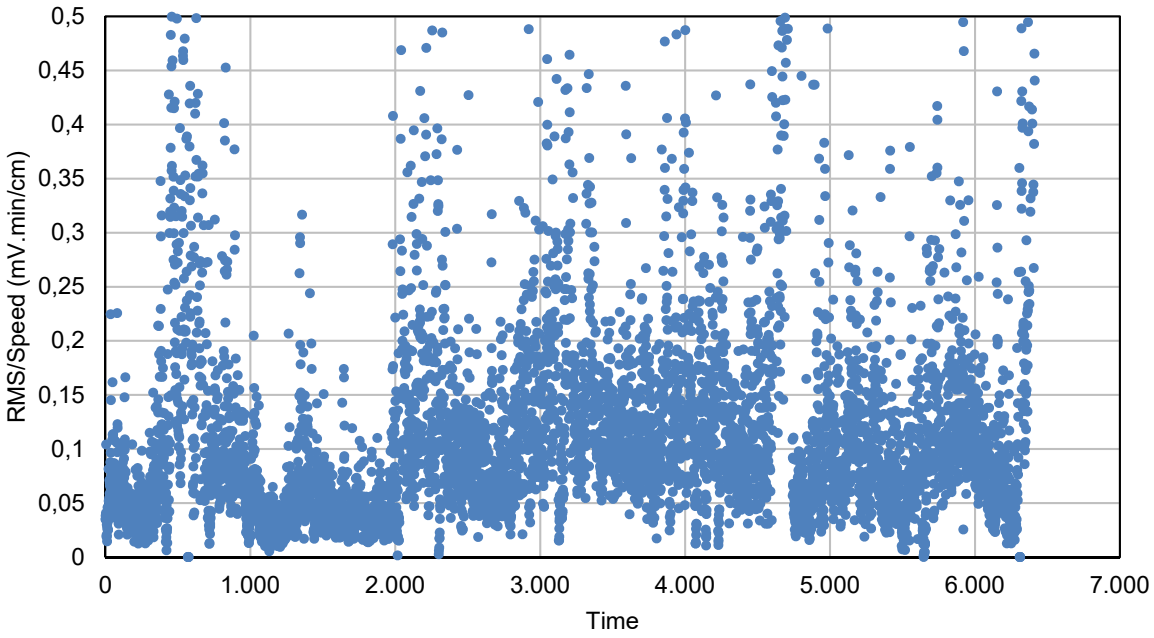

Graph 14.5: Normalized RMS of the signal for all samples in a time frequency of 0.2 seconds

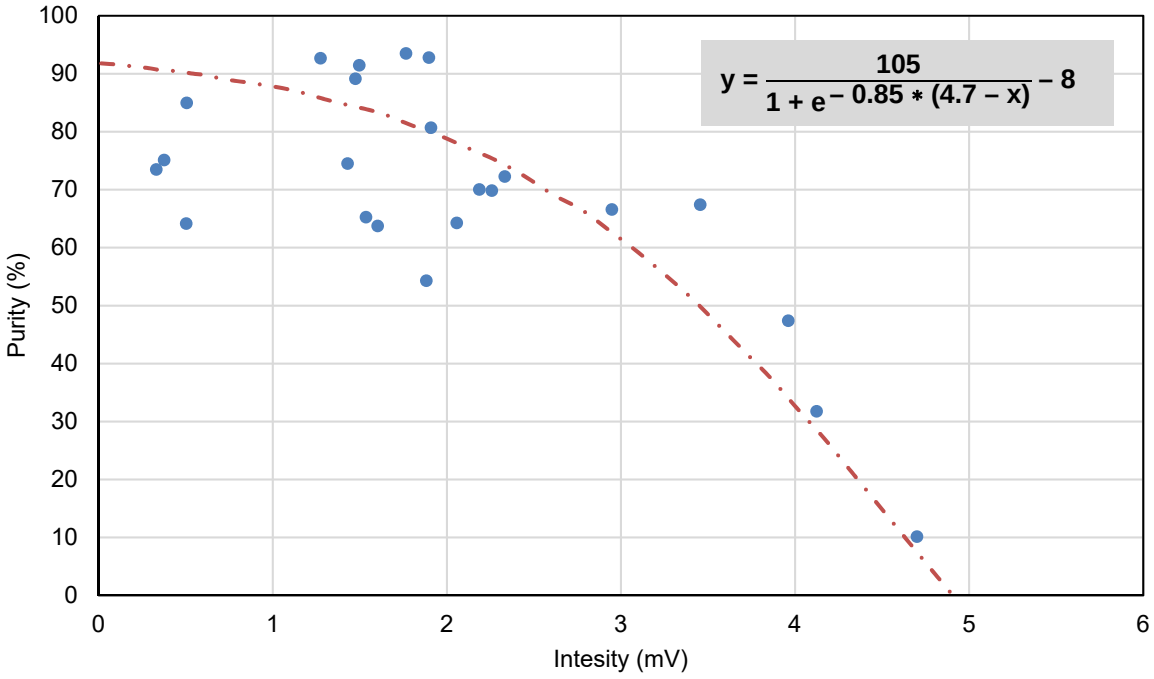

Graph 14.6: Relationship between the degree of purity and the standardized RMS signal values

The recorded and normalized signals were processed using two different methods similar to the results of the laboratory tests. The first method based on the so-called multivariate data analysis, while the second method based on statistical probability. In signal processing, the time signals were filtered after a spectral analysis and the determination of the energy density of the signals. The filtered time signals were then subjected to a Fourier transformation and over 500 signal properties were calculated.

The group of signal properties includes the signal intensity for certain frequencies and the RMS value for the entire filtered spectrum. This data was analysed with the PCR method and the correlation matrix for the calibration was calculated. Graph 14.7 shows the course of the signal intensity during the drilling process for the same hole as described above.

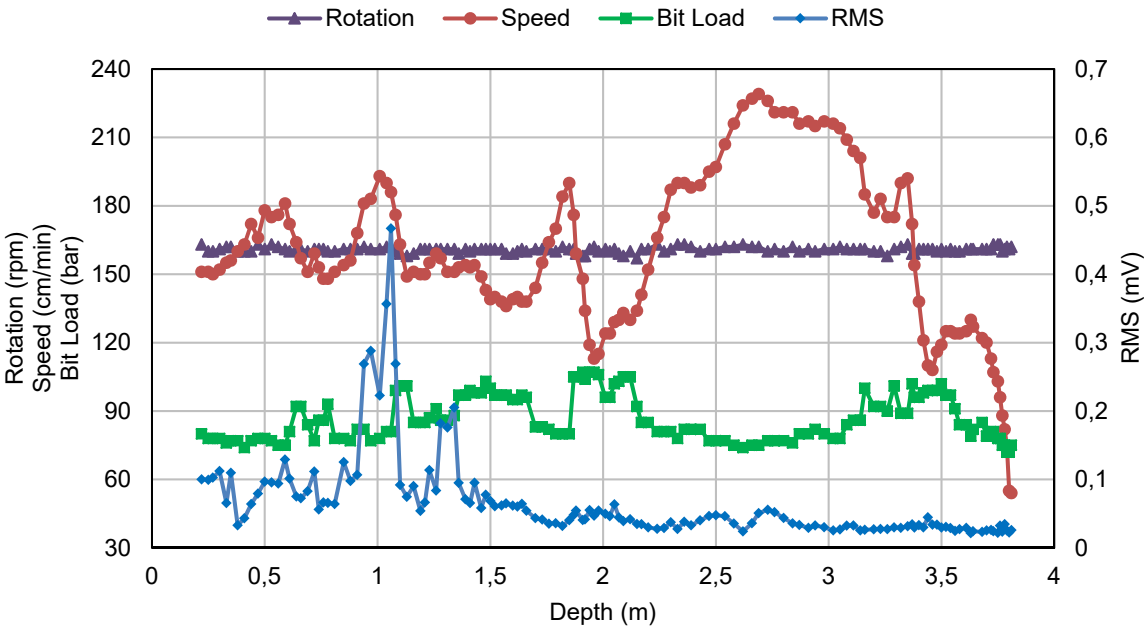

Graph 14.7: Machine data for hole 2 with RMS values

The RMS values remain low and relatively constant during the first 2 m depth. At about 2.75 m depth and 3 m depth they form two maxima. In the second method, the normalized signal intensities were calculated for every 200 milliseconds. These data were then classified and the distribution determined. In Graph 14.8 the distribution of the signal intensities is shown in a histogram.

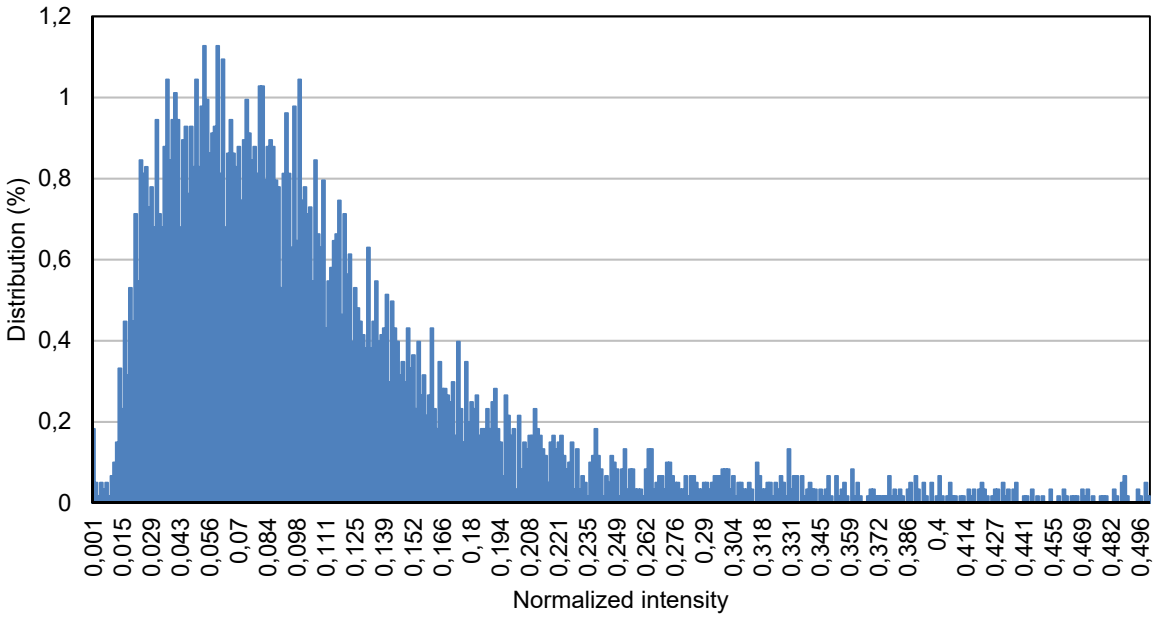

Graph 14.8: Distribution of normalized signal intensities for all samples

For the calculation of the calibration function, the samples were divided into 6 quality groups. The groups consisted of a group with purities of less than 46 %, a group with purities of 59.1 %, a group with purities of 68.5 %, a group with purities between 72 % and 80 %, a group with purities between 80 % and 90 % and a group with purities of more than 90 %. For these groups the distributions were determined from the normalized signals and probability plots were prepared. In Graph 14.9 the probability plots of the intensities of the respective groups are shown. Similar to the signal evaluation of the samples during the laboratory test, the probability was calculated with a cut off of 30 %. Graph 14.10 shows the probability for more than 30 %. The curves of the probability distributions were then smoothed and displayed in another diagram as a calibration function. The calibration function is shown in Graph 14.11.

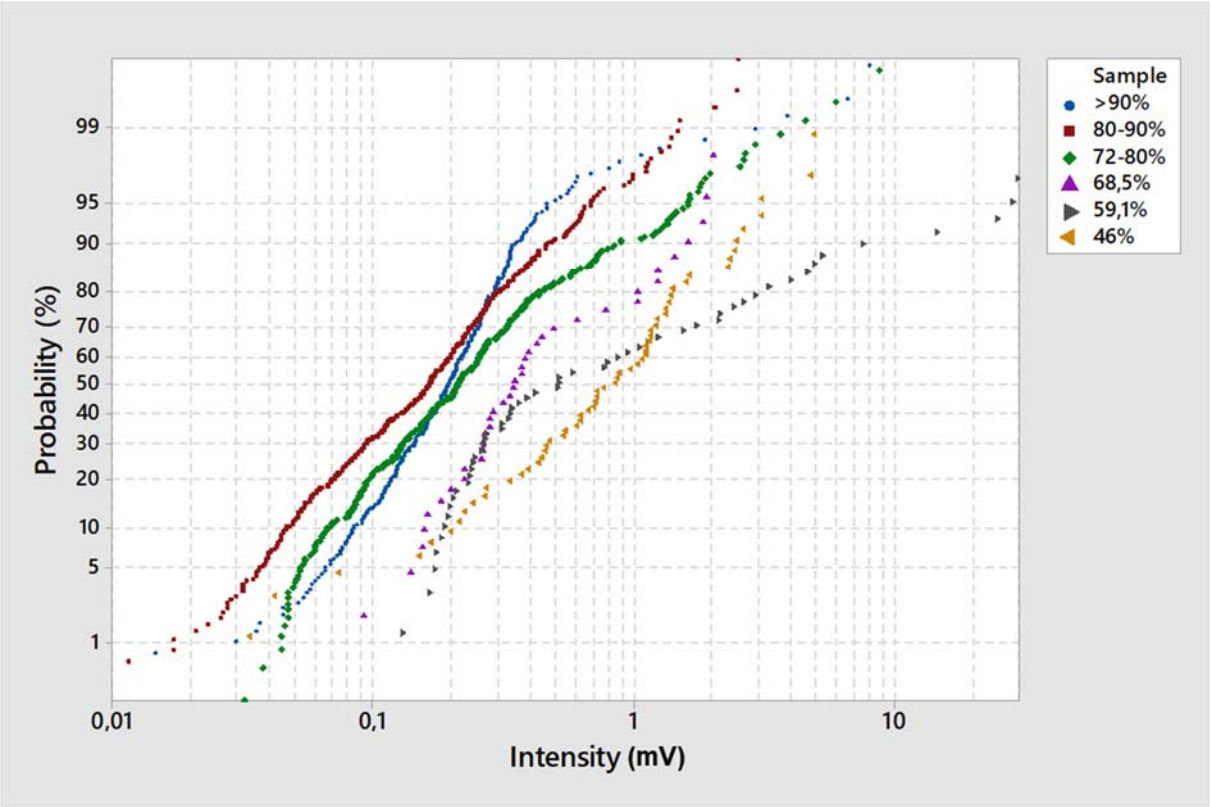

Graph 14.9: Probability Plot by quality groups

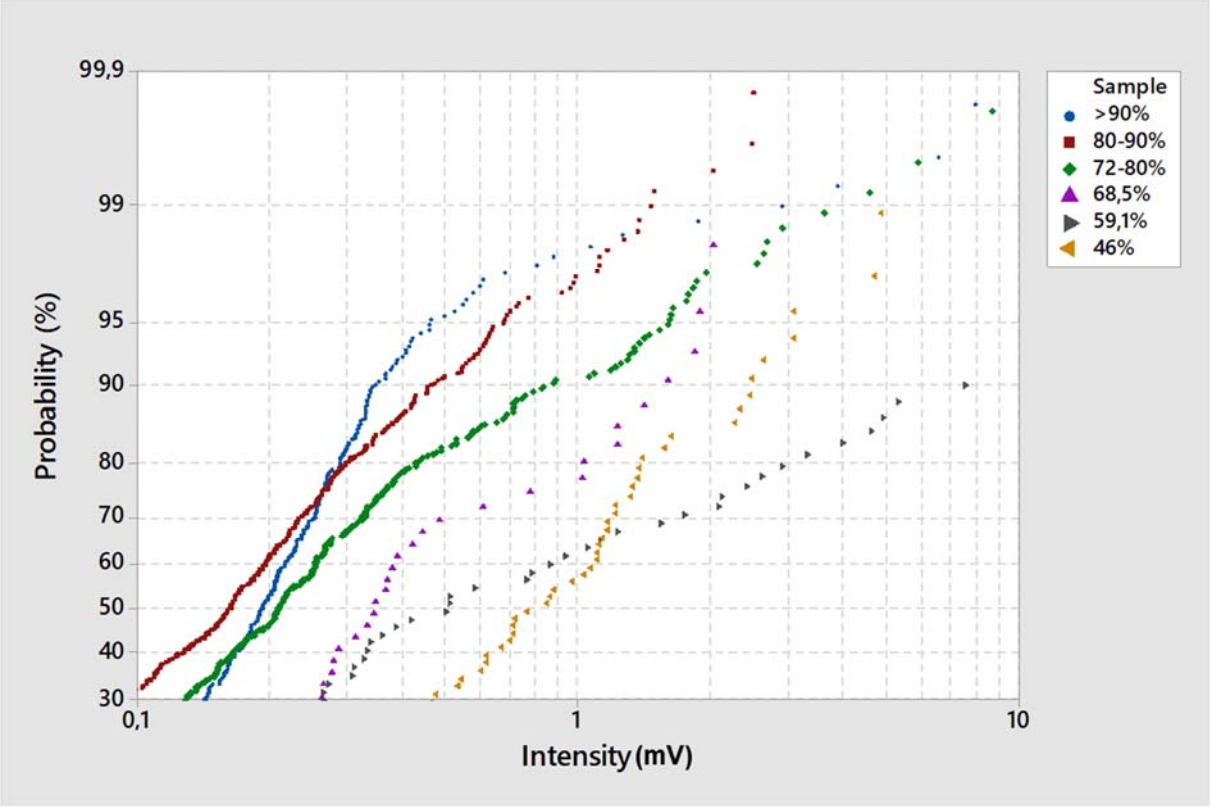

Graph 14.10: Probability Plot for sample groups at a cut-off of 30 % probability

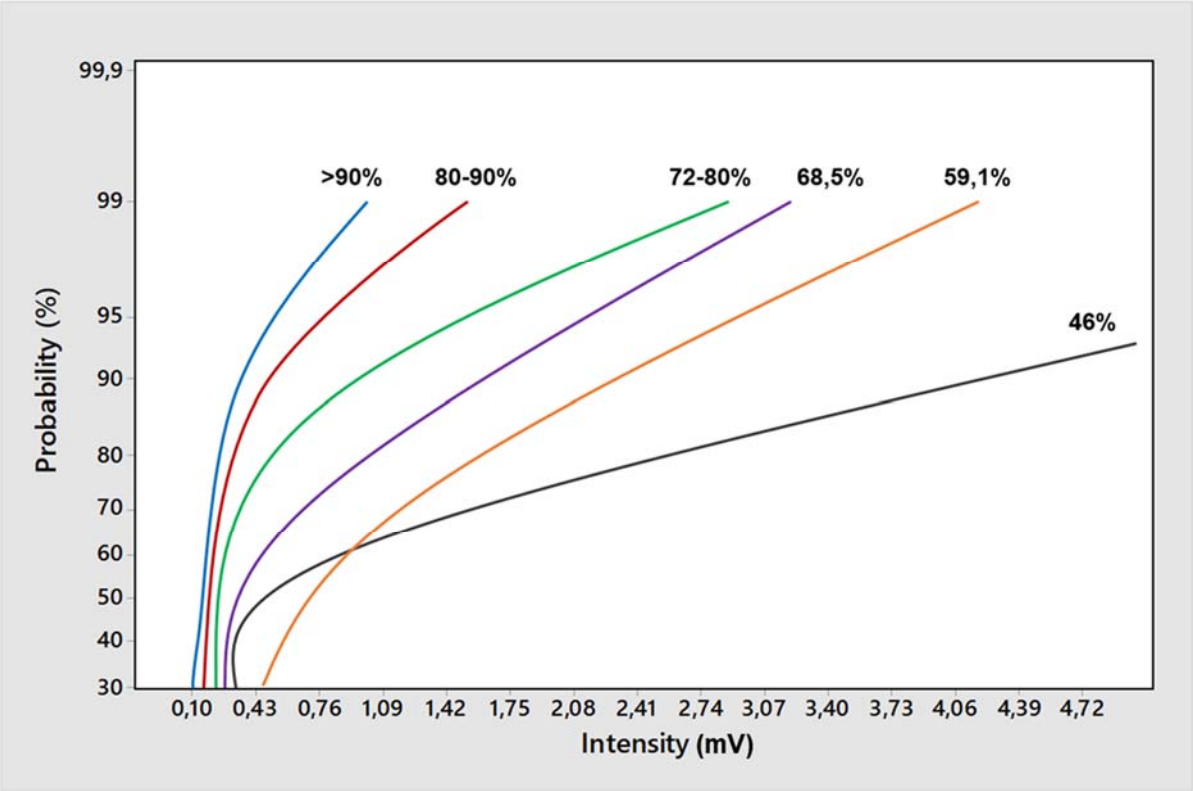

Graph 14.11: Interpolation graphs for Probability Plot at a cut-off of 30 % probability

14.4 Validation of the field test calibration algorithms

For the validation of the respective algorithms, 15 additional samples were used. The samples were first chemically analysed and the ore grade determined. The degree of purity of the samples was between 73.9 % and 88.52 %. The degree of purity of the samples is shown in Table 14.2. The signals of the samples were then normalized and processed as described above. In the first stage, the generated algorithm based on multivariate data analysis was used for the online analysis. The results of the validation are shown in Graph 14.12. The results of the online analysis are generally consistent with the chemical analysis. The differences between the results of the chemical analysis and the online analysis are between 2.19 % and 8.29 %, as can be seen in Table 14.3. Considering that, as mentioned above, these are composite samples from drill cuttings, the results are satisfactory and this accuracy is sufficient for online quality control in the mine.

Table 14.2: Purity of 15 validation samples

Sample	Purity-Laboratory (%)
1	70.85
2	88.52
3	76.63
4	72.50
5	73.20
6	74.50
7	82.60
8	82.66
9	77.53
10	81,78
11	69.50
12	82.39
13	88.10
14	63.79
15	80.59

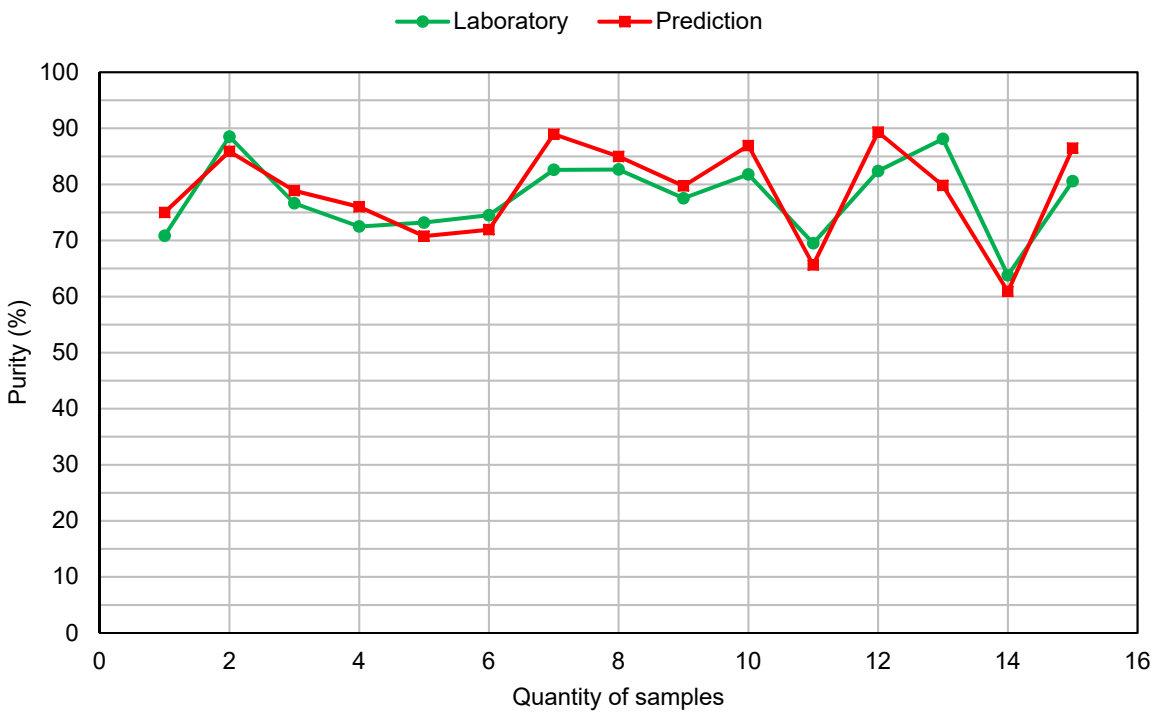

Graph 14.12: Comparison of the chemical analyses with the results of the multivariate method

Table 14.3: Comparison of the chemical analyses with the results of the multivariate method

Sample	Purity-Laboratory (%)	Purity-Online (%)	Deviation (Laboratory-Online) (%)
1	70.85	75.00	-4.15
2	88.52	85.88	2.64
3	76.63	78.88	-2.25
4	72,50	76.01	-3.51
5	73.20	70.76	2.44
6	74.50	71.92	258
7	82.60	88.95	-6.35
8	82.66	84.98	-2.32
9	77.53	79.72	-2.19
10	81.78	86.92	-5.14
11	69.50	65.64	3.86
12	82.39	89.32	-6.93
13	88.10	79.81	8.29
14	63.79	60.90	2.89
15	80.59	86.46	-5.87

In the second stage, the validation of the algorithm according to statistical probability was carried out. First, the probability plots of the measured signals of the 15 samples were created. Then the intensities of the respective samples were calculated at a probability of 90 %. These values were inserted into the previously created probability calibration curves and the degree of purity was determined. The result of the validation is shown in Graph 14.13 and Graph 14.14. The results show the fluctuations in the sample qualities very well. The deviation between the chemical analysis and the online analysis is between 1.42 % and 10.53 %. However, the absolute deviation is relatively high at 10 %. Nevertheless, the accuracy of the analysis for quality management in the mine is within the tolerable range, see Graph 14.15 and Table 14.4.

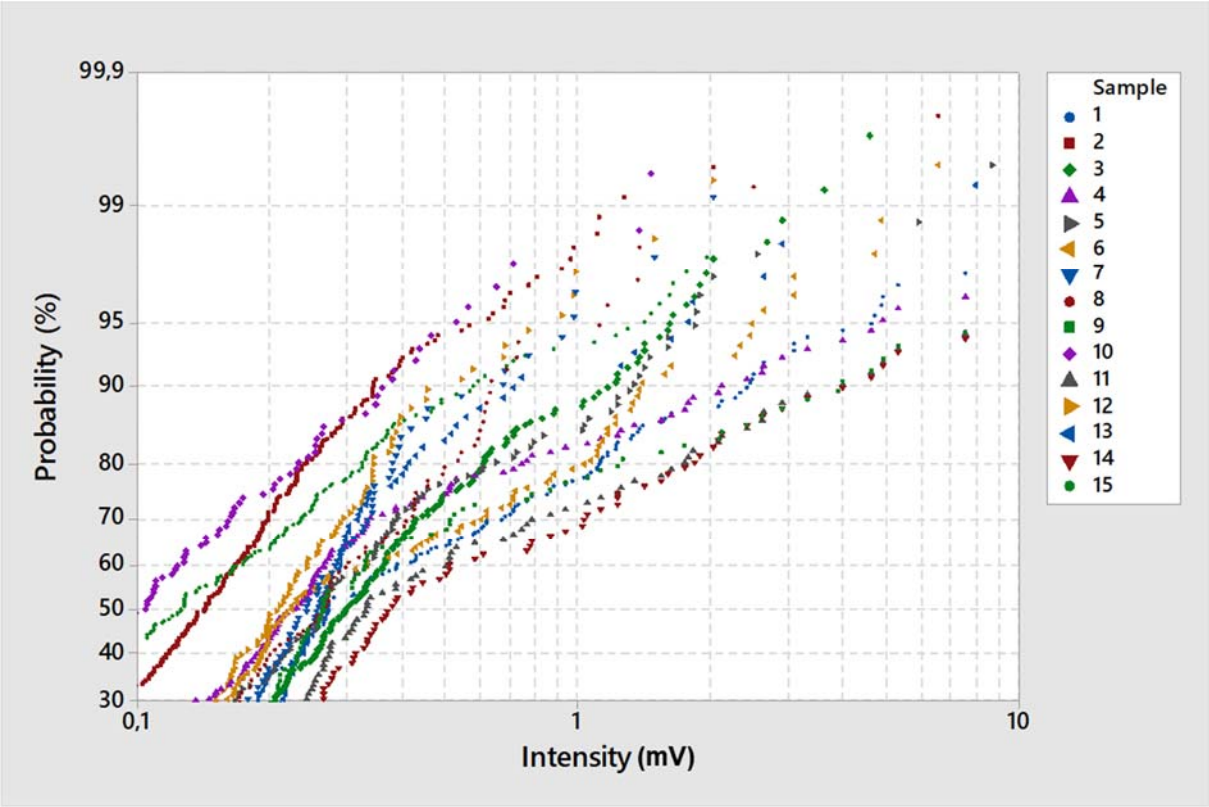

Graph 14.13: Probability Plot at a cut-off of 30 % probability

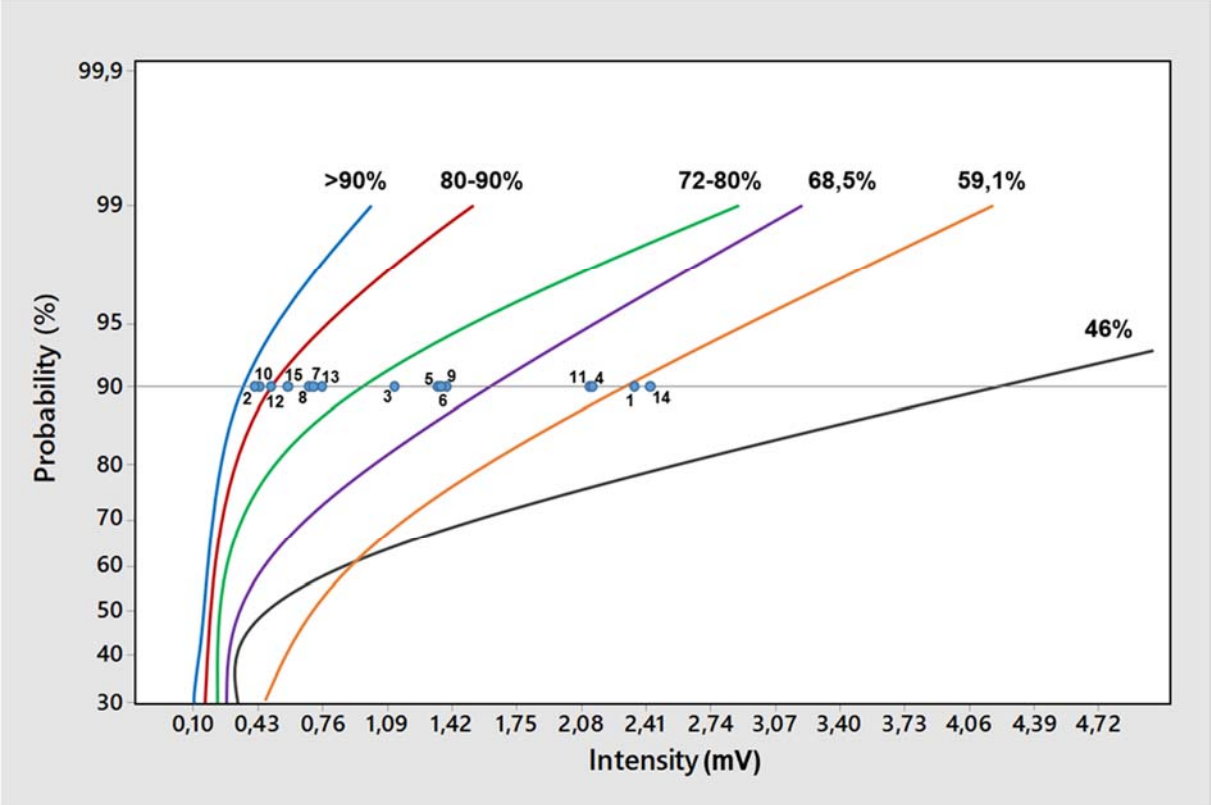

Graph 14.14: Intensity of the signals of the samples at a probability of 90 % entered in the calibration curves

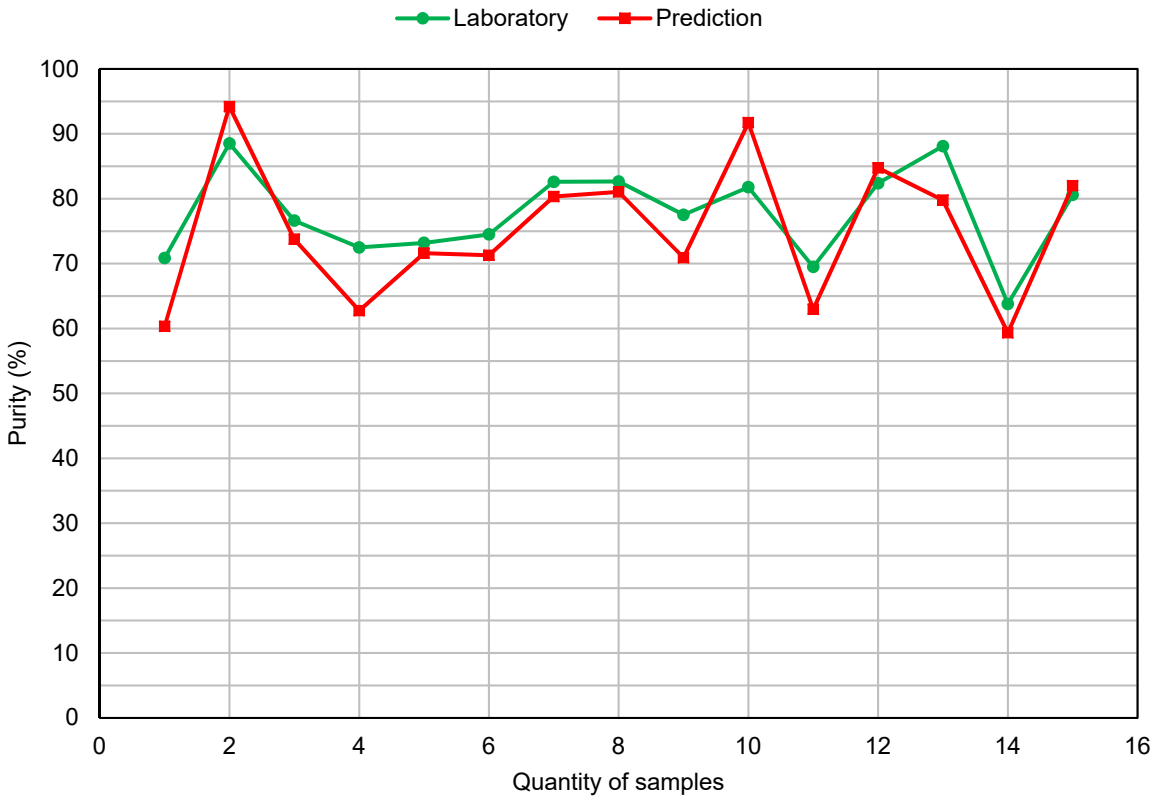

Graph 14.15: Comparison of the chemical analyses with the results of the probability method

Table 14.4: Comparison of the chemical analyses with the results of the probability method

Sample	Purity-Laboratory (%)	Purity-Online (%)	Deviation (Laboratory-Online) (%)
1	70.85	60.32	10.53
2	88.52	94.20	-5.68
3	76.63	73.77	2.86
4	72.50	62.76	9.74
5	73.20	71.62	1.58
6	74.50	71.28	3.22
7	82.60	80.34	2.26
8	82.66	81.05	1.61
9	77.53	70.91	6.62
10	81.78	91.71	-9.93
11	69.50	62.97	6.53
12	82.39	84.76	-2.37
13	88.10	79.78	8.32
14	63.79	59.33	4.46
15	80.59	82.01	-1.42

14.5 Summary of the field test

The field tests have shown that the developed online analyser is suitable for use in the mine. The analyser can be easily attached to a drilling machine. The idea to use the flow of the cuttings in a dust collector for the collision of the cuttings with the oscillator has been confirmed. The flow is very similar to the discharge from a Venturi nozzle.

The cuttings flow with high velocity into the dust collector and collide with the oscillator. The position of the oscillator results in the generation of sufficiently intensive signals. The integration of the electronic unit into the machine was possible without any problems. For the accuracy of the analysis it is important to use the machine data. The combination of the signals from the collision of the cuttings with the oscillator and machine data is useful. For the calibration of the online analyser both the method of statistical probability and the method of multivariate data analysis can be used. The validation results have shown that both algorithms are suitable for online analysis. The accuracy of the algorithm based on multivariate data analysis is higher. The comparison of the results is shown in Table 14.5. It is possible to increase the accuracy of the analyser. For this purpose, the calibration data should be extended. Overall, the results of the field test confirm the scientific research hypothesis.

Table 14.5: Comparison of the results of the chemical analysis and online methods

	Purity (%)				
Sample	Laboratory	Multi Correlation function	Deviation (Laboratory-MCF)	Probability	Deviation (Laboratory-Probability)
1	70.85	75.00	-4.15	60.32	10.53
2	88.52	85.88	2.64	94.20	-5.68
3	76.63	78.88	-2.25	73.77	2.86
4	72.50	76.01	-3.51	62.76	9.74
5	73.20	70.76	2.44	71.62	1.58
6	74.50	71.92	2.58	71.28	3.22
7	82.60	88.95	-6.35	80.34	2.26
8	82.66	84.98	-2.32	81.05	1.61
9	77.53	79.72	-2.19	70.91	6.62
10	81.78	86.92	-5.14	91.71	-9.93
11	69.50	65.64	3.86	62.97	6.53
12	82.39	89.20	-6.93	84.76	-2.37
13	88.10	79.81	8.29	79.78	8.32
14	63.79	60.90	2.89	59.33	4.46
15	80.59	86.46	-5.87	82.01	-1.42

15 Summary and outlook

One of the most important tasks of mining and processing is the control of ore grade. The most efficient use of deposits and maximizing economic profit depends on the effectiveness of ore recovery. This can be achieved by reducing ore dilution and achieving sustainable ore grade control. The determination of the ore grade starts with the exploration of a deposit and continues throughout the life of the mine. While the determination of the ore content in the exploration phase is the basis for the calculation and classification of resources, the ore grade control in the mining phase is carried out continuously to validate the predicted ore content and to control the entire process chain from the extraction of raw materials to the processing and production of the final product. In the mining phase, samples are taken from the mine face, from cuttings from blast holes, from the muckpile, from the stockpiles and during the processing, crushing, sorting, classifying and so on. All these measures are aimed at increasing ore recovery, optimising the treatment processes and thus reducing costs. Manual sampling and analysis is time consuming and costly. For this reason, online analysers are sometimes used in mining, which are usually designed according to the radiation measurement principle. The main disadvantage of these analysers is their sensitivity to dust, vibrations and atmospheric influences such as temperature and humidity. Furthermore, the application of these technologies is limited due to radiation. The development of an online analyser without these disadvantages is one of the most important tasks in mining and processing. Ideally, an online analyser to be developed for use in mining should be used at the beginning of the process chain. In this case the information about ore grade is available relatively early. In this way the processes could be controlled in time. The development of such an online analyser is the subject of this thesis. Based on the state of the art a hypothesis for the development was made. The hypothesis assumes that in a mass flow of grains the ore grade can be determined by passive acoustic measurement, provided that the ore and waste have different densities. The objective of the development was to implement such an analyser in the drill rig to measure the ore grade of the cuttings.

Online analysis of the drill cuttings would provide tremendous support for exploration and ore grade control. In open pit mining, on average one blast hole is drilled per five hundred tonnes of ore. In open pit mines, more than ten thousand drill holes are drilled annually.

The hypothesis was tested in several successive stages. First, the basis of the acoustic measurement was explained.

To determine the necessary requirements for the online analyser, the influences of the material and the mass flow on the passive acoustics were determined on a theoretical basis. In addition, the necessary configuration of the electronics for signal acquisition, signal processing and methods of data classification was determined. Based on this information, an online analyser was designed for laboratory use. The online analyser is designed to simulate the flow conditions of the cuttings in the borehole. The sample to be analysed is sucked from a container through a venturi nozzle and mixed and accelerated with the compressed air. The accelerated air-solid mixture hits the oscillator. A sensor is mounted in the oscillator. As a result of the collision of the sample with the oscillator, vibrations are generated which are recorded by the sensor and sent to the electronic unit for signal processing. The signals are evaluated by software after processing. After a preliminary calibration, the processed signals are converted into ore grade with the software. Two different algorithms were developed for the evaluation. One algorithm is based on the statistical probability calculation, the second algorithm was developed according to the principle of multivariate data analysis.

The individual components of the analyser were selected and dimensioned on the basis of theoretical investigations. The laboratory tests were carried out with gypsum, anhydrite and dolomite and mixtures of these minerals. After the basic verification of the hypothesis, the previously theoretically worked out influences of the grain size, the grain size distribution, the velocity and concentration of the mass flow as well as the moisture were determined in several tests. These test series confirms the hypothesis. An online determination of gypsum and anhydrite or dolomite is possible provided that the particle size of the gypsum particles does not exceed 18 % of the particle size of the anhydrite or dolomite. This detection limit results from the difference in density between the respective materials of about 0.52 kg/cm³. The greater the difference in density of the materials, the more the grain size of the materials can differ. In the second stage of the research, investigations were carried out to determine ore grade. For this purpose, samples of gypsum and anhydrite of different purity were prepared in the laboratory. The investigations show that, depending on the algorithm used, the results of the online analysis and chemical analysis of the samples vary between 0.07 % and 11.52 % and 0.84 % and 19.77 % respectively. In 87 % of the analyses

the deviations between online analysis and laboratory are less than 8 %. In 73 % of the cases the deviation is even less than 5 %.

Based on the experience with the laboratory online analyser and the results of the test series, an online analyser for field tests was designed. The analyser was installed in the dust collector. The drill cuttings produced during drilling hit the oscillator at high speed. A sensor, which is integrated in the oscillator, records the oscillations that occur because of the collision. The signal processing takes place in the electronic unit, which is integrated in the driver's cab. The processed signals are transmitted wirelessly to a computer. With the developed software the ore grade is calculated. Compared to algorithms developed for the laboratory unit, the algorithms for analysis in the field consist of an extended model in which the machine data are recorded every second. The machine data includes drilling speed, drilling force and bit rotation speed. This data is used to normalize the sensor signals.

In a first phase the online analyser was tested in an underground gypsum mine for its mechanics and electronics. Afterwards the Online Analyser was integrated into a drilling rig to produce blast holes in a gypsum open pit mine. The field tests were carried out in two stages. In a first series of tests 8 boreholes were drilled. From the drillings 24 samples were taken. These samples were chemically analysed in the laboratory and used as a basis for the calibration of the online analyser. After the calibration of the analyser, 15 further drillings were carried out in a second stage. The drill cuttings were analysed online, and the ore grade of the gypsum was determined. For validation, samples were taken from the dust collector and analysed in the laboratory. The online analysis was again carried out with both algorithms. The comparison of the results shows that the online results based on the multivariate data analysis differ between 2.25 % and 8.99 % from the laboratory analysis. 66 % of the results deviate less than 5 %. The results of the online analysis based on statistical probability differ between 1.42 % and 10.53 % from the laboratory results. In this case, the results of 53 % of the analysis deviate less than 5 % from the laboratory results.

These deviations are not absolute values, but relative values. There are many reasons for this. In laboratory analysis, only a few grams of sample are analysed. The samples come from the dust collector. An absolute homogenisation of the whole cuttings before sampling is not possible. It cannot be excluded that the cuttings from a drill hole in the dust collector are contaminated with the remains of cuttings from previous drill holes

still in the dust collector. Considering the fact that the online analyser analyses the entire cuttings and that contamination with other substances can be excluded due to the analysis method, the results of the online analysis are good, and the determined deviation is tolerable. Currently one drilling rig is equipped with the developed online analyser. Data is continuously recorded, and the ore grade is calculated online. In this phase the analyser will be tested for its availability. Afterwards the developed analyser will be installed in further drilling rigs. In addition, implementations of the online analyser are being tested in processing. The combination of the online analyser with the drilling rig allows an early detection of the ore grade. Before the ore is blasted and processed, information about the ore grade is available. From this information, dynamic online deposit modelling can be performed. The control of the ore grade enables the optimization of the entire process chain in mining and processing. Because the analysis with the developed analyser is based on the density difference of materials, the analyser is suitable for ore grade determination in metallic deposits. However, when used in polymetallic deposits, the analyser will only calculate the percentage of ore without detailed information on the individual components.

16 Bibliography

[1] Polytec GmbH (2007) Prozesskontrolle mit NIR-Spektroskopie. Berlin. Polytec GmbH

[2] Shankar, V. (2015) Field Characterization by Near Infrared (NIR) Mineral Identifiers. Procedia Earth and Planetary Science 11, 198–203

[3] Himmelsbach, C.; Thalmann, C.; Petitat, M. et al. (2014) Online Analysis Technologies. DRAGON

[4] Vinzelberg, G. (2008) Laserinduced Fluorescence as Sensor for Mining Dissertation. Fakultät für Georessourcen und Materialtechnik. Rheinisch-Westfälische Hochschule Aachen. Aachen

[5] Pavićević, M.K.; Amthauer, G. (2000) Mikroskopische, analytische und massenspektrometrische Methoden. Stuttgart, Schweizerbart

[6] Fricke-Begemann, C.; Jander, P.; Wotruba, H.; Gaastra, M. (2010) Laser-based online analysis of minerals. Zement, Kalk, Gips International 63, 65–70

[7] Ekkhart, M. (2008) Grundlagenuntersuchung der Möglichkeiten einer Online Analyse mit Hilfe der Laser induzierten Plasmaspektroskopie (LIPS) am Beispiel von Kalkstein Dissertation. Fakultät für Energie- und Wirtschaftwissenschaften. Technische Universität Clausthal. Clausthal Zellerfeld

[8] Khodkar, A. (2009) Untersuchung zur Optimierung der Lagerstättenerkundung mittels Analyse des Bohrkleins. 1. Aufl. Clausthal-Zellerfeld, Papierflieger

[9] Schwedt, G.; Schreiber, J. (1996) Taschenatlas der Analytik. 2. Aufl. Stuttgart, Thieme

[10] Dhanjal, S.K.; Young, L.; Storer P. (2006) Automatic Control of Cement Quality using On-Line XRD. Piscataway, NJ, IEEE Operations Center, 289-305

[11] Evans Analytical Group (2009) TN 109 EAGLABS X-ray Diffraction (XRD) Services Technique Note. Sunnyvale. Evans Analytical Group

[12] Foster, S.; Bond, J. (2006) The history and future of nuclear elemental analyzers for product optimization in the cement industry. Piscataway, NJ, IEEE Operations Center, 237-254

[13] Thermo Fisher Scientific Inc. (2007) CBX-M (CrossBelt Xpert-Minerals) Online PGNAA Elemental Analyzer. Thermo Fisher Scientific Inc.

[14] Gottwald, W.; Heinrich, K.H. (1998) UV/VIS-Spektroskopie für Anwender. Weinheim, Wiley-VCH

[15] Lehmann, T. (2009) UV/VIS-Spektroskopie. Berlin. Freie Universität Berlin

[16] Dehler, M. (2011) Color versurs NIR/XRT. AT Mineral Processing 52, 68–75

[17] John, H.J. (2008) Vorrichtung zum Bearbeiten und Verfahren zum Bestimmen eines Lockergesteins. 102008043886

[18] Tudeshki, H.; Hertel, H.; John, H.J. (2012) Baugrunderkundung mittels akustischem GeoScanner. BBR - Fachmagazin für Brunnen und Leitungsbau, 40–45

[19] Tudeshki, H.; Hertel, H. (2012) Lagerstättenerkundung in gewachsenem Lockergestein mit dem akustischen GeoScanner. SDAG Schriftenreihe Geo Hannover 80

[20] Povey, M.; Tong, J.; Nelson, P.V.; Jones, G.M. (2002) Particle measurement by acoustic speckle. 6481268

[21] Tudeshki, K. (2016) Verfahren zum Bestimmen der Korngrößenverteilung von Granulaten in einen Förderstrom und Messeinrichtung. 102015116376

[22] Tipco GmbH (2016) Verfahren zum Bestimmen der Korngrößenverteilung von Granulaten in einen Förderstrom und Vorrichtung zur Durchführung des Verfahrens. 102015116379

[23] Tudeshki, H.; Vogler, K.; Korei, H.; Weigel, C. (2019) Online-Korngrößenanalyse von Gesteinskörnungen. Gesteins Perspektiven, 18–20

[24] Tudeshki, H.; Korei, H. (2018) Verfahren zum Bestimmen des Mischverhältnisses von einem Gemenge aus granularen Feststoffen mit unterschiedlicher Dichte in einen Förderstrom. Mining, 73–78

[25] Tudeshki, H.; Korei, H. (2018) Online Erkennung von Rohstoffen während des Bohrvorgangs. Mining, 17–21

[26] Tudeshki, H.; Korei, H. (2019) Method and device for determining the qualitative proportions of a plurality of fractions of a blend. WO 2019/238274A1

[27] Voigt, W.; Tudeshki, H. (2016) Apparatus and method for blending loose rock material. 3183623

[28] Alessandro, B.; Cristina, C.; Roberto, M.; Erlado, P. (2011) Acoustic emissions for particle sizing of powders through signal processing techniques. Mechanical Systems and Signal Processing 25, 901–916

[29] Kupyna, A.; Rukke, E.O.; Isaksson, T. (2008) The effect of flow rate, accelerometer location and temperature in acoustic chemometrics on liquid flow: Spectral changes and robustness of the prediction models Chemometrics and Intelligent Laboratory Systems. Chemometrics and Intelligent Laboratory Systems 93, 87–97

[30] Goldsmith, W. (2015) Impact: The theory and physical behaviour of colliding solids. 1960. Aufl. Mineola, NY, Dover Publications

[31] Benes, P.; Zenhula, K. (2000) New design of the two-phase flowmeters. Sensors and Actuators 86, 220–225

[32] Syvitski, J.P.M. (2010) Principles, Methods and Application of Particle Size Analysis. Cambridge University Press

[33] Zogg, M. (1993) Einführung in die mechanische Verfahrenstechnik: Mit 29 Tabellen und 32 Berechnungsbeispielen. 3. Aufl. Stuttgart, Teubner

[34] Masuda, H.; Yoshida, H.; Higashitani, K. (2006) Powder technology handbook. 3. Aufl. Boca Raton, Taylor & Francis

[35] Rhodes, M. (2013) Introduction to Particle Technology. Somerset, John Wiley & Sons Incorporated

[36] Robertson, E.C.; Robie, R.A.; Books, K.G. (1958) Physical properties of salt, anhydrite and gypsum. Preliminary report. U.S. Geological Survey. United States Department of the interior geological survey, Trace Elements Memorandum Report 1048, 38 p

[37] Worthoff, R.; Siemes, W. (2012) Grundbegriffe der Verfahrenstechnik: Mit Aufgaben und Lösungen. Weinheim, Wiley-VCH Verlag GmbH & Co. KGaA

[38] Eckstein, L.; Dellmann, T. (2012) Mechatronische Systeme in der Fahrzeugtechnik: Vorlesungsumdruck. 5. Aufl. Aachen, fka Forschungsgesellschaft Kraftfahrwesen

[39] Eckstein, L.; Dellmann, T. (2014) Mechatronische Systeme in der Fahrzeugtechnik. Forschungsgesellschaft Kraftfahrwesen mbH

[40] Edison, J.; Lee, K. (2003) Sharing a common sense of time. IEEE Instrumentation and Measurement Magazine 6, 26–32

[41] Bernard, M. (2015) Big Data: 20 Mind-Boggling Facts Everyone Must Read. Forbes https://www.forbes.com/sites/bernardmarr/2015/09/30/big-data-20-mind-boggling-facts-everyone-must-read/#7e2c684d17b1 . (zuletzt eingesehen am 05.10.2020)

[42] Jolliffe, I.T. (1986) Principal Component Analysis. New York, NY, Springer

[43] Mitchell, H.B. (2010) Multi-sensor data fusion: An introduction ; with 59 tables. Berlin, Springer

[44] Pedregosa, F.; Varoquaux, G.; Gramfort, A.; Michel, V.; Thirion, B. (2011) Machine Learning in Python. Journal of Machine Learning Research 12, 2825–2830

[45] Zhang, P.; Peng, J.; Riedel, N. (2005) Discriminant Analysis: A Unified Approach, 514–521

[46] Hardoon, D.; Szedmak, S.; Shawe-Taylor, J. (2004) Canonical Correlation Analysis: An Overview with Application to Learning Methods. Neural Computation 16, 2639–2664

[47] Hyvärinen, A.; Karhunen, J.; Oja, E. (2001) Independent Component Analysis. New York. JOHN WILEY & SONS, INC.

[48] Risidanto, D.; Kusnadi, D. (2010) The Application of a Probability Graph in Geothermal Exploration. Bali. Department of Energy and Mineral Resources, Proceedings World Geothermal Congress

[49] McQueen, K.G. (2015) Identifying geochemical anomalies. department of Earth and Marine Sciences

[50] Breiman, L. (2001) Random Forests. University of California. Machine Learning, 45, 5–32

[51] Chollet, F. (2018) Deep learning with Python. Shelter Island, NY, Manning

[52] Brownlee, J. (2019) How to Configure the Number of Layers and Nodes in a Neural Network. Machine Learning Mastery Website machinelearningmastery.com/how-to-configure-the-number-of-layers-and-nodes-in-a-neural-network/

[53] Abadi, M.; Barham, P.; Chen, J.; Chen, Z. (2016) Proceedings of OSDI ’16: 12th USENIX Symposium on Operating Systems Design and Implementation: November 2-4, 2016, Savannah, GA, USA. Berkeley, CA, USENIX Association

[54] Rindler, W. (1977) Essential Relativity: Special, General, and Cosmological. Berlin, Heidelberg, Springer

[55] Levinzon, F. (2015) Piezoelectric Accelerometers with Integral Electronics. Cham, s.l., Springer International Publishing

[56] PCB Piezotronics Introduction to ICP Accelometers. PCB Piezotronics https://www.pcb.com/resources/technical-information/introduction-to-accelerometers#collapse10 . (zuletzt eingesehen am 05.10.2020)

[57] Analog Devices (2018) Single Supply, 24-Bit, Sigma-Delta ADC with ±10 V and 0 mA to 20 mA Inputs. Analog Devices

[58] Fox Valve Eductors for Pneumatic Conveying with No Moving Parts. Fox Valve https://www.foxvalve.com/solids-conveying-eductor-systems/introduction/ . (zuletzt eingesehen am 05.10.2020)